Translation Initiation with 70S Ribosomes
A Single Molecule Study

Cristina Remes

JÜLICH
Forschungszentrum

Schriften des Forschungszentrums Jülich
Reihe Schlüsseltechnologien / Key Technologies   Band / Volume 184

Translation Initiation with 70S Ribosomes A Single Molecule Study

Cristina Remes

To the memory of Prof. Dr. Knud Nierhaus,

whose scientific work and enthusiasm

will remain an enormous source of inspiration in the ribosome research.

Contents

Summary

Until now, three initiation pathways for ribosomal protein synthesis have been described: the 30S-binding mechanism of canonical mRNAs, which assumes that the first step is binding of the small subunit to the start codon of the mRNA with the help of initiation factors, the rare initiation of leaderless mRNAs by full 70S ribosomes, and the 70S-scanning mode through which the second cistron of a polycistronic mRNA is translated.

According to the standard model from classical textbook, translation of canonical mRNAs occurs exclusively via the 30S-binding mechanism, which requires dissociation of subunits. In contrast to this, we demonstrated here using an *in vitro* transcription-translation system that canonical mRNAs can be also initiated by full 70S ribosomes, without dissociation. The standard and non-standard initiation events were quantified with single molecule experiments, since only by tracking one particle at a time one can identify and count parallel mechanistic initiation pathways.

To perform single molecule experiments, the sample preparation had first to be optimized by establishing the protocols for reassociation of ribosomes, biotinylation and labeling. The reassociation procedure involves purification of tightly-coupled 70S from *E. coli*, dissociation into subunits and reassociation to form 70S monomers, and it leads to a highly pure sample, in which the endogenous bacterial mRNAs and factors are discarded. Concerning the biotinylation, two approaches are presented: on the one hand, *in vivo* biotinylation of the uL4 ribosomal protein, and on the other hand, binding of a biotinylated oligonucleotide to an RNA loop engineered on the small subunit. The first approach lead to a 1/4 decrease in activity of the modified ribosomes, in contrast to the second method, which did not affect the activity of the ribosomes. In addition to this, ribosomes were fluorescently labeled for single molecule experiments, using two strategies: unspecific labeling of accessible lysines with NHS dyes and labeling via oligonucleotide binding on engineered loops of rRNA. In both cases, the samples were characterized in regard to the labeling ratio, presence of aggregates and free dye, and activity. The first method allowed multilabeling of ribosomes, but a 1/3 decrease in activity was observed, while the second approach yielded site-specifically single labeled ribosomes with an activity comparable to the wild type.

The second step was improving the stalling properties of the DNA used for GFPem synthesis. A poor stalling efficiency would release the GFPem from the ribosomal complexes, so it would not be detected on a wide field. Moreover, the ribosomal subunits would dissociate, meaning that the 70S which initiated translation would not be identified. Previous studies used the secretion monitor (SecM) arrest sequence to stall ribosome nascent chains. However, the SecM showed unsatisfactory stalling characteristics in our experiments, considering that most of the translated protein was released from the ribosome. Therefore, a new SecM arrest sequence was designed (SecMstr), that was proven to have enhanced stalling properties, achieving an almost absolute stalling of the ribosomes (>95%). The good stalling properties allowed also the quantification of the active fraction of ribosomes in an *in vitro* transcription-translation kit and the average number of productive cycles the ribosomes can perform in these conditions.

Moreover, the techniques for single molecule experiments were optimized. In order to limit the bleaching and blinking of the fluorophores, two oxygen scavenging systems were studied: the protocatechuic acid/protocatechuate-3,4-dioxygenase (PCA/PCD) system in combination with Trolox, and the Glucose oxydase/catalase (Gox) system. The first one considerably improved the detection of Cy5, both in Two-Colour Coincidence Detection (TCCD) and wide field measurements. For specific tethering of biotinylated ribosomes on modified glass slides, a protocol for surface coating using a mixture

of PEG and bioPEG has been developed, focusing on obtaining a low fluorescence background, good blocking properties and maintaining the activity of the immobilized ribosomes.

After achieving an optimized system, the study on translation initiation was performed, using site-specifically single labeled reassociated ribosomes, and the canonical mRNA containing the SecMstr in order to stall the produced GFPem on the ribosomes. The initiation modes were quantified with TCCD experiments, demonstrating that from the total successful translation events, 30% occurred by initiation with 70S, and 70% occurred via the 30S-binding mode. This is the first study that investigates and quantifies initiation of canonical mRNAs by full 70S ribosomes, without dissociation into subunits. Furthermore, the optimized system presented here can be used in wide field measurements to get insights into the kinetics of the processes involved in this non-standard initiation mechanism. Moreover, optimization of the stalling properties of the SecM arrest sequence in combination with single molecule studies offers a broad spectrum of further studies on transcription, translation and co-translational protein folding.

Zusammenfassung

Bisher wurden in der Literatur drei Initiierungswege für die Proteinsynthese beschrieben: der 30S-Bindungsmechanismus der kanonischen mRNAs, welcher als ersten Schritt die Bindung der kleinen Untereinheit an das Startkodon mittels Initiierungsfaktoren annimmt, die seltene Initiierung von mRNAs ohne Leadersequenz durch 70S Ribosomen, und der 70S-Scanning Initiierungsmodus, bei dem das zweite Cistron einer polycistronischen mRNA durch Translation übersetzt wird.

Das Standardmodell aus dem klassischen Lehrbuch nimmt an, dass Translation der kanonischen mRNAs ausschlielich über den 30S-Bindungsmechanismus abläuft. Dieser Mechanismus setzt die Dissoziation der ribosomalen Untereinheiten voraus. Im Gegensatz dazu zeigen wir hier in einem *in vitro* Transkription-Translationssystem, dass Translation der kanonischen mRNAs auch durch vollständige 70S Ribosomen initiiert werden kann, ohne Dissoziation der Untereinheiten. Die Initiierungsereignisse, die nach dem klassischen und nicht-klassischen Modell abgelaufen sind, wurden quantitativ durch Einzelmolekülexperimente untersucht. Einzelmoleküluntersuchungen sind für diese Studie ausschlaggebend, da es für die Identifizierung und Quantifizierung der möglichen Initiierungswege unbedingt erforderlich ist, einzelne Moleküle zeitlich verfolgen zu können.

Um für die Studie erforderlichen Einzelmolekülexperimente durchführen zu können, musste zunächst der Prozess der Probenvorbereitung optimiert werden. Dafür wurden die Protokolle für die Reassoziation, für die Biotinylierung und für die Markierung der Ribosomen etabliert. Die Reassoziationsprozedur besteht dabei aus der Herauslösung der fest gekoppelten 70S aus *E. coli*, der nachfolgenden Dissoziation in Untereinheiten und anschließenden Bildung von 70S Monosomen durch Reassoziation der Untereinheiten. Diese Prozedur liefert Ribosomen von sehr hoher Reinheit, ohne bakterieneigene mRNAs und andere Faktoren. Bei der Biotinylierungsprozedur werden zwei Wege vorgestellt: zum einen, die *in vivo* Biotinylierung des ribosomalen uL4 Proteins und zum anderen, die Kopplung eines biotinylierten Oligonukleotiden an eine RNA Schleife, die an die kleine Untereinheit der Ribosomen angebracht wurde. Die in vivo Biotinylierung führt zur Senkung der Aktivität der modifizierten Ribosomen um 25%, im Gegensatz zum zweiten Ansatz, der die Aktivität der Ribosomen unbeeinträchtigt lässt. Zur Durchführung der Einzelmoleküluntersuchungen müssen die Ribosomen mit Fluoreszenzfarbstoffen markiert werden. Hierfür wurden zwei Methoden gewählt: einerseits die ortsunspezifische Markierung der zugänglichen Lysine mit NHS-Ester Farbstoffen und die ortspezifische Markierung durch Bindung von Farbstoff gekoppelten Oligonucleotiden an die hergestellten rRNA Schleifen. Die fluoreszent markierten Ribosomen wurden für beide Szenarien untersucht, und ihr Markierungsanteil, das Vorhandensein von Aggregaten und von freiem Farbstoff, und das Niveau der ribosomalen Aktivität wurden gemessen. Die erste Methode ermöglichte die multiple Markierung von Ribosomen, allerdings wurde ein Abfall der ribosomalen Aktivität um 1/3 ihres Wertes im Originalzustand ohne Markierung beobachtet. Die zweite Methode ermöglichte die ortsspezifische Einzelmarkierung der Ribosomen, die ein mit dem unmarkierten Zustand vergleichbares Aktivitätsniveau zeigen.

Der zweite Schritt beinhaltete die Verbesserung der Fixierungseigenschaft der DNA, die für GFPem Synthese verwendet wurde. Eine unzureichende Fixierung hätte eine Freisetzung der GFPem aus dem ribosomalen Komplex zur Folge, so dass es nicht mehr im Zusammenhang mit dem synthetisierenden Ribosom im Weitfeldmikroskop gemessen werden könnte. Darüber hinaus könnten sich die ribosomalen Untereinheiten trennen, was bedeuten würde, dass jene 70S Ribosomen, die möglicherweise eine Translation initiierten, als solche nicht mehr erkannt werden könnten. Frühere Arbeiten verwendeten eine Sekretionsmonitor-Fixierungssequenz (SecM), um ribosomale Elongationsketten zu halten. Allerdings offenbarte SecM in unseren Experimenten eine unbefriedigende Fixierungseigenschaft, da

sich das Groteil von hergestellten Proteinen von Ribosomen loslösen konnte. Es wurde daher eine neue SecM Fixierungssequenz (SecMstr) entworfen, die Fixierungseffizienz stark steigern konnte - sie zeigte eine fast vollständige Fixierung von Ribosomen (>95%). Die hohe Fixierungseffizienz erlaubte auch die Quantifizierung des Anteils der aktiven Ribosomen in einem *in vitro* Transkription-Translationssystem. Dort wurde ebenfalls die mittlere Zahl der produktiven Synthesezyklen ermittelt, die Ribosomen unter diesen Bedingungen ausführen konnten.

Weiterhin wurden die spektroskopischen Methoden für die Einzelmolekültersuchungen optimiert. Um das Ausbleichen und das Blinken der Fluorophoren zu vermindern, wurden zwei Sauerstoff-szehrungssysteme untersucht: das Protocatechusäure/Protocatechuat-3,4-Dioxygenase (PCA/PCD) System in Kombination mit Trolox, und die Glukose Oxydase / Katalase (Gox) System. Das erste System verbessert stark die Photostabilität von Cy5, sowohl in Zweifarben-Koinzidenzdetektion (Two-Colour Coincidence Detection, TCCD) als auch in Weitfeldmessungen. Für die spezifische Fixierung der biotinylisierten Ribosomen auf modifizierten Glasdeckgläsern wurde ein Protokol zur Beschichtung der Deckgläser mit einer Mischung aus PEG und bioPEG entworfen. Besonderer Fokus lag dabei auf einem niedrigen Niveau des Fluoreszenzhintergrundes, der Herstellung von einer guten spezifischen Bindung und der Fähigkeit, die fixierten Ribosomen aktiv zu halten.

Nach der Optimierung des gesamten Verfahrens wurde die Studie zur Translationsinitiierung durchgeführt. Dabei wurden Ribosomen mit ortsspezifischen fluoreszenten Einzelmarkierungen verwendet. Kanonische mRNA mit integrierter SecMstr Sequenz wurden dabei eingesetzt, um hergestellte GFPem Moleküle an Ribosomen gebunden zu halten. Die verschiedenen Initiierungswege wurden durch TCCD Experimente quantifiziert. Es hat sich gezeigt, dass aus der Gesamtzahl der erfolgreichen Translationen 30% auf die Initiierung mit 70S, und 70% auf die Initiierung durch 30S-Bindung fielen.

Die hier vorgestellte Studie ist somit die erste, welche Initiierung der kanonischen mRNAs durch vollständige 70S Ribosomen, die nicht in Untereinheiten dissoziieren, bestätigt und quantifiziert hat. Das optimierte System kann im weiteren Verlauf für die Untersuchungen mit Weitfeldmikroskopie verwendet werden, um noch mehr Einsicht in die Dynamik der Prozesse liefern, die dem Initiierungsmechanismus der 70S Ribosomen zugrunde liegen. Ausserdem bietet die optimierte SecM Fixierungssequenz in Kombination mit Einzelmolekülmessungen ein breites Spektrum an weiteren Studien der Transkription, Translation und der co-translationalen Proteinfaltung.

Part I.

Introduction

1

General Information

1.1. The Ribosome and Ribosomal Subunits

The ribosome is a 2.5 MDa ribonucleoprotein particle, that synthesizes proteins, using the mRNA as a template and aminoacyl-tRNAs as building blocks. In bacteria, the ribosome (70S) consists of two subunits: the small (30S) subunit and the large (50S) subunit, approximately twice as large as the first one, each with specific roles in translation of proteins. The RNA component is about two thirds of the total mass of the ribosome.

Determining the ribosome structure by X-ray crystallography is problematic, because of the internal flexibility of the complex, the size of the asymmetric unit, the crystal variability and sensitivity to radiation damage. The first successful attempts to crystallize ribosomes were achieved in the 1980s, by the group of Ada Yonath, using samples of *B. stearothermophilus* ribosomes. Improvements in the quality of the crystals and the measurement techniques were later achieved, so that the structure of both subunits at atomic resolution was determined in the past years ([Clemons et al., 2001], [Ban et al., 2000]).

Since obtaining crystals from ribosomal complexes raises many problems and has major limitations, it is easier to investigate them by cryo-electron microscopy (cryo-EM). This technique is suitable for large, stable molecules that can withstand electron bombardment without structural change, and it has the advantage that the sample does not require absolute homogeneity. High resolution has been achieved recently ([Hashem et al., 2013], [Shalev-Benami et al., 2016], [Sprink et al., 2016]), with the development of direct electron detectors, that outperform film or digital cameras, and improvement in the image analysis ([Cheng, 2015]).

The basic architecture of the prokaryotic ribosome is shown in Fig. 1.1 The interfaces of both subunits, especially the part that binds the mRNA and the tRNA, are protein-free, with the exception of protein S12 in the small subunit ([Ramakrishnan and Moore, 2001]). The ribosomal proteins have both a globular domain, found on the surface of the ribosome, and long extensions which penetrate into the

structure of the RNA, stabilizing its tertiary structure. The mRNA binding site is located in a cleft between the "head" and the "body" of the 30S subunit, where the codons interact with the anticodons of the tRNA. Both subunits contain three binding sites for accommodation of tRNAs that are in three different functional states (Fig. 1.7). The A site binds the aminoacyl-tRNA that will be incorporated into the polypeptide chain, the P site accommodates the peptidyl-tRNA and the E (exit) site contains the deacylated tRNA before it is released from the ribosome ([Steitz, 2008]).

The catalytic site of the protein synthesis, where the peptide bond is formed, is located on the large subunit, at the peptidyl-transferase center (PTC), where the 3' ends of the tRNAs located in the P and A sites are in close proximity. The structure of ribosomes with substrate analogues bound to the PTC was determined by crystallography, and the position of the PTC was located in the central loop of the domain V of the 23S rRNA ([Nissen et al., 2000]).
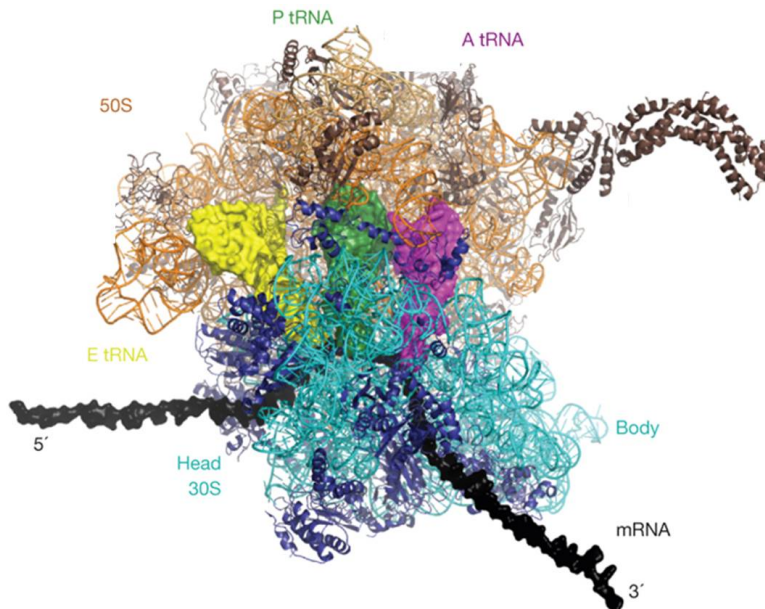
Figure 1.1.: The 70S ribosome, with mRNA and tRNAs located in the A, P and E site ([Schmeing and Ramakrishnan, 2009])

The 30S subunit is composed of a 1500 nucleotide RNA (16S rRNA) and 21 proteins, and it has two main functions in protein synthesis. It resolves the base pairing between the codon on the mRNA and the complementary anticodon on the transfer RNA (tRNA), ensuring accuracy in translation ([Carter et al., 2000]). Additionally, together with the 50S subunit, it moves the mRNA and the corresponding tRNA by precisely one codon, during translocation.

The small subunit of *Thermus thermophilus* ribosome was crystallized and resolved at 3 Å resolution by Wimberly et. al ([Wimberly et al., 2000]). The overall shape can be divided into a head, neck, platform and body and it is largely defined by the RNA component. The secondary structure of the 16S rRNA contains over 50 regular double helices connected by single-stranded loops. Stacking of the helical elements forms three compact domains: the 5' domain, the central domain and the 3' major

domain, and one extended domain: the 3'-minor domain. These structures are tightly connected in the neck region, forming the most functionally important part of the 30S subunit. The proteins are distributed asymmetrically, concentrated in the top, sides and back of the subunit.

The 50S subunit consists of two ribosomal RNAs, the 23S (2900 nucleotides) and the 5S rRNA (120 nucleotides), and 33 proteins. It has a more compact structure than the small subunit, composed of a rounded base with three almost cylindrical extensions: the L1 protuberance, the central protuberance and the L7/L12 stalk. The large subunit catalyses the peptide bond formation in the PTC, and it contains the binding site of GTP-binding proteins that assist the ribosome in translation. The first high-resolution structure of the 50S was solved by Ban et. al ([Ban et al., 2000]) using X-ray crystallography. The six domains of the 23S rRNA and 5S rRNA have an irregular, highly asymmetric shape, that fit together to create a compact RNA mass. The proteins are located throughout the structure, mostly concentrated on the surface, but do not extend beyond the borders of the rRNA. They have globular domains on the outer surface of the subunit and they protrude with extended, irregular loops and termini between the RNA helices, stabilizing its structure.The 5S rRNA does not interact with the 23S rRNA directly, but it attaches to the subunit via a large number of ribosomal proteins that bind both RNA domains.

An important feature of the 50S subunit is the exit tunnel (Fig. 1.2) that the newly synthesized protein traverses before exiting at the cytoplasmic region. Emerging from the PTC, the diameter of the tunnel is 10 Å wide at its narrowest and 20 Å at its widest point next to the exit, and the length is 100 Å, accommodating 30-40 aminoacids of the nascent chain. The wall of the tunnel is formed by the 23S rRNA and loops of the ribosomal proteins that face the interior: L4, L22, L24, and proteins that are in close proximity: L23, and L29.

It has been shown that some nascent chains are being folded already in the exit tunnel, when they contain a transmembrane sequence, but not when they contain a sequence of ten nonpolar residues ([Nilsson et al., 2015], [Woolhead et al., 2004]). Moreover, the trigger factor (TF), which interacts with the exit of the tunnel through proteins L23 and L29, allows folding of small size proteins as they emerge from the ribosome ([Ferbitz et al., 2004], [Schlünzen et al., 2005]).

1.2. Messenger RNA (mRNA)

In bacteria, precision of translation is ensured at two levels: the mRNA and the initiation factors. The majority of the prokaryotic mRNAs contain, upstream the start codon, an untranslated region (UTR), a purine-rich structure called the Shine-Dalgarno (SD) sequence, which has a complementary sequence with the 3' end of 16S rRNA component of the 30S subunit: the anti-SD sequence, aSD ([Shine and Dalgarno, 1974], [Steitz and Jakes, 1975]). This complementarity is used for correctly positioning the AUG start codon in the P site of the ribosome during initiation.

The SD-aSD interaction has been visualized in *Thermus thermophilus* 30S subunits, by X-ray crystallography ([Yusupova et al., 2001]). Around 30 nucleotides are wrapped in a groove that encircles the neck of the 30S subunit, while the SD-aSD structure forms a helical complex above the platform and behind the head of the 30S subunit. At the subunit interface, eight nucleotides are centered between the A and the P site, bound exclusively to the 16S rRNA (Fig. 1.3).

It has been shown that in bacteria the sequence of the mRNA modulates translational pauses, important in folding and protein targeting. In particular, rare codons which pair to less abundant tRNAs are translated slowly ([Jansen et al., 2003], [Angov et al., 2008]). Moreover, the presence of an internal
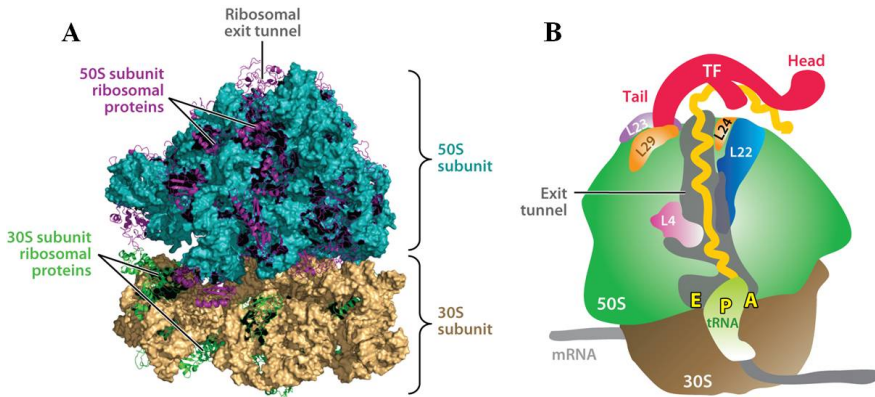
Figure 1.2.: The exit tunnel (A) Crystal structure of the ribosome at 3.5Å resolution. The 23S and 5S rRNA is depicted in turqoise, and the 16S rRNA in beige. The ribosomal proteins are shown as ribbons, in green (30S) and in purple (50S) (B) Schematic representation of a vertical section of the 70S ribosome, showing the proteins near or close to the exit tunnel and the ribosome-associated TF. [Fedyukina and Cavagnero, 2011]
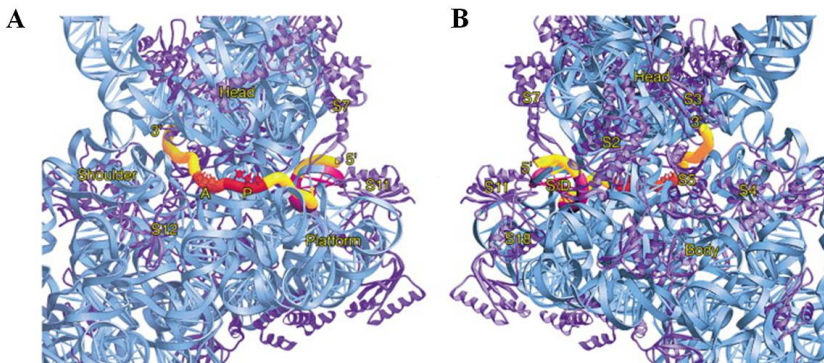
Figure 1.3.: Interaction of the mRNA with the 30S subunit (view from the subunit interface (A) and solvent (B)). The head, platform, shoulder and body of the subunit, and ribosomal proteins involved in mRNA-30S interaction are indicated ([Yusupova et al., 2001])

SD sequence in the structure of the mRNA promotes pausing *in vivo*, presumably for modulating the transcription-translation coupling ([Li et al., 2012]).

1.3. Initiation Factors

Proper initiation requires three factors (IF) in bacteria: IF1, IF2·GTP and IF3, and a specialized initiator tRNA, the fMet-tRNA. In short, the functions of the initiation factors are described as following: IF3 is a subunit dissociation factor, IF2 is a GTPase that hydrolyses GTP when the 50S binds the 30S

initiation complex, and together, IF2 and IF3 position the initiator tRNA in the P site, establishing the interaction with the AUG codon ([Hartz et al., 1989], [Meinnel et al., 1999]). IF1 is an essential factor for cell viability, and it assists the other two initiation factors to select the initiator tRNA once the 70S initiation complex has been formed ([Hartz et al., 1989]).

1.3.1. Initiation Factor 1

IF1, the smallest of the three initiation factors, is a monomeric protein consisting of 71 aminoacids. The 3D structure, determined by NMR spectroscopy ([Sette et al., 1997]), is very similar to the structure of the oligonucleotide-binding protein family, characterized by a five-stranded β-sheet, closed to form a β-barrel and capped by an α-helix. Current evidence shows that IF1 interacts with the 16S rRNA of the 30S subunit, in the A region, through mostly electrostatic interactions ([Dahlquist and Puglisi, 2000]). Binding to the 30S subunit leads to a structural rearrangement of the helix h44 within the subunit, functionally important during decoding, allowing the proper fit of codon-anticodon ([Carter et al., 2001]). In addition, in the new conformational state, h44 allows extensive contacts with the 50S subunit, which explains the higher affinity of subunits in presence of IF1 (Fig. 1.4). Moreover, IF1
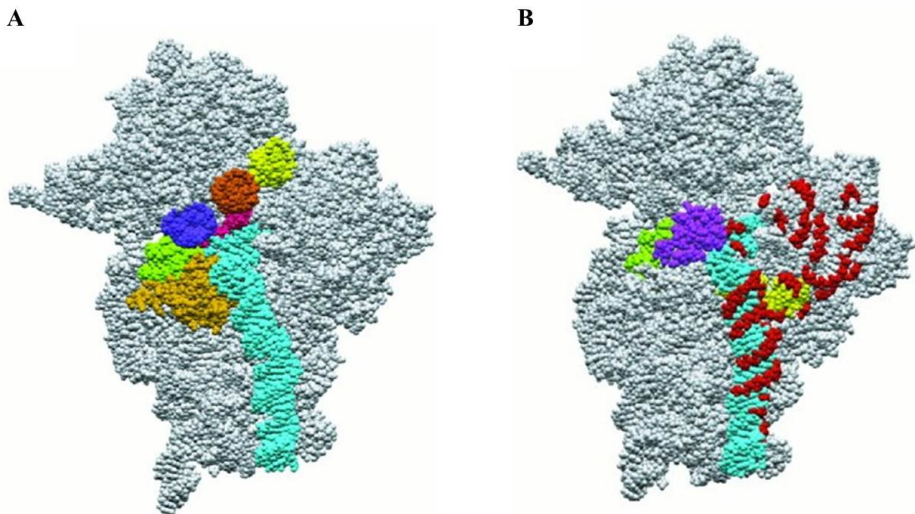
Figure 1.4.: Interaction of IF1 with the 30S subunit. (A) Overview of the IF1 (purple) interaction with the 30S subunit (grey), showing helix 44, S12 and the 530 loop in cyan, light orange and green, respectively, and the A, P and E site in dark blue, dark orange and yellow, respectively. (B) Conformational changes in the 30S subunit on IF1 binding, with loop 530 (purple), and helix 44 in the presence (cyan) and absence (yellow) of IF1. Regions that are exposed to the 50S subunit are shown in red. ([Carter et al., 2001]

modulates the interaction of IF2-fMet with the 30S, by increasing its activity when IF1 is bound and promoting its release when IF1 is released ([Celano et al., 1988]). Also, the presence of IF1 accelerates the IF3-dependent dissociation, with a 25-fold increase dissociation rate ([Pavlov et al., 2008]).

1.3.2. Initiation Factor 3

IF3 is a 180 aminoacids protein, containing two functionally independent globular domains, separated by a flexible hydrophilic linker. The structure has been elucidated by X-ray crystallography ([Biou et al., 1995]) and NMR spectroscopy ([Fortier et al., 1994], [Garcia et al., 1995]). The two domains interact independently with the 30S subunit: the C domain binds first, through some of the loops and α helices, allowing the consequent binding of the N-domain ([Sette et al., 1999]) via a lower number of α helices. Docking of IF3 in the small subunit takes place in the E-site region, as reported in crystallography ([Pioletti et al., 2001]) and cryo-EM ([Allen et al., 2005], [McCutcheon et al., 1999]) studies, and inhibits association of subunits ([Kaempfer, 1972]).

The conformation of IF3 bound to the 30S-initiation has been elucidated with single molecule experiments ([Elvekrog and Gonzalez, 2013]). The study shows that the system converts into at least three distinct conformational states, demonstrating that there is a conformational equilibrium of IF3 in the 30S initiation complex, that can be modulated by IF1 and IF2. In this model, IF3 bound to the 30S initiation complex can have at least three major conformations, whose thermodynamic stability depends on the composition of the complex. In the case in which the complex carries all three initiation factors and a properly base-paired initiator tRNA, the equilibrium is shifted to a conformation of IF3 that signals proper selection and leads to rapid 50S joining (Fig 1.5, A). In contrast, when the correct tRNA is missing, the conformational equilibrium will be shifted to a structure that is not conductive to rapid 50S binding (Fig 1.5, B).
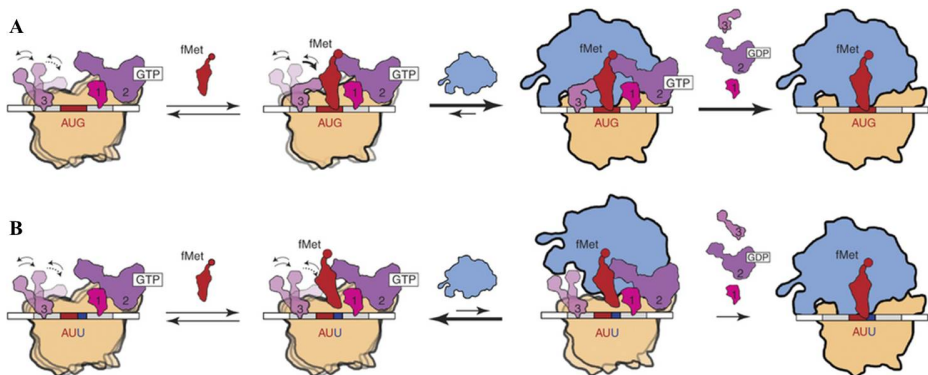
Figure 1.5.: Mechanism of IF3-induced recognition and selection of correct initiation complexes. IF3 bound to the 30S-initiation complex is in a conformational equilibrium, that is shifted to the state which leads to stable 70S complexes, only when the initiator tRNA is properly base paired to a start codon (A). Otherwise, the equilibrium is shifted to a conformational structure that does not lead to successful 70 S complexes (B) ([Elvekrog and Gonzalez, 2013])

IF3 is not required for mRNA binding to the ribosome ([Calogero et al., 1988]), but it induces repositioning of the mRNA from the "stand-by" site into the "P-decoding site" of the subunit, in the mRNA channel ([La Teana et al., 1995]). This shift was correlated to the correct selection of the initiation codon by the IF3.

1.3.3. Initiation Factor 2

From the three bacterial initiation factors, IF2 is the largest (100 kDa), composed of two compact domains (the C-domain and the G-domain) and a flexible region (the N-domain), with at least four active sites: the binding site for GTP, the 30S subunit, the 50S subunit and fMet-tRNA ([Gualerzi et al., 1991], [Gualerzi et al., 2001]). It forms a complex with the initiator tRNA and GTP ([Gualerzi et al., 1991]), that is then delivered to the 30S subunit, in the P site region, to form the 30S-initiation complex ([Simonetti et al., 2008]). In the GTP bound state, IF2 makes strong contacts to the 30S subunit. IF2 has binding sites on both subunits, and it accelerates subunit joining. After recruitment of the 50S subunit to the 30S initiation complex, GDP hydrolysis occurs, and the GDP bound to IF2 produces a conformational change resulting in a reduced interaction with the ribosome ([Myasnikov et al., 2005]). The cryo EM structure of IF2-bound 70S initiation complex was solved using non-hydrolizable GTP analogues ([Allen et al., 2005], [Myasnikov et al., 2005]), and shows structural rearrangements in comparison to the 30S initiation complex and the GDP form of the 70S initiation complex. These structures prove that during hydrolysis, inter-subunit rotation occurs, and the 3' end of the initiator tRNA is accommodated in the P site of the ribosomal complex ([Sprink et al., 2016], Fig. 1.6).

The inter-subunit rotation was also confirmed with single molecule FRET experiments ([Marshall et al., 2009]). The results show that a significant electrostatic energy barrier is required for accommodation of the 50S subunit. In this respect, initiation factors, mostly IF2, bury nearly half of the negatively charged 30S and 50S subunit interface, decreasing the energetic barrier and therefore, stabilizing the newly formed 70S initiation complex.
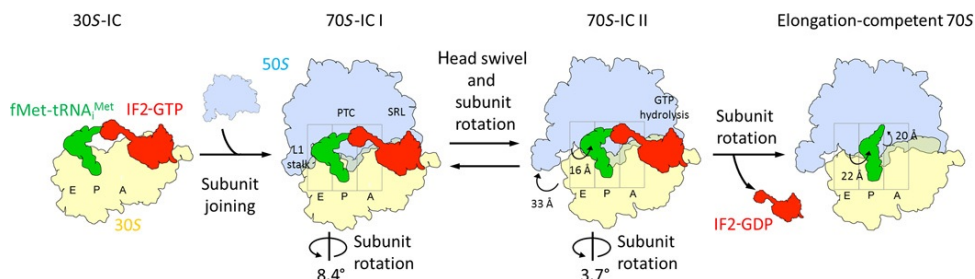
Figure 1.6.: IF2 (red) induces binding of the 50S subunit (blue) to the 30S-initiation complex (yellow), leading to a inter-subunit rotation, with the formation of the 70S-initiation complex (70S IC-1). In order to reach the elongation state, the 30S completes the back rotation IF2-GDP dissociates and the tRNA is shifted to the P site([Sprink et al., 2016])

Moreover, it has been shown that IF2 selectively stimulates translation of leaderless mRNAs (detailed in 1.6.2.1), *in vivo* and *in vitro* ([Grill et al., 2000]).

1.4. Bacterial Translation

In bacteria, transcription and translation are coupled in time and space. The ribosome starts initiation of mRNA immediately as the ribosomal binding site has emerged from the RNA channel of the RNA polymerase (RNAP). In addition to this, translating ribosomes modulate transcription by physically blocking backtracking of the RNAP ([Saeki and Svejstrup, 2009]). This cooperation makes sure that

the rate of transcription is determined by the codon usage and nutrient availability under various growth conditions ([Proshkin et al., 2010]).

In translation, the sequence of codons in a mRNA directs the synthesis of a polypeptide chain. This process takes place on the ribosome, with high accuracy. *In vivo*, ribosomes translate 18 amino acids/s, while in a cell-free transcription-translation system, the number decreases to 1.5 amino acids/s.

Bacterial translation can be divided into three main steps: initiation, elongation and termination (Fig. 1.7). The initiation step, the most regulated and the rate-limiting phase of translation, requires free subunits that have been split by the ribosome recycling factor (RRF) during a previous termination event. The first step is binding of initiation factors, initiator tRNA (fMet-tRNA) and mRNA to the 30S, to form the 30S-initiation complex. At this point, fMet-tRNA is bound to the A site of the subunit. IF2 promotes the recruitment of a 50S subunit, which leads to the formation of the 70S initiation complex and the subsequent release of IF3. After GTP hydrolysis, the fMet-tRNA shifts to the P site, in a step which prepares the ribosome for the elongation step. *In vivo*, initiation occurs at a rate of 2.8 $\mu M^{-1}\text{s}^{-1}$, several orders of magnitude faster than *in vitro* ([Marshall et al., 2008]).

The elongation step is a repetitive process in which the ribosome selects the tRNAs corresponding to the codons on the mRNA, and the peptide bonds are synthesized to form the protein chain. The selection of the correct tRNA is made through a two-step mechanism, facilitated by the elongation factor Tu (EF-Tu), a ribosome-activated GTPase. The incoming tRNA is accommodated in the A site of the ribosome, via codon-anticodon interactions, so that the aminoacyl residue docks in the peptidyl transferase centre of the large subunit. This step leads to formation of the peptide bond, and the nascent chain is transferred from the P-site tRNA to the aminoacyl group of the A-site tRNA, so that a deacylated (uncharged) tRNA is located at the P site and the peptidyl-tRNA carrying the polypeptide chain is bound to the A site. The mRNA is then shifted on the ribosome by one codon, in order to place the deacylated tRNA in the E site and the peptidyl-tRNA in the P site, thus providing an empty A site for the next aminoacyl-tRNA. This process is called translocation, and is catalyzed by the elongation factor G (EF-G). The pre- and post-translocation states, separated by a high activation energy barrier of 80-90 kJ ([Schilling-Bartetzko et al., 1992]), have been both visualized with cryo-EM.

The elongation cycle stops at the appearance of a stop codon in the A site of the ribosome. This process is facilitated by codon specific release factors (RF): RF1 decodes the stop codons UAG and UAA, while RF2 decodes UGA and UAA. The protein is released and the ribosome is disassembled into subunits by the ribosome recycling factor (RRF), EF-G and IF3, preparing a new cycle of initiation ([Kisselev et al., 2003], [Kisselev and Buckingham, 2000]).

1.5. Trans-translation. The tmRNA Ribosome Rescue System

Ribosome stalling during translation is a serious problem for cell survival, and bacteria have developed rescue systems to ensure that the protein synthesis is not interrupted in order to maintain cell viability. Stalling usually occurs when when a codon is missing in the decoding center and ribosomes are trapped at the 3' end of a mRNA, and it leads to termination or arrest of elongation. Moreover, the presence of specific motifs in the polypeptide chain or depletion of a tRNA or a release factor can lead to stalling in the middle of a mRNA. In most cases, the ribosomes do not immediately dissociate when such events take place, since the complex is stabilized by interactions with the peptidyl-tRNA and the mRNA ([Keiler and Feaga, 2014]). Therefore, the bacterial rescue system is challenged to hydrolyse
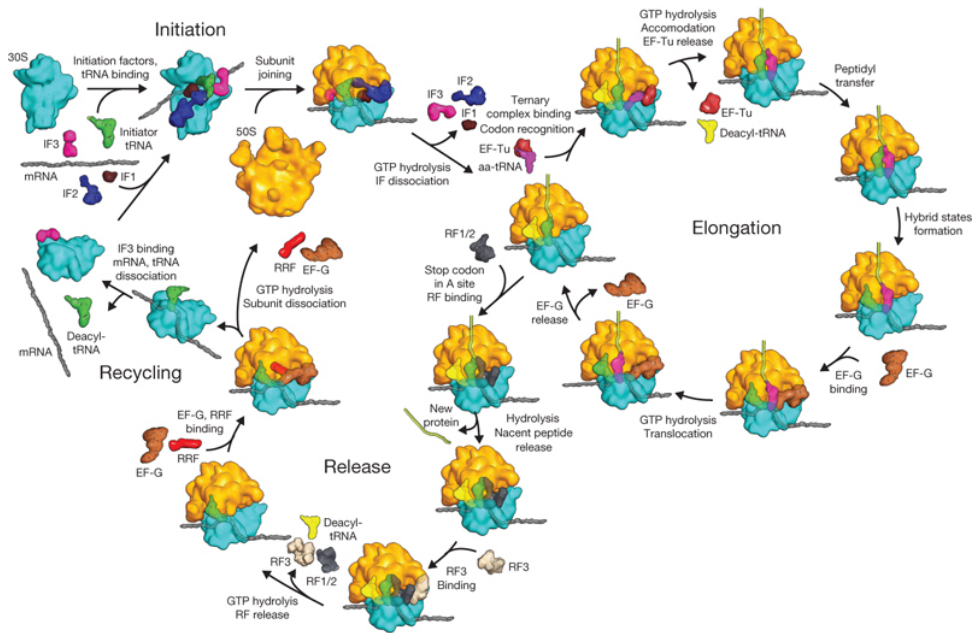
Figure 1.7.: An overview of translation in prokaryotes ([Schmeing and Ramakrishnan, 2009]).

peptidyl-tRNA of the defective ribosomes (non-stop ribosomes), but avoid hydrolysis of peptidyl-tRNA of the elongating ribosomes. This is achieved by trans-translation, using a specialized RNA molecule, transfer-messenger RNA (tmRNA), and a small protein SmpB.

The tmRNA, first described by [Keiler et al., 1996], and named according to the ability to function as both tRNA and mRNA, is a highly structured RNA with 5' and 3' ends forming a tRNA cloverleaf-like structure that resembles the Ala-tRNA ([Komine et al., 1994], [Gutmann et al., 2003]).

The first step of trans-translation is positioning of the alanyl-tmRNA, SmpB and EF-Tu complex, in the A site, since there is no codon in this position. The tRNA-like domain is accommodated so that the tRNA-like part is placed in the PTC center, and EF-Tu is released. The peptidyl transfer reaction follows, resulting in the transfer of the already formed polypeptide to the alanine attached to the tmRNA, and the polypeptide-tmRNA-SmpB is translocated to the P site. At this point, the reading frame of the tmRNA is located in the mRNA channel, and the initial mRNA is released and degraded. Because the tmRNA contains a stop codon, termination proceeds, the ribosome dissociates into subunits and the protein is released and degraded by proteases. ([Keiler, 2015], Fig. 1.8)
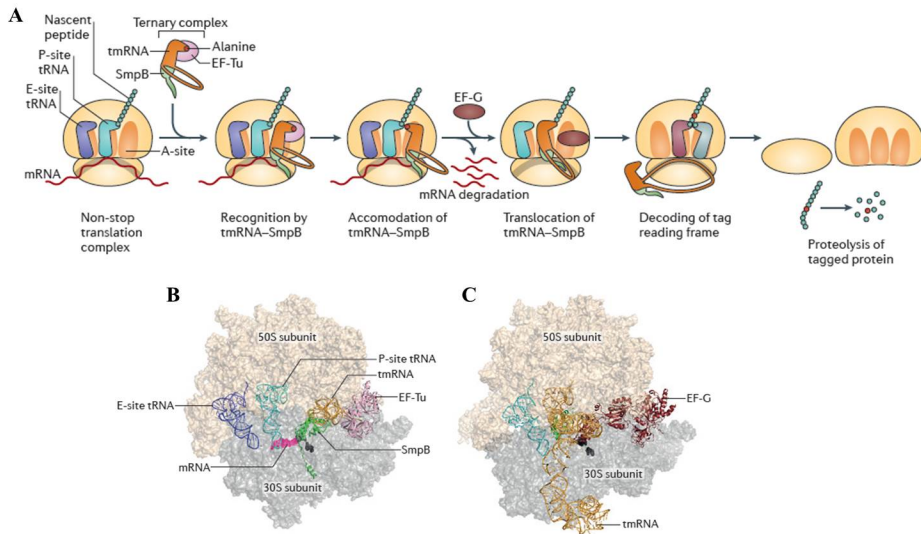
Figure 1.8.: (A) Mechanism of trans-translation (B) Cryo-EM structure of the tmRNA-SmpB complex in the A site of the ribosome (C) Cryo-EM structure of the post-translocation complex, with the tmRNA-SmpB in the P site of the ribosome ([Keiler, 2015])

1.6. Modes of Translation Initiation

1.6.1. 30S-binding Initiation

Translation initiation in bacteria has been studied in detail in the last decades. Studies ([Pon and Gualerzi, 1984], [Gualerzi and Pon, 1990], [Simonetti et al., 2008], [Fabbretti et al., 2007], [Dallas and Noller, 2001], [Antoun et al., 2006], [Julián et al., 2011]) put forward a general accepted textbook knowledge, the 30S-binding initiation mode, according to which initiation requires a pool of free 30S and 50S subunits to occur.

This mechanism, illustrated in Fig 1.9, postulates that the first initiation step in prokaryotes is binding of mRNA SD-sequence to the 16S rRNA anti-SD element of the 30S subunit ([Shine and Dalgarno, 1974]), together with the three initiation factors (IF1, IF2-GTP and IF3, described in Section 1.3) and the initiator tRNA, $\text{fMet} - \text{tRNA}^{\text{fMet}}$. This structure is called the 30S-initiation complex, and it has a high affinity for 50S subunits. As soon as a 50S subunit joins the complex, IF3 (the anti-association factor) is released, GTP is hydrolysed to GDP, and in a concerted manner, both IF2 and IF1 are then released. This mechanism leads to formation of the 70S initiation complex, which then enters the elongation phase of the translation process.
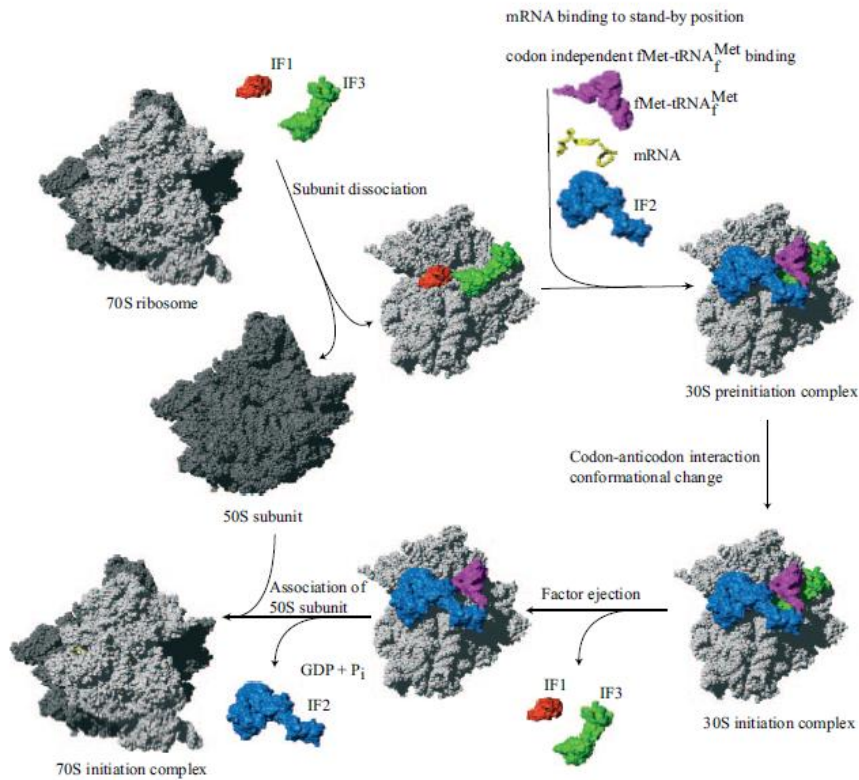
Figure 1.9.: The 30S-binding initiation mechanisms for translation of canonical mRNAs. ([Laursen et al., 2005])

1.6.2. Initiation with 70S Particles

In the current literature, cases of initiation with 70S ribosomes were already described, in addition to the 30S-binding type: translation of leaderless mRNA (lmRNA), translation of bi-cistronic mRNAs and translation by ribosomes with tethered subunits. These examples are detailed in the following sections.

1.6.2.1. Initiation of Leaderless mRNAs

In a leaderless mRNA (lmRNA), the start codon is either preceded by only a few nucleotides or it starts directly with a 5'-terminal AUG sequence. The lmRNA has no 5'-UTR and no SD-sequence. In many archeal prokaryotes, the majority of the mRNAs are leaderless ([Slupska et al., 2001], [Brenneis et al., 2007]), while in bacteria, the lmRNAs are widespread, but not dominant ([Zheng et al., 2011]), and their occurence has been correlated with extreme environmental conditions. In many *Streptomyces* species, antibiotic resistant genes are leaderless. In the *E. coli* genome, three lmRNAs have been identified:

viz. racR, *ymfK* and *rhlB* ([Romero et al., 2014]). It was suggested ([Moll et al., 2002]) that the lmRNAs are remnants of ancestral mRNAs, considering that they can be translated by both eukaryotic and prokaryotic systems, and are found in high abundance in mammalian mitochondria ([Christian and Spremulli, 2010]).

It was commonly believed that the efficiency of translation depends on the primary and secondary structure of the initiation regions of the mRNA. However, since the lmRNA lacks these structures, a new mechanism has been proposed. It has been shown that in presence of an initiator tRNA, 70S ribosomes have an approximately 10 fold higher affinity for the 5'-AUG of the lmRNA than 30S subunits, since immediate coding region downstream of the start codon of lmRNA can hardly provide sufficient interactions with the 30S subunit to ensure the formation of a thermodynamically stable binary complex ([Grill et al., 2000]). This observation lead to the conclusion that initiation of lmRNAs is performed by both 30S subunits, and by full 70S ribosomes, without dissociation into subunits. Moreover, Ueda et. al demonstrated that in an *in vitro* transcription-translation kit, and excess of fMet-tRNA, initiation of lmRNAs by 70S ribosomes can occur in absence of initiation factors ([Udagawa et al., 2004]).

The initiation of lmRNA via the 30S initiation complex is dependent on the concentration of initiation factors: high concentrations of IF2 stimulate translation, while IF3 has an inhibitory effect ([Grill et al., 2001]).

In the presence of kasugamycin, *in vivo* translation of canonical mRNAs stops, while translation of lmRNA is not inhibited ([Kaberdina et al., 2009]). In these conditions, stable 61S ribosomes are accumulated, which are able to translate selectively lmRNAs, both *in vitro* and in *in vivo*. The 61S ribosomal particles lack more than six proteins of the small ribosomal subunit, including the proteins S1, S2, S6, S12, S18 and S21. The ribosomal protein S1 is functionally important for initiation of canonical mRNAs, since it facilitates mRNA binding, and protein S21 stimulates the SD-aSD interaction. These facts can explain why the canonical mRNAs can not be translated by the protein-depleted ribosomes. Since the missing proteins were evolutionary added after the separation of the kingdoms ([Mears et al., 2002]), it has been suggested that the 61S particles are an ancient form of proto-ribosomes.

1.6.2.2. 70S Scanning Initiation

In bacteria, genes are transcribed from transcriptional units that contain several related genes, generating polycistronic mRNA. In *E. coli*, mRNAs are formed of 4 cistrons, with separate initiation sites (SD sequences and AUG initiation codons). The downstream cistron can be also translated by re-initiation, so that the 70S ribosome does not dissociate into subunits after translation of the previous cistron, but rather continues directly to the next cistron. The 70S-scanning initiation mode was postulated in 1966 ([Yanofsky and Ito, 1966]), and tested in several studies since ([Adhin and van Duin, 1990], [Petersen et al., 1976]), but the in-depth mechanism has been only recently investigated, by Yamamoto et. al ([Yamamoto et al., 2016]).

The results show that in an *in vitro* transcription-translation kit, polycistronic mRNAs are also translated by full 70S ribosomes, without dissociation into subunits after translation of the first cistron. The 70S scans the sequence surrounding the termination codon of the first cistron until it reaches the second Shine-Dalgarno sequence. This mechanism of initiation with 70S ribosomes has been proved to be frequent in *E. coli*, at least 50% of the initiation events using this mechanism.

Scanning is triggered by fMet-tRNA and does not require initiation factors, the SD sequence of the
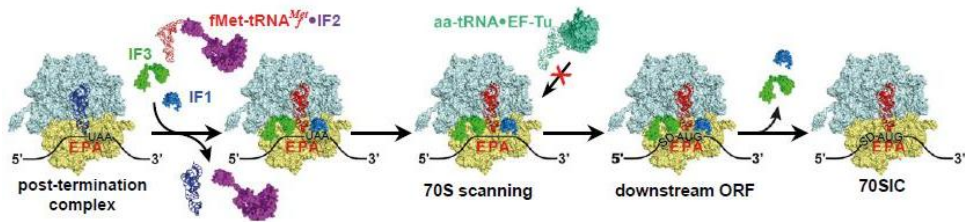
Figure 1.10.: 70S-scanning initiation mechanism ([Yamamoto et al., 2016])

second cistron is enough as a recognition element of re-initiation. IF3 is essential for the 70S-scanning mechanism, and IF1 was demonstrated to be highly stimulating (Fig. 1.10)

1.6.2.3. Protein Synthesis by Ribosomes with Tethered Subunits

A ribosome with covalently linked subunits has been recently engineered ([Orelle et al., 2015]), by adding an RNA linker between the 16S rRNA and 23S rRNA (Fig. 1.11), and named Ribo-T (Fig. 1.11). The linker, binding the H101 of the large subunit with the helix h44 of the small subunit, was designed long enough to allow the 10 Å ratcheting of the subunits during protein synthesis.
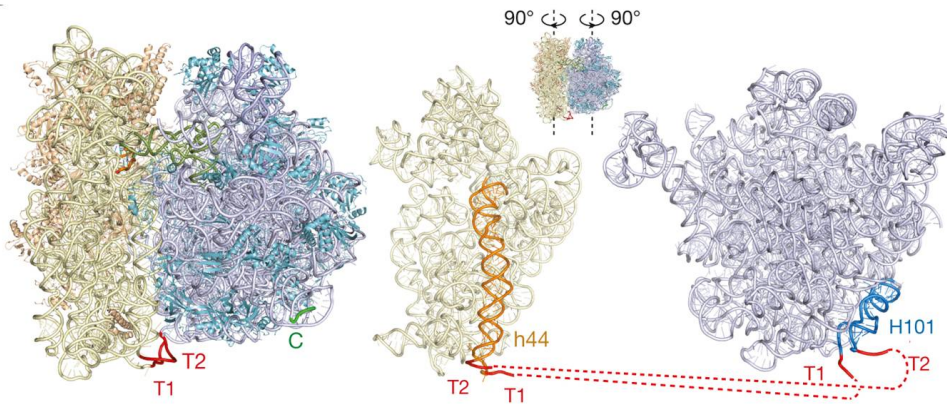
Figure 1.11.: The location of the tethers in the *E. coli* ribosome (T1 and T2) ([Orelle et al., 2015])

The gene encoding the mutant rRNA was introduced in a plasmid carrying the wild-type rrnB rRNA operon under the control of the native constitutive promoter P1P2, which was then transformed in a Squires strain, lacking chromosomal rRNA. Therefore, all the ribosomes contained in the end exclusively the chimera RNA 16S-23S, confirmed by agarose gel electrophoresis. The Ribo-T ribosomes are capable of successfully synthesizing proteins both *in vitro* and *in vivo*. This result contradicts the current knowledge that translation requires reversible exchange of subunits, since dissociation can not occur in this case.

2

Evidence of 70S Initiation of Canonical mRNAs. Motivation of this Study.

2.1. Why initiation with 70S?

Previous studies ([Katranidis et al., 2009], [Uemura et al., 2008]) show that fluorescently labeled 70S ribosomes, biotinylated at one subunit (50S or 30S, respectively), and tethered specifically on a modified microscopy glass slide, are able to translate canonical mRNAs to produce GFP in an *in vitro* transcription-translation system. Translation and correct folding of GFP was monitored in real time, using a TIRF microscope, so that colocalization of blue and red fluorescence was counted as a successful translation event. The studies show that approximately 10-15% of the 70S ribosomes produced a bound mature GFP.

According to the previously described hypothesis (Section 1.6.1), the tethered 70S ribosomes dissociate during the initiation step. Considering that the concentration of the ribosomes on a glass slide covered with 50 μL reaction mix is lower than 1 fM, dissociation into subunits would lead to diffusion of the non tethered subunit in the solution (Fig. 2.1). However, this events would not lead to successful translation of GFP, since the probability that the subunits form a 70S initiation complex after dissociation is extremely low after they have diffused in the solution.

Our hypothesis is that in the experiments mentioned above, GFPem was translated by full 70S ribosomes, without dissociation into subunits.

2.2. Why single molecule studies?

In single molecule studies, the molecular properties are measured one particle at a time, so that distributions of molecular properties are directly evaluated, in contrast to the ensemble experiments, where

Figure 2.1.: Motivation of this study. GFP production by tethered ribosomes can not be explained by the 30S-binding initiation (A). We assume that translation took place with full 70S ribosomes, without dissociation into subunits (B).

only the average effect of the sample is measured. Events that would be otherwise averaged in ensemble measurements can be detected at single molecule level. As a result, single molecule techniques can directly characterize short and rare events, as well as parallel reaction pathways, all of which are not easily assayed in heterogeneous and asynchronous ensembles.

Indeed, it is expected that translation initiation occurs via several pathways, so that single molecule studies offer the possibility to identify and quantify these events. In the particular case of this study, the challenge is to distinguish after translation, the molecules of GFP bound to a labeled ribosome from the GFP bound to a non labeled ribosome. This can be achieved exclusively with single molecule methods, since in ensemble experiments only an average fluorescence signal of the sample can be measured.

Part II.

Materials and Methods

3

Materials and Buffers

3.1. Chemicals

If not stated otherwise, all chemicals used in the present study were of analytical grade and purchased from Sigma Aldrich Co., St. Louis, Missouri, USA.

From Sigma Aldrich Co., St. Louis, Missouri, USA:

- sucrose BioUltra, for molecular biology, $\geqslant 99\%$ (HPLC)

From Rapp polymere GmbH, Germany:

- PEG-NHS ester
- biotin-PEG-NHS ester

From AppliChem GmbH, Darmstadt, Germany:

- Tris-HCl: Tris Hydrochloride, buffer grade
- Tryptone
- Yeast Extract
- Agar for Molecular Biology

From MP Biomedicals, South Chilicothe Rd, Aurora, USA

- EDTA: ethylenediamine tetraacetic acid

From ROTH GmbH, Karlsruhe, Germany:

- NaOH: sodium hydroxyde $\geqslant 99\%$ p.a.

- Tween20
- Glycerin $\geqslant 99.5\%$ p.a., water-free

From Merck Millipore:

- NH_4Cl: ammonium chloride p.a.
- Tween20

From Thermo Fischer Scientific (Waltham, MA, USA)

- Agarose UltraPure for gel electrophoresis

3.2. Consumables

- Sekusept Aktiv (ECOLAB Healthcare, Monheim am Rhein, Germany)
- RNase ZAP (Thermo Fischer Scientific, Waltham, MA, USA)
- SUPERase In RNase Inhibitor, 20 U/μL (Thermo Fischer Scientific, Waltham, MA, USA)
- cOmplete Protease Inhibitor Tablets, EDTA Free (Roche, Basel, Switzerland)
- RNAse-free pipette tips: Biozym Scientific GmBH (Hessisch Oldendorf, Germany)
- RNase-free eppendorf tubes
- Roti-PVDF Membrane, pore size 0.2 (Carl-Roth, Karlsruhe, Germany)
- RNA Loading Dye, 2x (New England Biolabs, Ipswich, MA, USA)
- Quartz Cuvette, 3 mm path length (105.251-QS, Hellma, Mühlheim, Germany)
- High precision glass slides (170 $\pm$ 5 μm, No. 1.5H, Marienfeld Superior, Germany)
- TetraSpeck Fluorescent Microsphere Standards, 0.1 μm (Thermo Fischer Scientific, Waltham, MA, USA)

3.3. Fluorescent Dyes

From AttoTec GMbH, Siegen, Germany:

- Atto488 NHS ester

From GE Healthcare Life Sciences, UK:

- Cy5 NHS ester

3.4. Vectors and Oligoucleotides

From Invitrogen, Carlsbad, California, USA

- pRSET

From Eurofins Genomics, Ebersberg, Germany: Functionalized oligonucleotides:

- 50S-Cy5: (5') GAGGCCGAGAAGTG-Cy5 (3')
- 30S-Bio: (5') GGGAGATCAGGATATAAAG-bio (3')
- 30S-Cy3: (5') GGGAGATCAGGATATA-Cy3 (3')

3.5. Kits and Enzymes

- QIAprep Spin Miniprep Kit (Qiagen, Hilden Germany)
- PURE in vitro transcription-translation system (New England Biolabs, Ipswich, MA, USA)
- WesternDot 625, Western Blot Kit (Thermo Fischer Scientific, Waltham, MA, USA)
- Restriction Enzymes were purchased as "Fast Digest" from Fermentas, St. Leon-Rot, Germany: Hind III
- Antarctic Phosphatase (New England Biolabs, Ipswich, MA, USA)
- Protocatechuate 3,4-dioxygenase from the *Pseudomonas* species, molecular weight: 700 kDa (Sigma Aldrich Co., St. Louis, Missouri, USA.)

3.6. Instruments

- Ultracentrifuge Optima L-70K (Beckman, Krefeld, Germany)
- Ultracentrifuge Optima XPN-80 (Beckman, Krefeld, Germany)
- Ultracentrifuge Optima MAX-XP (Beckman, Krefeld, Germany)
- Centrifuge Avanti J-20XP (Beckman, Krefeld, Germany)
- Centrifuge 5417 R (Eppendorf, Wesseling-Berzdorf, Germany)
- Centrifuge Allegra X-15R (Beckman, Krefeld, Germany)
- NanoDrop 2000 UV-VIS spectrophotomeret (Thermo Fisher Scientific, Waltham, MA)
- Semi Dry Blotter Unit Model V20-SDB, 20 x 20 cm (SCIE-PLAS, Cambridge, UK)
- Biocomp Piston Gradient Fractionator Model 152 (Science Services, München, Germany)
    1. Gradient Master Model 108 (Science Services, München, Germany)
    2. Fraction Collector Model 2110 (BIO RAD, München, Germany)

3. UV Monitor Model EM-1, dual-wavelength detector for liquid chromatography (BIO RAD München, Germany)

- Cell disruptor

- Autoclave: Fedegari FVA3A/A1 Automated Saturated Steam Sterilizer (Fedegari Autoklaven AG, Bedano, Switzerland)

- Glovebox (Weidner, Hardegsen, Germany)

- Lyophilizer: Christ Alpha 1-2 LD Plus Freeze Dryer (Shrewsbury, UK)

- Gel Imaging System: ChemiDoc MP System (BIO RAD, München, Germany)

- Wide-field microscope

  1. Microscope body: Olympus IX-81 (Olympus, Hamburg, Germany)

  2. Objective: Olympus UApoN, 100x, NA=1.49

  3. Lasers (Coherent Inc., USA)

     a) Red laser: Obis 637-140

     b) Blue laser: Sapphire 488-200

  4. Dual-band dichroic mirror, ZT488/640rpc (Chroma Technology Corp, Bellows Falls, USA)

  5. Dual-band emission filter, ZET488/640m (Chroma Technology Corp, Bellows Falls, USA)

  6. Image-splitter Optosplit II (Cairn Research Ltd, Faversham, UK)

  7. EMCCD camera (Andor iXon Ultra 888, Andor Technology Ltd., Belfast, UK)

- Microtime 200 (Picoquant, Berlin, Germany)

  1. Microscope body: Olympus IX-81 (Olympus, Hamburg, Germany)

  2. Objective: UPLSAPO 60x, PlanApochromat, N.A. 1.2, W.D. 0.28, F.N. 26.5, water immersion, cover glass tickness 0.13-0-21, (400 - 900) nm (Olympus, Hamburg, Germany)

  3. Laser Driver: PDL828 "Sepia-II", Computer Controlled Multi-Channel Picosecond Pulsed Diode Laser Driver (PicoQuant GmbH, Berlin, Germany)

  4. TCSPC-Acquisition unit: "HydraHarp-400", Picosecond Histogram Accumulating Real-Time Processor, Time-Correlated Single Photon Counting System with USB interface (PicoQuant GmbH, Berlin, Germany).

  5. Avalanche Photo Detectors - APD:

     a) 2 x Photon Counting Module, SPCM-CD3307M and SPCM-AGR-14 (Perkin Elmer, Wood Bridge, Ontario, Canada).

     b) 2 x Single Photon Counting Module, L-SPAD, VLoK silicon avalanche photodiode (Laser Components, Olching, Germany) with quenching electronics (PicoQuant GmbH, Berlin, Germany).

  6. Laser Heads (PicoQuant, Berlin, Germany):

a) Red laser: LDH-D-C 640B

b) Blue laser: LDH-D-C 485B

7. FCU-II Fiber coupling unit (PicoQuant, Berlin, Germany).

8. 50/50 Beam Splitter (Linos Photonics, Göttingen, Germany).

9. Polarizing Beam Splitter Cube (Linos Photonics, Göttingen, Germany).

10. Pinhole: 30, 75 μm.

11. Major dichroic: 470/640 nm fitc/Cy5pc (AHF, Tübingen, Germany).

12. Minor dichroic: 600dcr (Chroma Technology, Bellows Falls, VT, USA).

13. Emission filters:

a) Red: HQ 690/70M 202814 (Chroma Technology, Bellows Falls, VT, USA).

b) Blue: XF 3003 520DF40 (Omega Optical Inc., Battleboro, VT, USA)

- UV 2401 PC Spectrophotometer (Shimadzu, Duisburg, Germany).

- Spectrofluorophotometer QM-7 (Photon Technology International, Birmingham, NT, USA).

- pH-meter S20-SevenEasy mit InLab Micro Electrode (Mettler Toledo, Giessen, Germany).

- "Zepto" plasma cleaner (Plasma Surface Technology, Diener Electronic GmbH, Ebhausen, Germany).

3.7. Bacterial Strains

3.7.1. General Considerations

When purifying ribosomes from bacteria, one has to keep in mind that a high ribonuclease activity of the strain itself leads to the degradation of the ribosomal RNA. The comparison between the quality of the rRNA of the ribosomes from a strain with high and a low RNase activity is clearly seen by agarose gel electrophoresis. The degraded RNA is detected as a smear (Fig. 3.1, A), while intact rRNA from the RNase deficient strains shows clear RNA bands (Fig. 3.1, B). Therefore, the choice of a strain with low RNase activity is essential.

Moreover, the cell cultures must be harvested in the early exponential phase, usually at an OD_{600} of 0.7, the stage in which the ribosomes are highly active. Before harvesting, the cultures were kept on ice for 1h in order to allow the run-off of the ribosomes, and avoid the formation of polysomes.

After harvesting, the cells were frozen in liquid nitrogen and stored at $-80°C$ until further use.

3.7.2. The CAN 20/12-E Strain

The CAN 20/12-E strain, provided by Murray Deutscher's laboratory (University of Miami Miller School of Medicine), is a K-12 derivative lacking the exoribonucleases RNase BN, RNase II, RNase D,
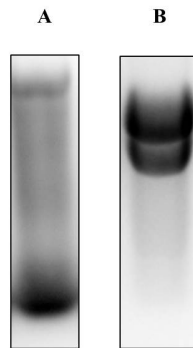
Figure 3.1.: Agarose gel electrophoresis of ribosomes prepared from a strain containing RNases: BL21 (A) and an RNase deficient strain: CAN20/12-E (B)

and RNase I ([Zaniewski et al., 1984]). The deletion of these RNases has no influence on cell growth or RNA synthesis.

The cultures have a regular growth curve, with a doubling time of 35 min at 37°C and shaking at 120 rpm, in DYT supplemented with Tet10. (Fig. 3.2)
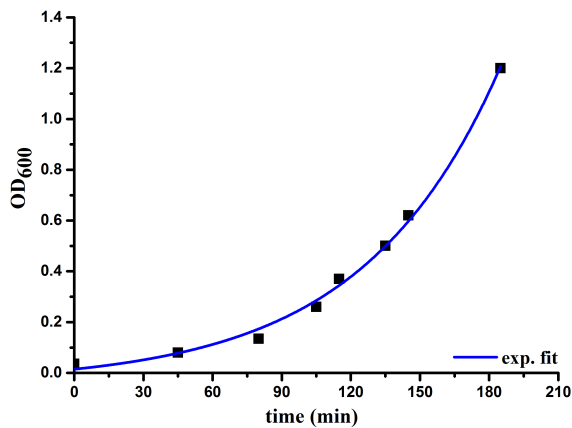
Figure 3.2.: Growth curve of the CAN 20/12-E strain, at 37°C, and shaking at 125 rpm.

3.7.3. The ZS-22 Strain

The ZS-22 strain, provided by Prof. Dr. Knud Nierhaus (Charité - Universitätsmedizin Berlin), was constructed by Dorywalska et. al ([Dorywalska et al., 2005]) in order to obtain a homogeneous sample of site-specifically labeled ribosomes.

In *E. coli*, the ribosomal RNAs are transcribed from seven operons. The repetitive nature of the rRNA genes impairs the introduction of mutations in the ribosomal RNA for a potential labeling strategy. Homogenous mutant ribosomes can be made by in vitro reconstitution, but the drawback of this technique is that the activity of the reconstituted ribosomes is usually low. Therefore, Dorywalska et al. used a Squires strain, in which all seven wild-type chromosomal rRNA copies were deleted. The rRNAs, engineered with helical extensions for oligonucleotide binding, were expressed by the plasmid PKK3535 ([Brosius et al., 1981], Fig. 3.3), under the control of the native constitutive promoter P1P2. The ZS-22 strain has the following modifications introduced on the PKK3535 plasmid:

- 50S subunit: hairpin 22 at helix H101 of the 23S rRNA

- 30S subunit: hairpin 68 at helix h10 of the 16S rRNA
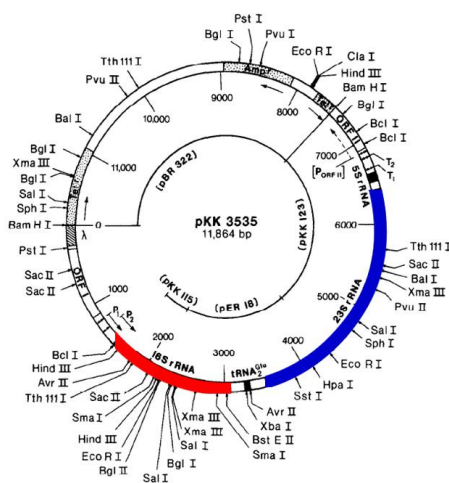
Figure 3.3.: The PKK3535 plasmid, containing rrnB operon, in which the 16S rRNA and 23S rRNA are marked in red and blue, respectively (adapted from [Brosius et al., 1981])

The engineered loops are presented in Fig. 8.1 and Fig. 8.2, in the results section.

Depending on the functionality that is needed to be introduced on the ribosome, several oligonucleotides were used in previous studies: fluorescently labeled oligonucleotides ([Aitken and Puglisi, 2010], [Tsai et al., 2012]) or both biotinylated and fluorescently labeled oligonucleotides (Uemura et al. [2008]).

The ZS-22 strain has a doubling time of 70 minutes, when grown in 2 L glass flasks filled with 300 mL DYT supplemented with Amp50, at 37°C, and shaking at 165 rpm. (Fig. 3.4). The slow growth compared to a usual *E. coli* strain is explained by the low copy of the rRNAs([Asai et al., 1999]).
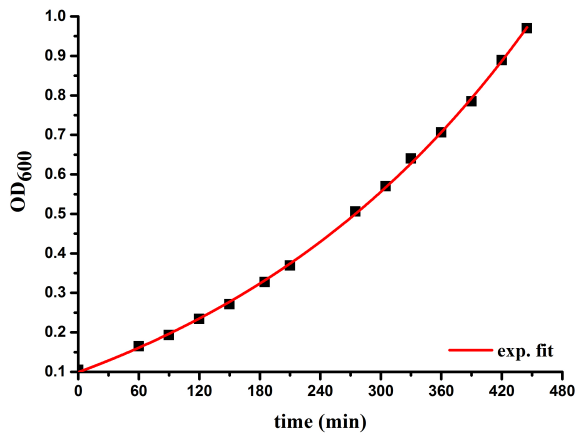
Figure 3.4.: Growth curve of the ZS-22 strain, at 37°C, and shaking at 165 rpm

3.8. Buffers

3.8.1. Purification of Ribosomes

Tico	Hepes, pH=7.6	20 mM
	$Mg(OAc)_2$	10 mM
	NH_4OAc	30 mM
	β-mercaptoethanol	4 mM
A30	Tris-HCl, pH=7.8	10 mM
	$MgCl_2$	10 mM
	NH_4Cl	30 mM
	EDTA	0.1 mM
	β-mercaptoethanol	7 mM
Glycerin solution C	A30	80%
	Glycerin	20% (v/v)
Dissociation Buffer	Hepes, pH=7.6	20 mM
	$Mg(OAc)_2$	0.97 mM
	NH_4OAc	200 mM
	β-mercaptoethanol	4 mM
Reassociation Buffer	Hepes, pH=7.6	20 mM
	KCl	30 mM
	$MgCl_2$	20 mM
	β-mercaptoethanol	4 mM

3.8.2. Labeling Buffers

NHS labeling	Hepes, pH=7.6	20 mM
	MgAc$_2$	10 mM
	NH$_4$OAc	30 mM

Tris-polymix	Tris-OAc, pH=7.5	50 mM
	KCl	100 mM
	NH$_4$OAc	5 mM
	Ca(OAc)$_2$	0.5 mM
	Mg(OAc)$_2$	10 mM
	β-mercaptoethanol	6 mM
	putrescine	5 mM
	spermidine	1 mM

The putrescine, spermidine and β-mercaptoethanol were added to the filtered and autoclaved buffer immediately before the experiment.

3.8.3. Microbiological Media

DYT	Tryptone	16%
	Yeast extract	10%
	NaCl	5%

The components were dissolved and the medium was autoclaved before use.

Agar plates	DYT	
	Agar	2.5% (w/v)

The mixture was autoclaved, mixed with a magnetic stirrer and when the temperature reached 30°C, the antibiotics were added.

Bacteria storage media	DYT	
	Glycerol	40% (v/v)

The mixture of the components was autoclaved, and cooled at room temperature. To 1 mL of bacteria, 1 mL storage media was added. The mixture was homogenized and stored at -80°C

3.8.4. Biotinylation

Bicine, pH=8.3	10 mM

The bicine buffer was slightly warmed and 12 mg biotin were added to 100 mL warm buffer.

3.8.5. Agarose Gel Electrophoresis

TAE Buffer	Tris-OAc, pH=7.6	40 mM
	AcOH	20 mM
	EDTA	1 mM
DNA Sample Buffer	TAE	1x
	Sucrose	40%
	Bromophenol blue	0.25%

3.8.6. Western Blot

Polyacrylamide (PAA) Gels	Stacking Gel (5%)	Separating Gel (15%)
dH$_2$O (mL)	2.4	5.7
30% Acrylamide/Bis (mL)	5	1.7
1.5M Tris-HCl pH 8.8/0.4% SDS (mL)	2.5	-
0.5M Tris-HCl pH 6.8/0.4% SDS (mL)	-	2.5
10% APS (μL)	50	50
TEMED (μL)	5	10
Total Volume (mL)	10	10

3.8.7. Competent Cells

SOB	Yeast Extract	0.5%
	Tryptone	2%
	NaCl	10 mM
	KCl	2.5 mM
	MgSO$_4$	20 mM

The components were dissolved, the buffer was filtered and autoclaved before using.

RF1 Buffer	RbCl	100 mM
pH=5.8	MnCl$_2$	50 mM
(acetic acid)	CaCl$_2$	10 mM
	KOAc	30 mM
	Glycerol	15%

Mix the components, adjust the pH to 5.8 and filter sterilize through a 0.22(μm) filter. Store at 4°C

RF2 Buffer	MOPS	10 mM
pH=6.8	RbCl	10 mM
(NaOH 0.1M)	CaCl$_2$	75 mM
	Glycerol	15%

Mix the components, adjust the pH to 6.8 and filter sterilize through a 0.22(μm) filter. Store at 4°C

3.8.8. Single Molecule Experiments

| Piranha Solution H_2O_2 | 1/3 (v/v) |
| H_2SO_4 | 2/3 (v/v) |

The solution should be always prepared by adding hydrogen peroxide in the sulfuric acid slowly, never in reverse.

| TP50 | Tris-OAc, pH=7.5 | 50 mM |
| | KCl | 50 mM |

4

Methods

4.1. Analytical Methods

4.1.1. Concentration Measurements for Ribosomal Particles

The concentration of the ribosomal particles was determined spectrophotometrically, with a NanoDrop by measuring the absorption of RNA at 260 nm, and using the following molar exctinction coefficients:

- 70S: 4.2 x 10^7 M^{-1} cm^{-1}

- 30S: 1.4 x 10^7 M^{-1} cm^{-1}

- 50S: 2.8 x 10^7 M^{-1} cm^{-1}

4.1.2. Agarose Gel Electrophoresis of DNA

Large DNA molecules migrate slower than the smaller ones in the presence of a electric field. Therefore, agarose gel electrophoresis is widely used in molecular biology to separate DNA molecules of different sizes. The gel was prepared by adding agarose in TAE buffer, usually 1% - 2% agarose (w/v), and heating the mixture up to the near-boiling temperature until it was completely dissolved. The agarose concentration was chosen according to the size of the DNA fragments that were separated (Table 4.1). The greater the agarose concentration, the smaller the pores created in the gel matrix, and the more difficult it is for large DNA fragments to move through the matrix.

The melted agarose was then cooled sufficiently before adding the stain and casting the gel. As a fluorescent stain, GelRed was used, which is an alternative for Ethidium Bromide, with better stability, higher sensitivity and less toxic effects. After the samples were loaded into the lanes, electrophoresis

Table 4.1.: Resolution of Linear DNA on Agarose Gels

Recommended % agarose	DNA size range (bp)
0.5	1000 - 30 000
0.7	800 - 12 000
1	500 - 10 000
1.2	400 - 7000
1.5	200 - 3000
2	50 - 2000

was performed, using a voltage of 200 V. The visualization of the bands was made using UV trans-illumination. The bands were cut from the gel, and extracted using commercially available kits

4.1.3. Agarose Gel Electrophoresis of RNA

The RNA integrity of a sample containing ribosomal particles can be assessed by non-denaturing agarose gel electrophoresis. Because the rRNA molecules are negatively charged, they will migrate towards the anode in the presence of an electric field. The migration speed is determined by the size of the particles.

The agarose gel electrophoresis of RNA is similar to the one of DNA. Additionally, the procedure has to be made in RNase free conditions. Usually, special running chambers, cleaned with RNase Zap, were used only for RNA work. Optimal separation is obtained when using a 2% agarose gel, and a running voltage of 180 V. Buffers must be fresh and cold, and the electrophoresis should be performed in the cold room, in order to avoid the RNA degradation.

4.2. Methods of Microbiology and Molecular Genetics

4.2.1. Growing and Storing *E.coli*

In all the experiments, the media used for growing E. coli was DYT (Section 3.8.3). To select for strains that contain specific plasmids, the appropriate antibiotic was added to the medium, in the following concentrations (unless stated otherwise):

- Ampicillin: 100 μg/mL (Amp100)

- Chloramphenicol: 10 μg/mL (Cm10)

- Tetracyclin: 10 μg/mL (Tet10). Tetracyclin is easily degraded by light. The stock solution and agar plates should be kept in the dark.

For long term storage, glycerol stocks of *E. coli* were prepared. Single colonies were picked and subsequently grown overnight in 5 mL DYT supplemented with antibiotic. To prepare a glycerol stock, 500 μL of the overnight culture were mixed with 500 μL DYT containing 80% Glycerol, so that the final concentration of Glycerol was 40%. After mixing, the stock was stored in sterile cryotubes at $-80°$C.

4.2.2. Preparation of Chemically Competent Bacteria

Bacterial cultures with a starting OD_{600} of 0.1 were prepared in SOB medium, from an overnight culture, and grown at $37°C$ and shaking at 120 rpm, until an OD_{600} of 0.3-0.4, then placed on ice for 30 min.

From this point on, the workplaces were particularly cleaned in order to avoid a possible contamination. The cells, buffers and centrifuges were kept at $4°C$ throughout the procedure. When possible, the techniques were performed in the cold room.

After cooling on ice, the bacteria were harvested at SX4750/3000 rpm/15 min (higher centrifugation speeds should be avoided, to avoid the damaging of the cells) and gently resuspended in 30 mL RF1 buffer by pipetting without forming air bubbles. After precisely 15 min, the cells were harvested by centrifugation (SX4750/3000 rpm/10 min) and resuspended gently in 10 mL RF2 buffer. The suspension was divided in aliquots of 100 μL, in sterile Eppendorf tubes, and after exactly 15 min, the cells were frozen in liquid nitrogen and stored at $-80°C$.

4.2.3. Transformation of Bacteria

A widely used method to introduce DNA in a bacterial cell (transformation) is by heat-shock. Chemically competent bacteria were slowly thawed on ice, mixed with 5 ng plasmid DNA, and incubated on ice for 15 min. The next step was the heat shock, at $42°C$, for 90 s, at which point the lipids of the bacterial membrane are becoming more fluid, and the DNA can be uptaken inside the cell. Then, the cells were placed on ice, for 120 s, when the cells come back to the initial size. Immediately after the heat-shock, DYT without antibiotics was added, and the cells were grown for 45 min at $37°C$, on a rotator wheel. The bacterial suspension was then harvested by a short centrifugation (Eppendorf/14000 rpm/1 min), 100 μL DYT was added and the dissolved pellet was plated on a DYT plate supplemented with the corresponding antibiotic(s).

4.2.4. Plasmid Isolation

Plasmids were isolated using kits purchased from Macherey-Nagel or Quiagen, according to the protocol provided by the manufacturer.

4.2.4.1. Minipreps

1. A 5 mL overnight culture of transformed bacteria was prepared, with the corresponding antibiotic

2. 3 mL culture was centrifuged using the Eppendorf centrifuge: 14000 rpm/1 min

3. The pellet was resuspended in 250 μL RESUSPENSION BUFFER (25 mM Tris-HCl, 50 mM glucose, 10 mM EDTA, pH 8)

4. The cells were lysed by adding 250 μL LYSIS BUFFER (1%) SDS, 0.2 N NaOH) and gently mixing for 5 min at room temperature.

5. The mixture was neutralized by adding cold 300 μL NEUTRALIZATION BUFFER, and mixing gently.

6. The sample was centrifuged at 14000 rpm/1 min.

7. The supernatant was collected and loaded in an anion-exchange column. The column was then centrifuged at 14000 rpm/1 min

8. The flow-through was discarded and the column was dried by centrifugation for 2 min. This step ensures that the ethanol is completely evaporated, since traces of ethanol can inhibit enzymatic reactions and transformations.

9. 100 μL ELUTION BUFFER (10 mM Tris-HCl, pH 8.5) was loaded onto the column, incubated for 1 min at room temperature and centrifuged at 14000 rpm/1 min.

10. The concentration of the miniprep was measured spectrophotometrically, using the Nanodrop, and stored at $-20°$C.

4.2.4.2. Midipreps

1. A 500 mL culture of transformed bacteria was prepared, using the corresponding antibiotic, and the cells were harvested by centrifugation: JLA 8.1000/6000 rpm/20 min/4°C

2. The pellet was resuspended in 8 mL RESUSPENSION BUFFER

3. The cells were lysed by addition of 8 mL LYSIS BUFFER, mixed gently and incubated at room temperature for 5 min

4. The mixture was neutralized by addition of 8 mL NEUTRALIZATION BUFFER, and mixing gently

5. The sample was centrifuged at SX4750A/4750 rpm/20 min/

6. The column was equilibrated with 12 mL EQUILIBRATION BUFFER

7. The supernatant was passed through the column by gravity flow

8. The column was washed with 5 mL EQUILIBRATION BUFFER, and afterwards, with 8 mL WASH BUFFER

9. DNA was eluted by addition of 5 mL of ELUTION BUFFER

10. DNA was precipitated by addition of 0.7 volumes cold isopropanol, and gently mixed and incubated for 2 min at room temperature.

11. The mixture was injected through a finalizer for DNA binding

12. The finalizer was washed with 2 mL cold 70% (v/v) ethanol, and dried 20 times

13. The DNA was eluted by passing 200 μL ELUTION BUFFER through the finalizer. This step was repeated twice, so that two samples were collected.

14. The concentration of the DNA was determined spectrophotometrically with the Nanodrop, and the samples were stored at -20°C

4.2.5. Linearization of Plasmids with Endonucleases

Linearization of the plasmid DNA was carried out by digestion with restriction endonucleases, using FastDigest enzymes, according to the manufacturer's instructions. Concerning the enzymatic activity, 1 μL of Fast Digest enzyme cleaves 1 μg of substrate DNA in 5 or 15 min in FastDigest buffer, at 37°C. Because of the short incubation times, the enzymes have no star activty.

The reactions were performed in triplicates of 10 μL, and contained 1 μg DNA, 1 μL of FastDigest enzyme and the FastDigest Buffer (10x) provided by the manufacturer. The mix was incubated for 15 min at 37°C.

After the linearization reaction, the 5' and 3' ends were dephosphorylated in order to prevent the re-circularization of the vector. Therefore, the mix was incubated with 1 μL Antarctic Phosphatase, in the recommended buffer, at 37°C for 30 min. The reaction was stopped by heat-inactivation of the enzyme at 37°C for 5 min.

The correct linearization of the vector was confirmed with Agarose Gel Electrophoresis, as described in Section 4.1.2. As a control, a sample containing the circular vector was loaded in the same gel. Typically, the uncut plasmids appear to migrate more rapidly than the same plasmids when linearized.

4.3. Purification of Ribosomes and Ribosomal Particles

4.3.1. General Considerations for Working with Ribosomes

The protocol for purification of ribosomal particles was adapted from previously described methods ([Bommer et al., 1997])

The ion composition of the buffers was kept close to the *in vivo* conditions, to preserve the activity of the ribosomes. The A30 buffer used in the first step of the purification contains a low amount of EDTA, which chelates the iron ions, in order to avoid the metal-induced RNA cleaving.

Throughout the procedure, special attention was given to preventing RNase contamination. In this respect:

- All working surfaces, plasticware and glassware were treated with RNaseZAP.

- All bufers were filter sterilized, autoclaved and stored at 4°C.

- The reducing agents (e.g. β-mercaptoethanol) were added to buffers immediately before use.

- RNase inhibitors were added to all buffers immediately before use: 1 μL/1 mL buffer.

- Protease inhibitors were added to all buffers immediately before use: 1 tablet/50 mL bufer.

- Only RNase-free pipette tips, eppendorf tubes and pipettes were used.

- The procedures were carried at 4°C, in the cold room.

- The centrifuges were prechilled before use.

- Gloves were changed frequently throughout the procedure.

- The centrifuge tubes, magnetic stirrers and glass spatulas were cleaned with Sekusept aktiv solution for 1h, washed with mQ water and autoclaved.

- The non-autoclavable tubes were cleaned in Sekusept aktiv solution for 1h, treated with RNase ZAP and washed with mQ water.

- The glass pipettes were sterilized at 180°C and stored in the cold room

4.3.2. Overview on Sucrose Gradient Centrifugation of Ribosomes

Density-gradient centrifugation was first established using swinging buckets, for separation of viruses, sub-cellular particles and nucleic acids ([Brakke, 1953]). The technique was described at that point as a "method for the separation of microscopic and submicroscopic particles, e.g. viruses, into zones by centrifuging."

During centrifugation in a sucrose gradient, particles of the same size, shape and density, sediment as a zone, until they encounter a medium of equal density, when equilibrium is reached. This allows the quantitative separation of particles with different buoyant properties.

Because of the difference in size and weight, the 70S, 50S and 30S particles have different buoyant properties and sedimentation rates, so they can be separated and purified in a sucrose gradient.

4.3.3. Methodological Information

In this study, the zonal rotor Type Ti-15 with B-29 core (Beckmann) was used when large amounts of sample (1000 - 6000 A_{260}) were available: for purification of tightly-coupled 70S and for ribosomal subunits. On the other hand, in the case of the reassociation reaction, which lead to low amounts of sample (usually 100 A_{260}), a swing rotor type 32 Ti (Beckmann) was used. (Table 4.2)

Table 4.2.: Specifications of the rotors used for rate-zonal centrifugation

	Ti-15 (B-29 core)	SW32 Ti
Maximum speed (rpm)	32000	32000
k-factor	468	204
Total volume (mL)	1350	6 tubes x 68.5 mL
Maximum flow rate	50 mL/min (gradient loading) 25 mL/min (sample loading)	n/a

4.3.3.1. Rate-zonal Centrifugation Using the Ti-15 Rotor

The zonal centrifugation using the Ti-15 zonal rotor was performed according to the manufacturer's instructions. The sample loaded in one run was 50 mL and it contained maximum 6000 A_{260}. An additional final concentration of 5% sucrose was added. The rotor was loaded from the inlet, at a speed of 2000 rpm, in the following order: 100 mL buffer, 50 mL sample, and the sucrose gradient, until the buffer loaded in the first step started to be pumped out from the outlet. In the end, 50% sucrose was

pumped in, until a total volume of 100 mL buffer has been pumped out.The last step creates a thin outer layer of 50% sucrose, to avoid the precipitation of particles on the wall of the rotor. (Fig 4.1).
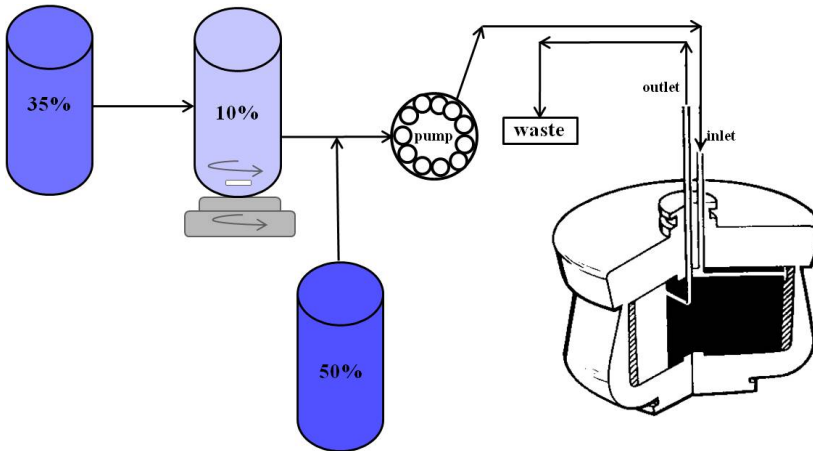

Figure 4.1.: Rate-zonal centrifugation in a Ti-15 zonal rotor

After loading, the centrifugation speed was increased, for an overnight run, allowing the particles to run through the gradient. The two end points of the gradient sucrose solutions and the overnight centrifugation speed was chosen according to the size of the particles to be separated. In the case of separation of the 70S ribosomes from factors, subunits and polysomes, a 10% - 35% sucrose gradient was used, and the speed was increased to 25 000 rpm, for 17 hours (Fig. 5.2). The ribosomal subunits were separated in a 6% - 35% sucrose gradient and required a higher centrifugation speed: 30 000 rpm for 17 hours (Fig. 5.4).

After the high-speed centrifugation, the sucrose gradient was fractionated, at a speed of 2000 rpm, by pumping 50% sucrose from the rotor inlet and collecting fractions of 50 mL from the outlet. Each fraction was thoroughly mixed for homogenization and the absorbance at 260 nm was measured using the Nanodrop. The absorbance of the collected fractions was plotted in the fractionation profile. The peaks were identified, the corresponding fractions were collected and centrifuged overnight for pelleting the ribosomal particles.

4.3.3.2. Rate-zonal Centrifugation Using the SW32 Ti Rotor

The SW32 Ti zonal centrifugation was used to purify the reassociated 70S ribosomes, when the sample contained less than 300 A_{260}. In this case, a 15% - 35% sucrose gradient was used, and the centrifugation speed for an optimal separation of ribosomal particles was 17 000 rpm, for 22 h (Section 5.5)

The SW32 Ti is a top-loading swinging bucket rotor. The sample tubes are loaded in individual buckets that hang vertically when the rotor is at rest. The sample is placed on top of the sucrose gradient before ultracentrifugation. During the ultracentrifugation step, the buckets swing out to a horizontal position, allowing the particles to be resolved in the gradient (Fig. 4.2).
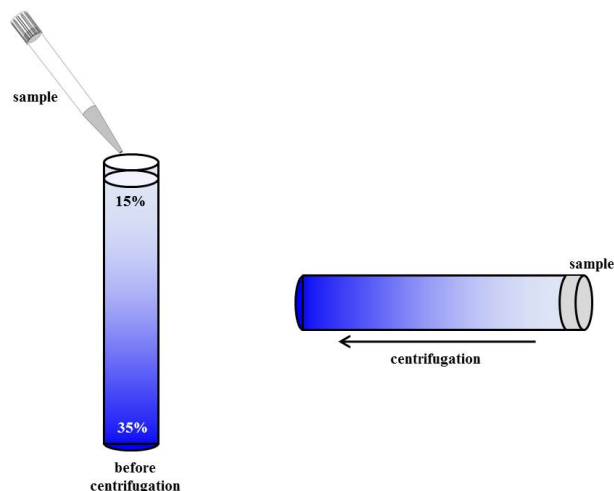
Figure 4.2.: Rate-zonal centrifugation in a SW32-Ti rotor

The sucrose gradient preparation and fractionation were performed using the Biocomp Gradient Station and Fractionator. The linear sucrose gradients were prepared with the tilted tube rotation method ([Coombs and Watts, 1985]), which requires having the two end point sucrose solutions layered in a centrifuge tube that is capped afterwards. The tube is then placed in a magnetic tube holder, which tilts it to the proper angle, rotates it at a fixed speed for a designated time, and brings it back to a vertical position.

Samples of maximum 500 μL were overlaid on top of each tube containing the sucrose gradient, and centrifuged overnight.

The fractionation of the gradient was performed with the Fractionation Unit of the Biocomp Gradient Station. Using a "trumpet tip" - like piston, the device is gradually compressing bands of gradient from horizontal discs into thin vertical columns (Fig. 4.3) in a capillary. The absorbance at 254 nm is measured in real time, using a dual-wavelength detector for liquid chromatography. Using this system, an ultra-high resolution profile of the gradient is reached. The fractions were collected in standard 12x100 mm tubes automatically, using the Fraction Collector.

In order to obtain a good resolution, the gradients were fractionated with the following settings:

- piston speed: 0.1 mm/sec
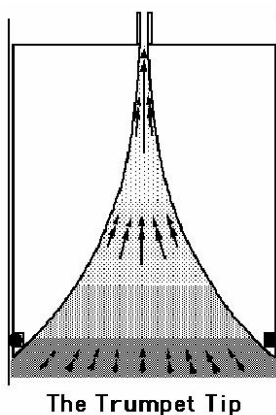- fraction size: 2 mm gradient
- number of fractions collected: 35

Figure 4.3.: The trumpet tip used for gradient fractionation

4.4. *In vivo* Biotinylation of Proteins

4.4.1. General Information

An approach for the *in vivo* biotinylation of proteins is using the BirA biotin-protein ligase, that covalently attaches d-biotin to biotin-acceptor peptides or proteins via an ATP intermediate (biotinyl $5'$-adenylate) in a highly efficient and targeted manner. The minimal acceptor substrate (AviTag) for BirA is the peptide:

G-L-N-D-I-F-E-A-Q-K-I-E-W-H ([Beckett et al., 1999])

This method involves the cotransformation, in bacterial cells, of two compatible plasmids, containing the N-terminal fusion of the AviTag to the protein of interest, and the BirA biotin-ligase, respectively. By addition of biotin in the culture media at the moment of induction, both the BirA enzyme and the fused protein are overexpressed. The enzyme specifically recognizes the N-terminal AviTag of the protein and binds the biotin covalently to the Lys residue.

4.4.2. Protocol

The AVB101 strain, commercially available from Avidity LLC, is an *E. coli* B strain (hsdR, lon11, sulA1) which contains the pBirAcm plasmid with an IPTG inducible BirA gene to over-express the biotin ligase. The pBirAcm vector can be extracted and transformed in another bacterial strain, or the AVB101 strain itself can be used for expression.

The gene encoding the protein to be biotinylated must be contained in a vector compatible with the pBirAcm plasmid (e.g. pAN, pBAD), together with the sequence encoding for the AviTag, at the desired position. The AviTag can be inserted at the N- or C-terminus of a protein, or at internal protein

locations, if the peptide domain forms a surface-exposed loop accessible to the BirA enzyme.

In this thesis, the bacterial cells were co-transformed with the BirA and the pAN5 plasmid, and plated on Cm10/Amp100 agar plates. An overnight culture was prepared starting from one colony grown in DYT with Cm10/Amp100. Starting from this culture, expression cultures were made, with an OD_{600} of 0.1, and grown at 37°C. When the OD_{600} reached the value of 0.4, the plasmids were induced by addition of 0.5 mM IPTG. At the same time, biotin solution, prepared as described in Section 3.8.4, was added in the medium at a final concentration of 50 μM.

The induction time can vary from 1h to 3h.

4.5. Labeling of Proteins Using NHS Fluorescent Dyes

One of the most common techniques for labeling peptides and proteins involve the use of chemical groups that react with the accessible primary amine groups ($-NH_2$), found at the N-terminus of each polypeptide chain and in the side-chain of Lysine residues. These amines are positively charged at physiologic pH, so they occur mostly at the outer surface of the biomolecules, being accessible for conjugation with a fluorescent reagent.

A popular example in this respect are the N-hydroxysuccinimide (NHS) ester functionalized fluorescent dyes, which react with primary amines in physiological to slightly alkaline conditions (pH 7.2 to 9) to yield stable amine bonds. (Fig. 4.4).
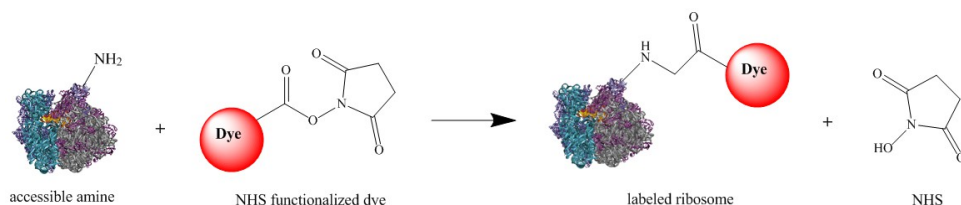
Figure 4.4.: NHS ester reaction scheme for chemical conjugation to an accessible primary amine on the surface of the ribosome

The hydrolysis of the NHS ester competes with the crosslinking reaction, so the dye solution should be prepared immediately before starting the labeling reaction. Moreover, the dyes should be stored as lyophylized aliquotes at -80°C, as described in Section 4.7.

The half-time of NHS esters is approximately 10 min at neutral pH. Therefore, the labeling reactions were performed at 37°C for 30 min.

4.6. Cell-free Protein Synthesis. The PURE System

4.6.1. Overview

One of the first approaches for producing an *in vitro* transcription-translation kit, in the early 1970s, was starting from crude extracts from *E.coli*, rabbit reticulocytes ([Pelham and Jackson, 1976]) or

wheat germ ([Roberts and Paterson, 1973]). However, these systems have a short lifetime because of the formation of toxic side products, and they don't have an optimal protein yield due to the leftover nucleases and proteases.

These *in vitro* kits were outperformed by the one produced from purified components, developed by Shimizu et al. in 2001 ([Shimizu et al., 2001]). This "protein synthesis using recombinant elements" (PURE) system contains all the resources necessary for transcription and translation, overexpressed in *E.coli* and purified with high specificity by His-Tag purification. Therefore, the system has no intrinsic nuclease or protease activity, and it is highly reproducible. The gene of interest should be under the control of the T7 promoter, since the system contains the T7 polymerase, a highly promoter-specific and fast-working enzyme.

Although the *in vitro* transcription-translation systems were originally developed as a fast and easy method to synthesize proteins, the PURE system became also a completely artificial framework to study transcription and translation. The system is basically made by mixing individually purified transcription and translation components, allowing omission or addition of specific or even modified molecules. By adding, for example, fluorescently labeled components, transcription or translation can be monitored at single molecule level.

For this study, the PURE System without ribosomes was used, since we want to study translation of our modified ribosomes.

4.6.2. Sample Preparation

When preparing samples for cell-free gene expression, a great emphasis was put on working at RNase free conditions. All the surfaces were cleaned with RNASE ZAP, and only RNAse-free pipette tips and pipettes were used. For time measurements using the fluorometer, the cuvette was treated with pirahna solution, rinsed with water and dried immediately before use.

The PURE system was used as described by the manufacturer. The kit is provided in two solutions "A" and "B", which were aliquoted and stored at -80°C.

Reactions of 25 μL were performed according to manufacturer's instructions, and contained:

- 10 μL Mix A

- 3 μL Factor Mix

- 500 nM ribosomes

- 5.5 nM plasmid (described in Section 9.2)

- 5 nM anti-sense tmRNA (AS-tmRNA), complementary to the sequence of tmRNA

- Tico buffer up to a final volume of 25 μL

In the reactions in which linear constructs were used, 5 nM anti-sense transfer-messenger RNA (AS-tmRNA), complementary to the sequence of the tm-RNA, was added ([Schaffitzel et al., 1999]). In this way, the function of the tmRNA of rescuing stalled ribosomal complexes ([Karzai et al., 2000], [Dulebohn et al., 2007]), described in Section 1.5 was suppressed.

The reactions can be scaled up according to the volume needed for the designed experiment. All the *in vitro* reactions were performed at 37°C.

4.7. Aliquotization of Dyes

The fluorescent dyes used in this study were bought as NHS-ester conjugates, and are susceptible to hydrolysis in water, the kinetics of which is dependent on pH. Therefore, dye aliquots were prepared in a nitrogen glovebox, using water-free DMSO.

First, the glovebox was equilibrated with nitrogen for 1h. Then, usually 1 mg of lyophilized dye was dissolved in 200 μL DMSO, to reach a concentration of 1-5 mM fluorescent dye. Aliquots of 5 μL were prepared, lyophilized at a pressure of 0.001 mBarr, and a temperature of -80°C for 2h, and stored at -80°C.

4.8. Preparation of Slides for Microscopy Techniques

FCS measurements were performed on PEG coated cover slips, in order to avoid the adherence of the molecules to the surface. For wide field measurements, biotinylated ribosomes were specifically tethered on the surface of biotin-functionalized PEG slides, using the biotin-streptavidin interaction.

Preparation of microscopy slides was performed in a clean airbox, to avoid contamination. The slides were cleaned first by incubation in piranha solution for 1h and then in a plasma cleaner for 5 min. Afterwards, they were incubated in a 2% solution of 3-aminopropyltriethoxysilane (APTES) in acetone, to introduce amino functionalization. The passivation was made by incubation in a PEG-NHS ester solution (200 mg/mL) in 100 mM NaHCO$_3$ (pH 8.5), for at least 2 h. For biotin-modified glass slides, the incubation was made in a mixture of 200 mg/mL PEG-NHS ester and 20 μg/mL biotin-PEG-NHS ester (Fig. 4.5).
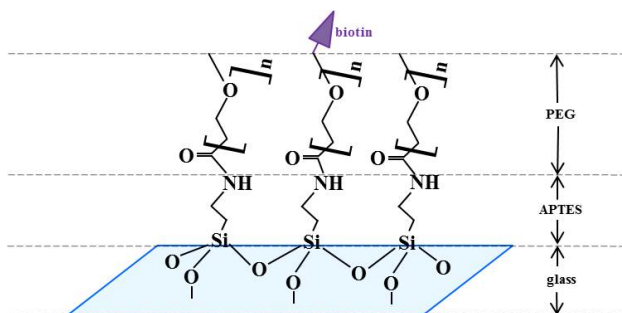

Figure 4.5.: Functionalization of glass slides for microscopy techniques

After preparation, the slides were either used immediately or stored at -20°C for further measurements.

4.9. Oxygen Scavenging System

Single molecule experiments require prolonged and stable fluorescence emission in the observation time. However, the usual fluorophores employed in these studies are characterized by fast photobleaching and intensity fluctuations (blinking), which impair correct analysis and limit the observation time. Several phenomena have been proposed as reasons for these effects: triplet state transitions ([Ha and Tinnefeld, 2012]), conformational isomers ([Widengren and Schwille, 2000]) and radical ions ([Zondervan et al., 2003]).

In this study, ribosomes were fluorescently labeled with Cy5, an activated carbonyl cyanine fluorophore, with high fluorescence quantum yield, high photostability and low pH sensitivity. Most cyanine dyes that have no sterical hindrance adopt the all-trans conformation in the ground state. By excitation, a photo induced isomerization occurs to a mono-cis non fluorescent conformation. For most excitation conditions relevant for single molecule experiments, an equilibrium is established between the two isomeric forms, where approximately 50% of the molecules are in the weakly fluorescent cis conformation. Also, following the excitation, Cy5 can undergo intersystem crossing and get trapped in the long-living dark triplet state.

It has been shown ([Rasnik et al., 2006]) that a concentration of 10 mM β-mercaptoethanol drastically affects the stability of Cy5, by shortening the fluorescence lifetime, and increasing the blinking events approximately 10 fold. The signal to noise ratio is also reduced in these conditions.

Molecular oxygen is primarily responsible for bleaching of fluorophores, either by directly interacting with the dye in the excited state or by producing free radicals. In order to remove the molecular oxygen from the buffers used in single molecule experiments, enzymatic oxygen scavenging systems are usually used. In this study, the protocatechuic acid/protocatechuate-3,4-dioxygenase (PCA/PCD) system was used, which has been proved ([Aitken et al., 2008]) to be more efficient than the Glucose oxydase/catalase system. PCD is a multimeric metalloenzyme with oxidizing properties achieved by a nonheme iron center, so it does not require further ions for its catalytic activity. The oxidation mechanism does not involve production of reactive species that could interfere with the dye stability or functionality of the studied biomolecules.
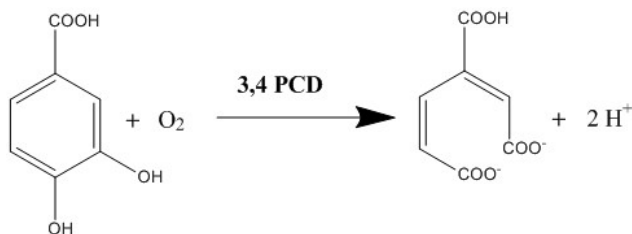

Figure 4.6.: The chemical reaction in the PCD system

On the other hand, molecular oxygen is efficient in quenching the dark triplet states of the fluorescent dyes. By removing the oxygen from the buffer, the lifetime of triplet states reaches a millisecond range, detected in single molecule studies as on and off states. Therefore, the triplet states are usually quenched in this case by adding Trolox, a water-soluble vitamin E derivative, in the buffer used for detection of single molecules.

The combination of Trolox with an oxygen scavenging system has been widely used for extending the observation time of single fluorophores ([Rasnik et al., 2006], [Aitken and Puglisi, 2010], [Uemura et al., 2010]). All single molecule experiments presented in this study were performed in the following conditions: 10 nM PCD, 2.5 mM PCA, and 1 mM Trolox.

The lyophilized powder of protocatechuate 3,4-dioxygenase from *Pseudomonas* species was resuspended in 50% Glycerol stocks in TP50 buffer (Section 3.8.8), and stored at -20°C. The protocatechuic acid (3,4-dihydroxibenzoic acid) solution was prepared fresh, in mQ water at a concentration of 100 mM in mQ water, and the pH was adjusted to 9 using NaOH. The Trolox solution was dissolved in methanol, to a final concentration of 100 mM, and stored at 4°C.

4.10. Confocal Fluorescence Detection

Fluorescence Correlation Spectroscopy (FCS) and single molecule two-colour coincidence detection (TCCD) measurements of freely diffusing fluorescent species were performed with a MicroTime 200 confocal microscope. The excitation light from pulsed lasers at 485 nm and 633 nm was focused with a water immersion objective 15 μm above the glass surface. The same objective was used for fluorescence collection in combination with a dual-band dichroic mirror. After focussing through a 30 μm (FCS) or 75 μm (TCCD) pinhole, the fluorescence was split into a blue and red detection channel by another dichroic mirror. 50/50 beam splitter cubes and appropriate emission filters (blue: 530/55, red: ET685/80 M) enabled detection on two single-photon avalanche diodes for each channel. The arrival time of each photon was recorded with a time-correlated single-photon counting (TCSPC) module.

4.10.1. Fluorescence Correlation Spectroscopy

Fluorescence Correlation Spectroscopy (FCS) measurements are performed with low concentration of labeled particles (nanomolar range) and low detection volumes (femtoliter range). In this way, the number of observed molecules is low enough so that each of them contributes substantially to the measured signal. In contrast to other fluorescence techniques, the parameters of interest are not emission intensity itself, but rather spontaneous fluctuations of intensity caused by deviations from a mean, due to the fact that a fluorophore enters or exits the confocal volume. These fluctuations of the fluorescence signal are quantified by temporally autocorrelating the recorded intensity signal.

An aspect that has to be considered when performing FCS is the afterpulsing of the detectors, due to scattered photons from the excitation pulse, resulting in a fast diffusing component in the autocorrelation function ([Enderlein and Gregor, 2005]). This artefact can be avoided by splitting the signal to two detectors and cross-correlating the counts of the two detection channels. Because afterpulsing occurs randomly, it will not be autocorrelated in the final analysis. Technically, the emission light was split by a 50/50 beam-splitter and detected by two SPADs ([Zhao et al., 2003]).

In standard FCS measurements, performed in aqueous solutions, containing nM concentration of labeled biomolecules and using a confocal microscope, the main contribution of the intensity fluctuations are diffusion and the triplet-state kinetics.

Practically, the fluorescence intensity, $F(t)$ is measured as a function of time. The autocorrelation function is defined as:

$$G(\tau) = \frac{\langle \delta F(t) \cdot \delta F(t + \tau) \rangle}{\langle F(t) \rangle^2}$$

where τ is the correlation time between a pair of photons detected at time t and $t + \tau$.

If only free diffusion is considered and the volume is calculated as an ellipsoidal 3D-Gaussian function, the theoretical autocorrelation $G_D(\tau)$ is:

$$G(\tau) = \frac{1}{N} \cdot \left[1 + \frac{\tau}{\tau_{DT}} \right]^{-1} \cdot \left[1 + \frac{\tau}{k^2 \cdot \tau_{DT}} \right]^{-\frac{1}{2}}$$

where:

- N is the average number of molecules in the observation volume

- τ_{DT} is the dwell time

- k, also called ellipticity, is the ratio between the major z_0 and the minor ω_0 axis of the observation volume: $k = \frac{z_0}{\omega_0}$

The value of the diffusion (dwell) time obtained by fitting the theoretical correlation function to the experimental data can be used to calculate the translational diffusion coefficient of the freely diffusing molecules:

$$D = \frac{\omega_0^2}{4 \cdot \tau_{DT}}$$

The spatial properties of the confocal volume must be determined precisely in order to obtain reliable diffusion coefficients. Therefore, before each series of measurements, a calibration was performed, using a fluorescent dye with the same spectral characteristics and a known diffusion coefficient.

4.10.2. Two-colour Coincidence Detection

Compared to surface-immobilized studies, solution-based single molecule experiments have the advantage that a large number of particles can be analysed. This is achieved by using a tightly focused Gaussian laser beam and confocal detection in order to obtain a small probe volume with a sample solution at picomolar concentration.

Two-colour coincidence measurements (reviewed in [Li et al., 2003], [Orte et al., 2010]) use two spatially overlapped lasers to excite two different colour probe molecules, and independent red and green detector channels are used for fluorescence detectors. If two fluorophores are bound to two subunits of the same biomolecule, one would expect to observe fluorescence bursts on both channels at the same time; on the contrary, a dissociated state of the biomolecule would result in single non-coincident bursts. It is then possible to quantitatively estimate the amount of bound/unbound biomolecules (Fig. 4.7).

Technically, the sample was diluted until a concentration of 0.01 ribosomes in the confocal volume was reached. Pulsed interleaved excitation (PIE) was applied ([Müller et al., 2005]) to identify two-colour
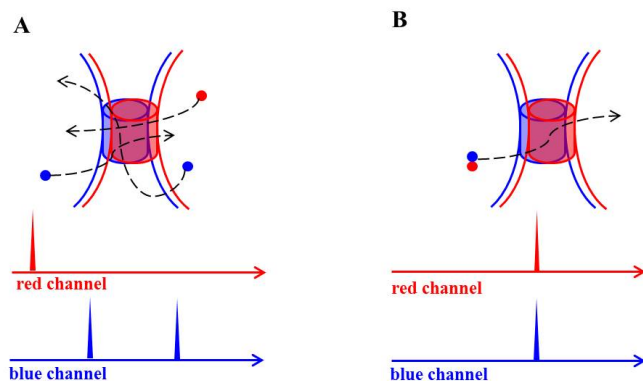
A

B

red channel

blue channel

red channel

blue channel

Figure 4.7.: In TCCD, non-associated moleculed do not give rise to coincident events (A), while the associated molecules give coincident bursts (B)

fluorescent species and sort out single-colour events. Data analysis was done with self-written Matlab routines (Mathworks, Natick, USA). In short, bursts were selected through the inter-photon distance and coincidence analysis was similar to the approach used by Li et al. ([Li et al., 2003]).

4.11. Widefield Imaging

The advantage of a wide field study is that a parallel measurement of hundreds of molecules is achieved, so that rare or non-synchronized events can be detected, and dynamic processes with time scales of ms-min can be monitored. For surface tethering, biotinylated ribosomes were specifically attached on glass surfaces functionalized according to Section 4.5. In order to limit the photobleaching and blinking of the fluorophores, the oxygen scavenging system described in Section 4.9 was added.

Surface imaging of RNCs was performed with an inverted microscope in widefield illumination mode. For excitation, lasers at 488 nm and 639 nm were focused on the back-focal plane of an oil-immersion objective. The fluorescent light was collected with the same objective and passed through a dual-band dichroic mirror as well as a dual-band emission filter. Simultaneous dual-colour imaging was implemented with an image splitter on an EMCCD camera. Images were acquired for 1.5 s at 10 mW (blue) and 7.5 mW (red) excitation power.

Chromatic aberrations were considered for data analysis. In this sense, TetraSpeck fluorescent microsphere standards (0.1 μm), labeled with four different fluorescent dyes (blue, green, orange and dark red), were unspecifically tethered on the surface of a glass slide, and imaged in the same conditions as the sample. The images were then spatially corrected using an in-lab written Matlab routine, so that a perfect overlap was achieved, and the same algorithm was then used to correct the sample images. The degree of colocalization was also analysed using Matlab routines.

Part III.

Results

5

Preparation of Reassociated 70S Ribosomes

5.1. General Considerations

Purification of ribosomes from bacteria requires harvesting the cells at a certain point of the growth phase, followed by the fractionation of the cells. Hence, the final product consists of ribosomes collected at a specific time point, when they were translating constitutive bacterial mRNAs and synthesizing proteins.

The main goal of this study is to optimize the labeling and productivity of the ribosomes in order to investigate the first step of the translation initiation with single molecule techniques. Therefore, the ribosomes that are already involved in translation are not interesting, since a ribosome that is already reading a mRNA will eventually dissociate into subunits before reading the mRNA encoding for GFP required in our experiments.

The problem can be overcome by employing "empty" ribosomes, prepared from 70S ribosomes purified from bacteria, dissociated into subunits, and reassociated to form 70S monosomes (Fig. 5.1). In this way, we remove the mRNAs that the ribosomes might be reading at the point we purified them from bacteria. In addition, these samples are of high purity, in the sense that we clean the ribosomes also from factors, tRNAs, subunits or polysomes that we co-purify from bacteria.

5.2. Preparation of Crude 70S Ribosomes

For a complete reassociation experiment, 15 g culture of the strain ZS-22 were used, obtained from 8 L bacterial culture harvested at an OD_{600} of 0.7.

The cells were washed, by dissolving the bacterial pellet in 100 mL A30 buffer and centrifuged: SX4750A/4750 rpm/20 min, followed by resuspension in 100 mL A30 buffer. The cells were homog-

Escherichia coli

crude 70S ribosomes
(mRNA, tRNAs, factors)

tightly-coupled 70S ribosomes
(mRNA, tRNAs)

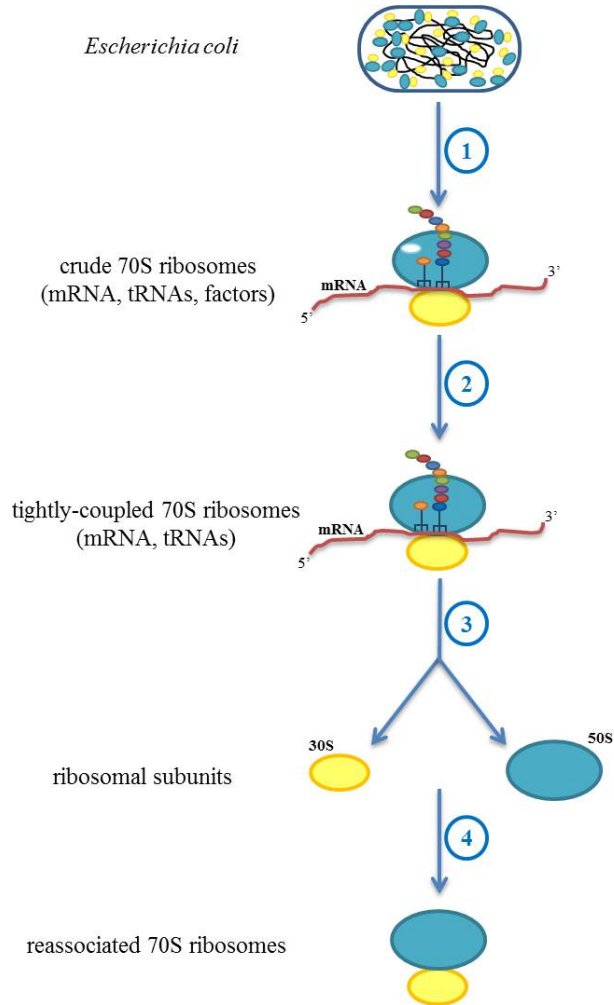ribosomal subunits

reassociated 70S ribosomes

Figure 5.1.: Preparation of reassociated 70S ribosomes. Bacterial cells are first fractionated to obtain crude 70S ribosomes (1), which are subjected to a rate-zonal centrifugation. The fraction corresponding to the tightly-coupled ribosomes is selected and purified (2). This sample contains mRNAs, tRNAs and factors. By dissociation of the tight couples into subunits (3), and reassociating them into 70S particles (4), we produce "empty" 70S ribosomes, which can be employed in studying initiation.

enized using a glass homogenizer, making sure that there are no clumps or aggregates before breaking them with a cell disruptor.

First, the outer surfaces of the cell disruptor were cleaned with RNase Zap and the machine was washed by passing RNase ZAP through the system, at 0.65 bar, followed by 200 mL autoclaved water and 100 mL A30 buffer for equilibration. The running temperature was set to $4°C$ to avoid the degradation of the ribosomes.

The bacteria were then disrupted by passing the suspension through the system, for three times, with a running pressure of 1.7 bar. In this manner, the cells were broken by forcing them through a 15 nm hole, thereby shearing the cell membranes. The mixture was collected in clean JA 25.50 tubes, and centrifuged: JA 25.50/11500 rpm/10 min to remove the unbroken cells. The supernatant was collected in JA 25.50 tubes and centrifuged at a higher speed: JA 25.50/16000 rpm/60 min in order to remove the cell debris.

The resulting supernatant, also called the S30 fraction, was overlaid on top of Glycerin Sol. C in 70-Ti tubes (2 volumes sample : 1 volume Glycerin solution C) and centrifuged overnight: 70-Ti/26500 rpm/14 h.

The sticky yellow pellet, composed of 70S crude ribosomes, was washed twice with 1 mL Tico, dissolved in 20 mL Tico buffer using a magnetic stirrer, and centrifuged: SX4750A/4750 rpm/20 min to remove the large aggregates. The supernatant was collected, adjusted to 10% Glycerol using autoclaved 100% Glycerol and Tico 10x, shock-frozen in aliquots of $6000 A_{260}$, and stored at $-80°$C.

Usually, a yield of $400 A_{260}$ crude 70S per gram cells can be expected. The Squires strains, however, lead to lower amounts, usually $250 A_{260}$ per gram cells.

5.3. Preparation and Characterization of Tightly Coupled 70S Ribosomes

The crude 70S sample contains not only 70S ribosomes, but also factors, tRNAs, subunits and polysomes, according to the status of the cell culture it was purified from.

In order to select the 70S monosomes from this mixture, the crude ribosomes were subjected to a sucrose gradient centrifugation in a Ti-15 rotor, using a $10 - 35\%$ sucrose gradient and a centrifugation speed of Ti-15/25000 rpm/17 h. The sucrose gradient was fractionated (Fig. 5.2), and the fractions corresponding to the 70S peak were collected in clean 45-Ti tubes and centrifuged: 45-Ti/24000 rpm/24 h. The pellet consists of pure tightly-coupled 70S ribosomes.

The purity and integrity of the rRNA was checked with gel electrophoresis, as described in Section 4.1.3. Three clear bands, corresponding to the 23S, 16S and 5S rRNA, were identified (Fig. 5.3, A).

Activity tests, described in Section 11.4, of the tightly coupled ribosomes were performed. The results show that approximately 40% of the ribosomes were active.

5.4. Preparation and Characterization of Ribosomal Subunits

In order to prepare subunits starting from 70S ribosomes, the concentration of Mg^{2+} was reduced to 0.97 mM and the concentration of $NH_4{}^+$ was increased to 200 mM (Dissociation Buffer conditions). The ribosomes dissociate when exposed to high concentrations of $NH_4{}^+$ (0.2 to 0.5 M) because these ions compete with the Mg^{2+} for metal binding sites at the subunits interface, causing dissociation ([Klein et al., 2004]).

The pellet taken from the previous centrifugation step, consisting of tightly coupled 70S ribosomes, was dissolved in Dissociation Buffer, using a magnetic stirrer, in the cold room. Usually, the procedure was carried out for minimum 4 h, to allow the complete dissociation of the 70S ribosomes into subunits.
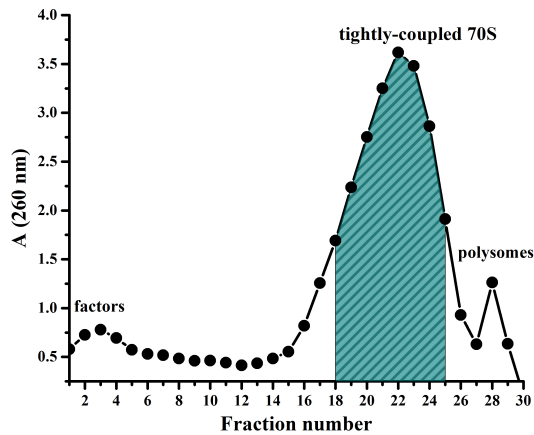
Figure 5.2.: Rate-zonal centrifugation for preparation of tightly-coupled 70S ribosomes
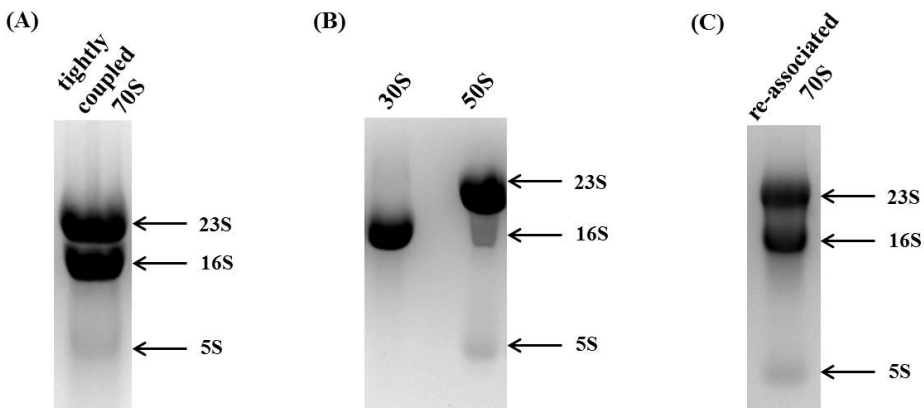

Figure 5.3.: The ribosomal particles can be identified by their electrophoretic behaviour in a 2 % agarose gel. The 70S monosomes: tightly-coupled (A) and the reassociated (C) display 3 bands, represented by the 23S, 16S and 5S rRNA. The 50S subunit shows two bands, corresponding to the 23S and 5S rRNA, while the 30S subunit shows one band, corresponding to the 16S rRNA.(B)

The sample was then subjected to a sucrose gradient centrifugation, using a $6 - 35\%$ sucrose gradient, and a centrifugation speed of 15-Ti/30000 rpm/17 h. All solutions used in this step were prepared using Dissociation Buffer.

The fractionation profile shows the dissociation of the 70S monosomes (Fig. 5.4). The two resulting peaks correspond to the small and the large subunit, respectively. The fractions were collected separately in clean 45-Ti tubes, and centrifuged: 45-Ti/35000 rpm/22 h. The pellets were then dissolved in
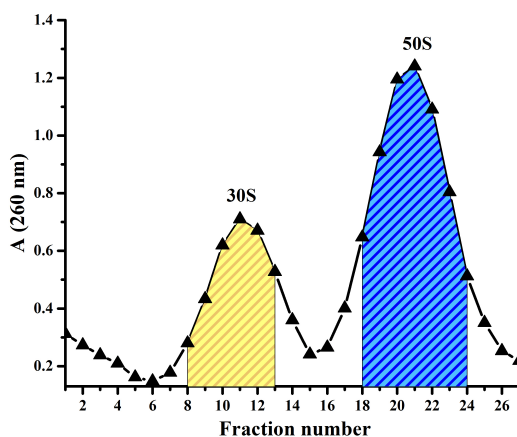
Storage Buffer, in the cold room, using magnetic stirrers.

Figure 5.4.: Rate-zonal centrifugation for preparation of ribosomal subunits

The purity and integrity of the subunits was confirmed with agarose gel electrophoresis. A pure 30S sample shows one band corresponding to the 16S rRNA, while a pure 50S sample presents two bands, corresponding to the 23S rRNA and 5S rRNA. (Fig. 5.3, B)

5.5. Preparation and Characterization of Reassociated 70S Ribosomes

In conditions of high Mg^{2+} concentration (20 mM Mg^{2+}/30 mM K^+), ribosomal subunits are able to form stable and active 70S particles ([Nierhaus, 2014]) The reassociation requires a high activation energy (80 kJ/mol) for the adaptation process of the 30S subunit, therefore the reaction needs a high temperature ([Blaha et al., 2002]).

The reaction was performed using a 50% excess of 30S with respect to 50S, at 40°C, for 45 min, and incubated on ice for 15 min. The high excess of 30S is needed to make sure that the whole amount of 50S is consumed. Otherwise, a considerable amount of 50S still present in the reaction mixture would eventually sediment very close to the 70S in the sucrose gradient, impairing the separation of the two peaks.

The sample was then subjected to a gradient centrifugation in a SW32 Ti rotor, as described before (Section 4.3.3.2), using a $15 - 35\%$ sucrose gradient, prepared in Reassociation Buffer. The ultracentrifugation was performed at 17000 rpm for 22 h. Afterwards, the gradient was fractionated (Fig. 5.5), the fractions corresponding to the 70S peak were collected in clean 45-Ti tubes, and centrifuged: 24000 rpm/24 h. Higher centrifugation speeds should be avoided, since they could lead to the dissociation of the 70S particles.
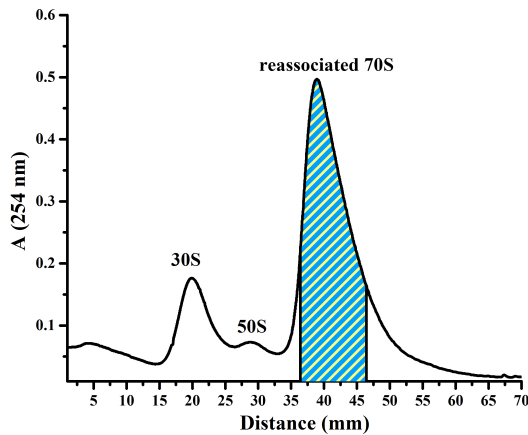
Figure 5.5.: Rate-zonal centrifugation for preparation of reassociated ribosomes

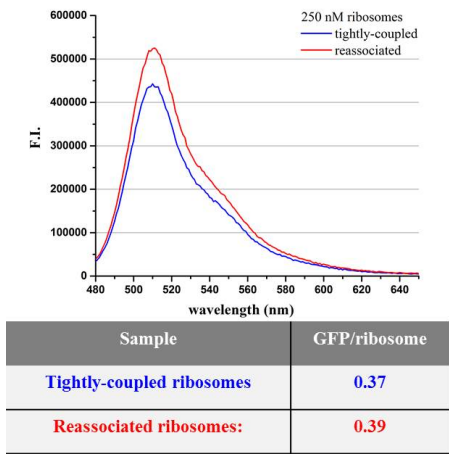| Sample	GFP/ribosome
Tightly-coupled ribosomes	0.37
Reassociated ribosomes:	0.39

Figure 5.6.: GFP production by 250 nM tightly coupled (blue curve) and reassociated (red curve) ribosomes

The pellet resulting after the overnight centrifugation, consisting of 70S reassociated ribosomes, was washed with 1 mL Tico buffer and dissolved in 50 μL Tico buffer, using a magnetic stirrer, in the cold room. The sample was adjusted to 10% glycerol, using autoclaved 100% glycerol and Tico 10X, aliquoted, shock-frozen and stored at -80°C.

Agarose gel electrophoresis confirm that the reassociated 70S ribosomes contain intact rRNAs (Fig. 5.3, C).

Activity tests, presented shortly in Fig. 5.6 and described in detail in 11.4, show that the reassociated ribosomes are as active as the tightly coupled ribosomes.

6

In vivo Biotinylation of Ribosomes

6.1. General Considerations

Using the previously described method (Section 4.4), the N-terminus of the ribosomal protein uL4 of the large ribosomal subunit was biotinylated *in vivo*. The CAN 20/12-E strain was transformed with two origin-compatible expression vectors, both inducible with IPTG (Fig. 6.1):

- PAN5 + AviTag-L4: we introduced the biotinylation AviTag upstream the uL4 gene

- pBirA plasmid: an engineered pACYC184 plasmid with the birA gene: isolated from the AVB101 strain (Avidity), to overexpress the biotin ligase
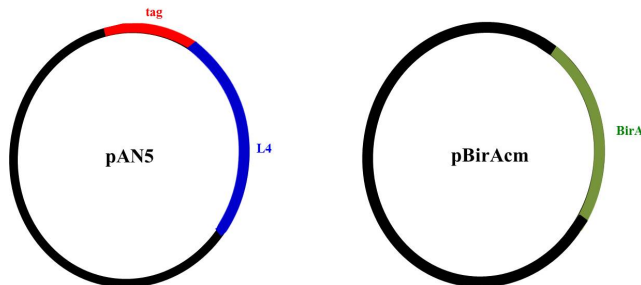

Figure 6.1.: The IPTG-inducible plasmids co-transformed in *E. coli* for *in vivo* biotinylation of ribosomes

By addition of d-biotin in the culture media and induction of the two plasmids, the biotin ligase and the AviTag-L4 were overexpressed. Subsequently, the biotin ligase attaches the biotin covalently to the N-terminus of the uL4 protein. This modified uL4 protein is then incorporated in the ribosome.

The crystal structure of the ribosomal protein uL4 shows alternating α/β fold and a large disordered loop region ([Worbs et al., 2000]). The C-terminal site, composed of two α helices, is required for

L4-mediated autogenous control of the S10 operon by interacting with the leader sequence of the S10 mRNA leader ([Lawrence et al., 2016]). The N-terminus consists of a disordered loop with flanking α helices, and is pointing outside of the ribosome (Fig. 6.2), so that addition of a 244 Da biotin molecule would not disturb the final structure.
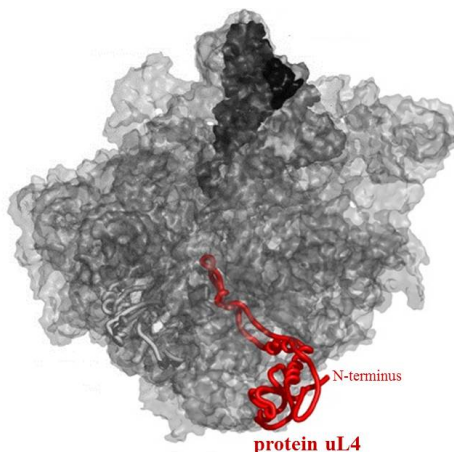

Figure 6.2.: Incorporation of the uL4 protein in the ribosome. The protein has a globular domain that sits on the surface of the 50S and an extended loop that penetrates the core of the subunit.

This approach leads to a competition between incorporation, into the ribosomes, of the wild type protein L4 expressed from the bacterial chromosome, and the over-expressed biotinylated uL4. Therefore, in the end a mixed population of particles was purified, containing both wild type and biotinylated ribosomes.

6.2. Procedure

First, the two plasmids were co-transformed in the CAN-20/12-E strain, by heat-shock, as described in Section 4.2.3. After transformation, the cells were plated on Cm10/Amp100 agar plates overnight, at 37°C. One colony was grown in 5 mL DYT supplemented with the same concentration of antibiotics. Then, starting from the 5 mL culture, overnight cultures of 100 mL were prepared, at 37°C and shaking at 120 rpm.

The expression cultures were prepared in 2 L flasks filled with 500 mL DYT supplemented with Cm10/Amp100, starting from an OD_{600} of 0.1. The cultures were grown at 37°C and shaking at 120 rpm, until an OD of 0.4. At this point, 5 mL of 5 mM biotin solution (see Section 3.8.4) was added to a final concentration of 50 μM biotin and the plasmids were induced by adding IPTG to a final concentration of 1 mM. The cells were grown further for 1 h. Longer induction times would eventually increase the degree of biotinylation, but a higher OD_{600} would compromise the quality of the ribosomal preparation. Usually, at the end of the procedure, the OD_{600} does not exceed the value of 1.

The cultures were placed on ice for 1 h, harvested by centrifugation, shock-frozen and stored at -80°C until further experiments.

6.3. Characterization

6.3.1. Identification Using Western Blot

The biotinylation of the ribosomal protein uL4 was confirmed by Western Blot. For immunodetection of the biotin, the Qdot625 streptavidin conjugate was used, consisting of nanometer scale crystals of a semiconductor material, coated to a polymer shell covalently coupled to streptavidin. Because of the high affinity of the streptavidin-biotin interaction, detection of biotin is highly specific and sensitive (Fig. 6.3).
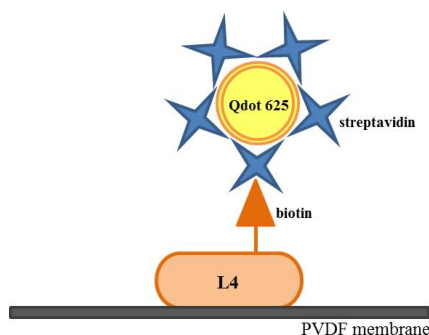

Figure 6.3.: Western Blot detection of biotinylated proteins using Qdot625 streptavidin

Samples of 20 μL containing 2 μM ribosomes were separated in 12% SDS-PAGE gels (prepared as described in 3.8.6). The transfer of proteins to a PVDF membrane was carried out in a semi-dry transfer chamber, in Transfer Buffer, at a constant voltage of 100 V for 2 h. The membrane was activated in advance, by incubating it in methanol for 2 min, then washing it with mQ water and equilibrating it in Transfer Buffer. The gels were also equilibrated in Transfer Buffer for 10 min prior to transfer.

After transfer, the blot was incubated in 20 mL Blocking Buffer for 1 h at room temperature, with gentle shaking. Then, the buffer was discarded and the membrane was washed three times for 15 min, with Wash Buffer. The volume of Wash Buffer depends on the size of the tray used for incubation (usually $10 - 20$ mL).

After washing, the membrane was incubated in 8 mL Qdot625 streptavidin conjugate solution, prepared according to the manufacturer's instructions: 4 μL Qdot625 streptavidin conjugate into 8 mL Blocking Buffer. The incubation was performed for 1 h at room temberature, in the dark.

The detection solution was discarded and the membrane was washed three times with Wash Buffer, for 15 min, in the dark, at room temperature. The final wash was made in mQ water, in the same conditions.

The blot was then quickly dried and immediately developed with a Gel Imaging System, using UV epi-illumination. Usually, exposure times of 20-60 s were necessary.

A signal at 25 kDa was detected, corresponding to the biotinylated protein uL4. As a negative control, CAN ribosomes, treated in the same manner, were loaded in the same gel.(Fig. 6.4)
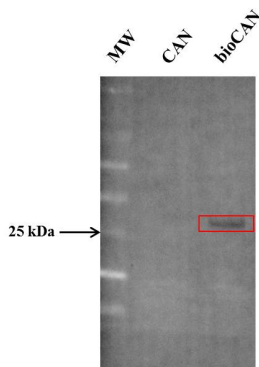

Figure 6.4.: Western Blot detection of the biotinylated protein uL4.

6.3.2. Activity of the Biotinylated Ribosomes

The activity of the biotinylated ribosomes, determined as described in Section 11, was slightly lower than the activity of the wild-type ribosomes (Fig. 6.5 and further explained in Section 11.4). The decrease in activity was caused by the fact that bacteria were harvested at a late exponential phase, characterized by a reduction in the ribosomal activity inside the cells.
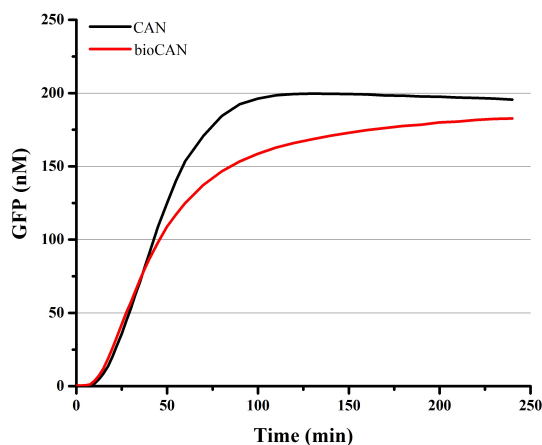

Figure 6.5.: Kinetics of GFPem production by 500 nM CAN (black curve) and bioCAN (red curve)

7

Fluorescent Labeling of Ribosomes Using NHS Functionalized Dyes

7.1. General Considerations

Ribosomes were labeled at the accessible primary amines using NHS dyes, as described in Section 4.5. Since there is a large number of lysines at the surface of the ribosome, this procedure leads to a high labeling ratio, presumably on both subunits. A drawback of this method is that it leads to a heterogeneous sample, with 70S particles labeled at different sites and with different numbers of fluorophores.

When adding fluorescent dyes on the ribosome, especially in the case of non-specific attachment, there is a high probability that "hot-spots" of the ribosome required for translation are blocked. Therefore, the activity of the labeled ribosomes must be tested and compared to the one of the unlabeled species.

7.2. Labeling Procedure

The fluorescent dyes: Cy5-NHS-ester or Atto488-NHS-ester, aliquoted as previously described (4.7), were dissolved in 5 μL DMSO, immediately before performing the labeling reaction.

The labeling procedure was adapted from existing protocols ([Milon et al., 2007]). First, the buffer in which the ribosomes were stored (Tico) was exchanged to Labeling Buffer (Section 3.8.2). A sample of $100 \mu L$ ribosomes was overlaid on top of 2 mL of 1.1 M sucrose in Tico, centrifuged: TLA 100.4/54000 rpm/2 h, and the pellet was dissolved in 100 μL Labeling Buffer using a magnetic stirrer, for 15 min, in the cold room.

The concentration of the ribosomes was adjusted to 5-10 μM and the NHS functionalized fluorescent dye (either Cy5-NHS or Atto488-NHS) was added in a 20 times excess. The reaction mixture was

incubated in a thermomixer at 37°C for 20 min. These conditions ensure a high labeling ratio and a good activity.

In order to remove the unreacted dye, the reaction mixture was overlaid on top of 2 mL of 1,1 M sucrose in Tico buffer and centrifuged: TLA 100.4/54000 rpm/2 h. The pellet consists of labeled ribosomes, while the dye remains as a band on top of the sucrose cushion after the centrifugation. The pellet was washed twice with 1 mL Tico, dried, and dissolved in 50 μL Tico, using a magnetic stirrer, in the cold room. The sample was then centrifuged: Eppendorf/14000 rpm/10 min to remove the aggregates, and the supernatant was collected and used for further experiments.

7.3. Characterization of the Labeled Ribosomes

7.3.1. Labeling Ratio

The concentration of both ribosomes and fluorescent dyes was measured by UV-VIS spectroscopy, with the Nanodrop, using the following molar exctinction coefficients:

- 70S: 4.2 x 10^7 M^{-1} cm^{-1} (λ_{max}=260 nm)
- Cy5: 250 000 M^{-1} cm^{-1} (λ_{max}= 649 nm)
- Atto488: 90 000 M^{-1} cm^{-1} (λ_{max}= 500 nm)

Using NHS functionalized dyes, an average labeling ratio of 7 Cy5/ribosome (Fig. 7.1) and 10 Atto488/ribosome was obtained. Previous experiments (data not shown) show that the 70S was labeled with an average of 3 dyes on the small subunit and 4 dyes on the large subunit in the case of Cy5. In the case of Atto488, the small subunit was labeled with 4 dyes and the large subunit with 6 dyes.
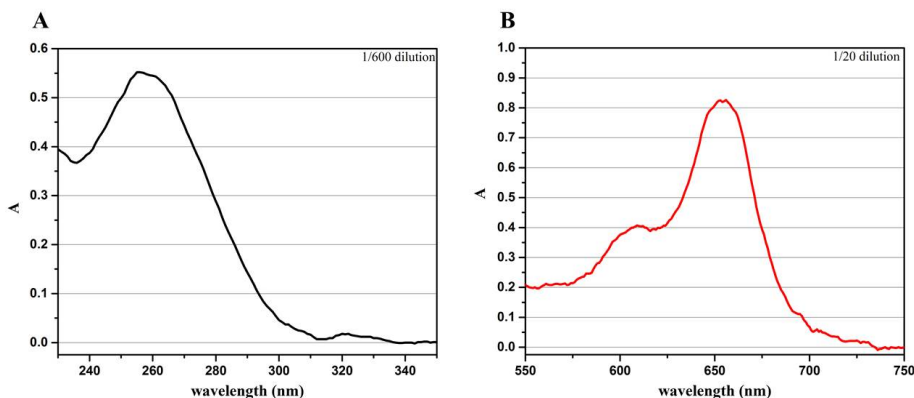

Figure 7.1.: Determination of the labeling ratio. (A) Measurement of the concentration of bioCAN ribosomes, and (B) Measurement of the concentration of Cy5

7.3.2. FCS

FCS measurements (described in Section 4.10.1) were performed to prove that the sample containing the Cy5 labeled ribosomes does not contain free dye or aggregates. The calculated diffusion coefficient was 21 μm^2/s, which is the expected diffusion of a labeled ribosome. This proves that the purification protocol allows a good separation of the excess of fluorophore and it confirms the fact that there are no aggregates in the sample.
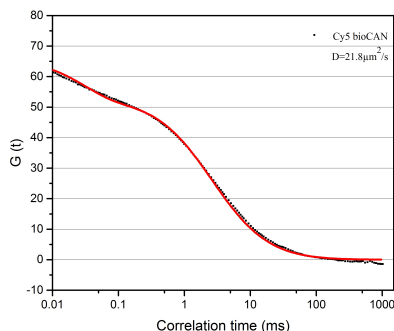

Figure 7.2.: FCS curve of bioCAN ribosomes labeled with NHS-Cy5

7.3.3. Activity of the Labeled Ribosomes

The activity test of the Cy5 bioCAN was performed as described in Section 11, and it shows that the activity of ribosomes decreased with 30% after labeling (Fig. 7.3, and further explained in Section 11.4.1).
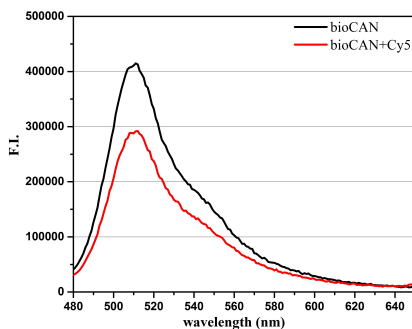

Figure 7.3.: GFPem production by 250 nM bioCAN (black curve) and 250 nM Cy5-bioCAN (red curve)

The labeled ribosomes can be stored overnight at $4°$C without any loss of activity.

8

Hybridization of Functionalized Oligonucleotides to Engineered Ribosomal RNA

8.1. General Considerations

As an alternative to non-specific labeling of the ribosome using NHS functionalized fluorescent dyes, Dorywalska et al. [Dorywalska et al., 2005] developed a method to site-specifically attach fluorescent dyes on the ribosome by hybridization of fluorescent oligonucleotides to engineered ribosomal RNA loops. The K_D of the resulting complex is 5 nM.

In this study, the bacterial strain ZS-22 was used, in which two hairpins were engineered (Fig. 8.1, Fig. 8.2).

- 50S subunit: hairpin 22 at helix H101 of the 23S rRNA

- 30S subunit: hairpin 68 at helix h10 of the 16S rRNA

According to the functionality to be introduced on the ribosome, the following oligonucleotides were used:

- 30S-Bio: (5') GGGAGATCAGGATATAAAG-bio (3'): $C_{stock} = 100\ \mu M$ (Eurofins), Fig. 8.1, A

- 30S-Cy3: (5') GGGAGATCAGGATATA-Cy3 (3'): $C_{stock} = 75\ \mu M$ (Eurofins), Fig. 8.1, B

- 50S-Cy5: (5') GAGGCCGAGAAGTG-Cy5 (3'): $C_{stock} = 100\ \mu M$ (Eurofins), Fig. 8.2
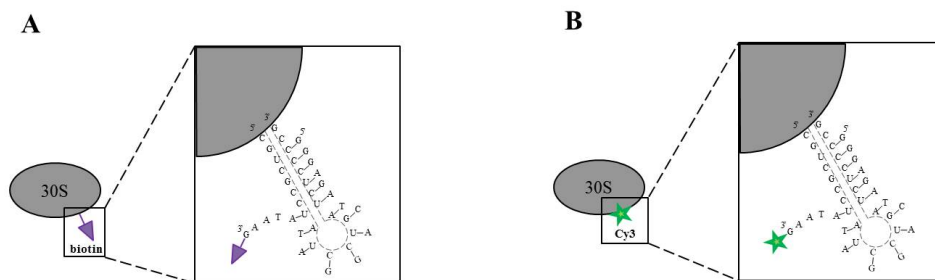
A

B

Figure 8.1.: Site specific labeling of the 30S subunit, using a biotinylated (A) or a Cy3-functionalized (B) olgonucleotide
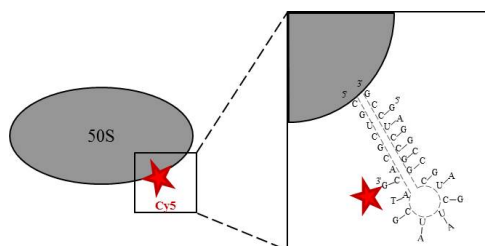

Figure 8.2.: Site specific labeling of the 50S subunit, using a Cy5-modified oligonucleotide

8.2. Labeling Protocol

The labeling method was adapted from the previously published protocols ([Dorywalska et al., 2005]). The buffer that lead to an optimal oligonucleotide binding and a good activity of the labeled species was a Tris-polymix buffer (Section 3.8.2).

The reaction was made by mixing 1-5 μM ZS-22 ribosomes with 30 times excess labeled oligonucleotide, and incubating the reaction at 37°C for 15 min and 30°C for 20 min, in a thermomixer. The labeled ribosomes were purified by overlaying the reaction mixture on top of 1 mL 1.1 M sucrose in Tris-polymix buffer and centrifugation: TLA 55/50000 rpm/17 h. The pellet was dissolved in 15 μL Tris-polymix buffer and the sample was centrifuged: Eppendorf/14000 rpm/10 min to remove aggregates. The supernatant, consisting of 70S labeled ribosomes, was collected and used for further studies.

Binding of the oligonucleotide was specific for the hairpin of the mutant ribosomes, since no label was detected in negative control samples containing ribosomes with no engineered loops (detailed in 8.3.2).

8.3. Characterization of the Labeled Ribosomes

8.3.1. Labeling Ratio

The concentration of the ribosomes and the fluorescent dyes were determined spectrophotometrically, with the Nanodrop , using the following exctinction coefficients:

- 70S: 4.2 x 10^7 M^{-1} cm^{-1} (λ_{max}=260 nm)
- Cy5: 250 000 M^{-1} cm^{-1} (λ_{max}= 649 nm)
- Cy3: 136 000 M^{-1} cm^{-1} (λ_{max}= 550 nm)

This protocol lead to a reproducible labeling ratio of 1 dye/ribosome, for both the Cy3 and Cy5 oligonucleotide. Fig. 8.3 shows the labeling ratio calculated for the ZS-22 reassociated 70S, labeled concomitantly with two oligonucleotides: Cy5 for labeling the large subunit and Cy3 for binding to the small subunit.
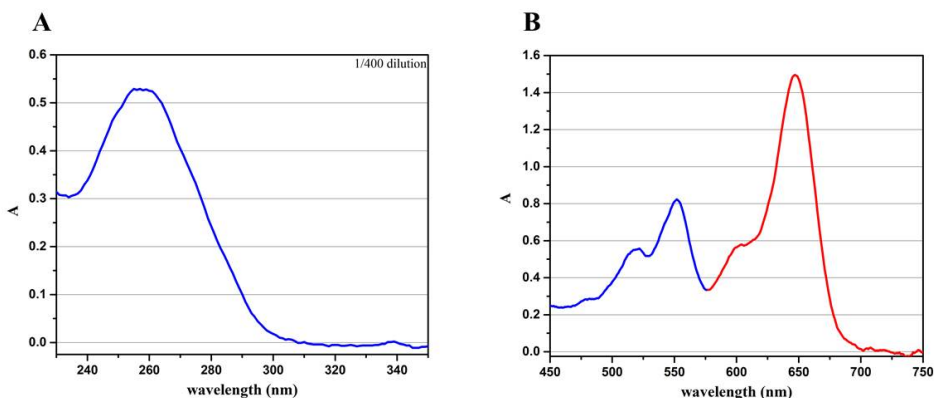

Figure 8.3.: Determination of the labeling ratio for double labeled ZS-22 ribosomes. (A) Measurement of the concentration of 70S, (B) Measurement of the concentration of Cy5 and Cy3.

8.3.2. Labeling Specificity

In order to confirm that the oligonucleotide binds exclusively the engineered loop and no unspecific binding is observed, negative controls were performed. Samples containing 50S from ZS-22 ribosomes, and 50S from bioCAN ribosomes were labeled in parallel with the Cy5 labeled oligonucleotide, as described before (Section 8.2). The diffusion coefficient of the two samples was measured with FCS (Section 4.10.1), and compared with the diffusion coefficient of the Cy5 labeled oligonucleotide, measured in the same conditions. The results, presented in Fig. 8.4 show that the diffusion coefficient of the labeled ZS-22 subunit is 25.8 $\mu m^2/s$, characteristic for labeled ribosomes, meaning that the labeling is specific and the sample contains no free unreacted oligonucleotide.The treated bioCAN subunit has a diffusion coefficient comparable to the one of the labeled oligonucleotide, supposedly due to the non perfect separation of the oligonucleotide in the purificaton step.
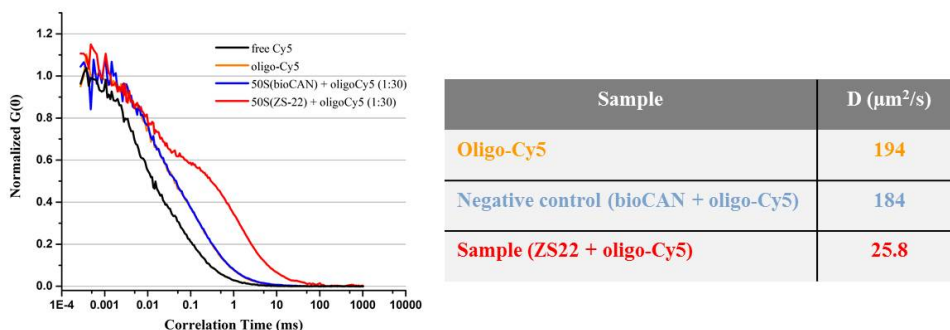
Sample	D (μm²/s)
Oligo-Cy5	194
Negative control (bioCAN + oligo-Cy5)	184
Sample (ZS22 + oligo-Cy5)	25.8

Figure 8.4.: (A) FCS curves of the labeled species: 50S from the ZS22 strain (red), 50S from the bioCAN strain (blue), oligo-Cy5 (orange) and Cy5 (black). (B) The diffusion coefficients of the species corresponding to the FCS curves in (A)

The control experiment proves that the labeled oligonucleotide binds only to the engineered loop, and no unspecific binding at the surface of the ribosome is observed. Moreover, the FCS data prove that the sample contains no free oligonucleotide and aggregates.

8.3.3. Detection of Biotin

The successful hybridizaton of the biotinylated oligonucleotide on the engineed loop of the rRNA was confirmed by agarose gel electrophoresis (Section 4.1.3). A sample containing 0.5 A_{260} (measured at a path length of 1 cm) of biotinylated ribosomes in RNA sample loading dye was run in a 2% agarose gel, at 200 V, for 20 min, in the cold room. Afterwards, the gel was incubated in a Qdot625 streptavidin conjugate solution for 30 min and washed two times with 20 mL mQ water, for 10 min. Detection was made using a Gel Imaging System. As a negative control, ribosomes without the biotinylated oligonucleotide were treated in the same manner as the sample, and loaded in the same agarose gel. The signal corresponding to the labeled biotin was detected only in the lane containing the sample, and not in the negative control (Fig. 8.5).

8.3.4. Activity

The activity of the labeled ribosomes was tested as described in Section 11 and compared to the activity of the unmodified ribosomes. The results, presented briefly in Fig. 8.6 and detailed further in Section 11.4.2 demonstrate that functionalization by hybridization of oligonucleotides to engineered loops does not influence the activity of the ribosomes.
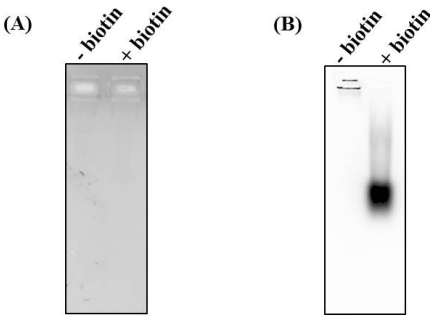
Figure 8.5.: Detection of biotinylated rRNA in a 2% agarose gel. The gel was imaged before labeling with the Qdot625 streptavidin conjugate (A) to test the background fluorescence of the samples. After labeling, the signal corresponding to a labeled rRNA is detected only in the positive sample.
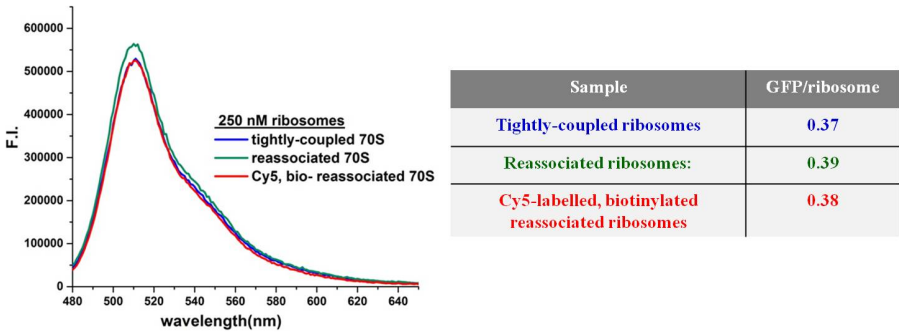

Sample	GFP/ribosome
Tightly-coupled ribosomes	0.37
Reassociated ribosomes:	0.39
Cy5-labelled, biotinylated reassociated ribosomes	0.38

Figure 8.6.: GFP production by 250 nM reassociated ZS-22 (green) and biotinylated, labeled ZS-22 ribosomes (red), measured as presented in Section 11.3

9

Optimizaton of the Plasmid for Single Molecule Experiments

9.1. General Considerations

The plasmid pRSET/GFPem was used as a bacterial expression vector. The pRSET vector carries a T7 promoter sequence, and is therefore suitable for the cell-free expression in the PURE system. Compared to the wild type GFP, the GFP Emerald (GFPem) derivative contains the S65T, S72A, N149K, M153T, I167T point mutations that improve the efficiency of maturation and folding at 37°C, and increase the intrinsic brightness ([Shaner et al., 2005]).

After a ribosome has reached a stop codon in a mRNA, the produced protein is released and the subunits dissociate in order to start a new translation step. In our experiments, to identify successful translation and folding of proteins (GFPem) on ribosomes with single molecule experiments, it is essential that the GFPem stays bound on the ribosomes, otherwise the dissociation would occur. Moreover, in order to test whether the subunits are dissociating during the first step of translation initiation, it is highly important that the 70S ribosomes do not dissociate after translation of the GFPem construct and start a new translation step.

To achieve protein stalling on the ribosomes, previous studies used the SecM translation arrest sequence ([Uemura et al., 2008], [Rosenblum et al., 2012], [Evans et al., 2005], [Cabrita et al., 2009], a 17-residue peptide sequence which interacts with the ribosomal exit tunnel to halt translation elongation. However, our experiments show that the SecM has a rather weak stalling efficiency, insufficient for single molecule experiments.

Therefore, the plasmid DNA containing the SecM sequence was optimized for better stalling efficiency, following suggestions from a recently published study ([Cymer et al., 2015]). A new variant of the SecM was constructed, which should offer a stronger translation arrest, and we named it SecMstr (Fig. 9.1). The stalling efficiency of the SecMstr and SecM constructs was then compared, using two

different methods: co-precipitation and confocal fluorescence detection (Section 9.3).

9.2. Plasmid Design

The pRSet plasmid contained, downstream the GFPem gene, a C-terminal extension composed of a 30-residue linker rich in Gly and Ser, followed by the SecM or SecMstr arrest sequence. The C-terminal extension spans the ribosomal tunnel, allowing the GFPem to emerge and completely fold while being still attached to the ribosome due to the SecM arrest sequence. (Fig. 9.1)
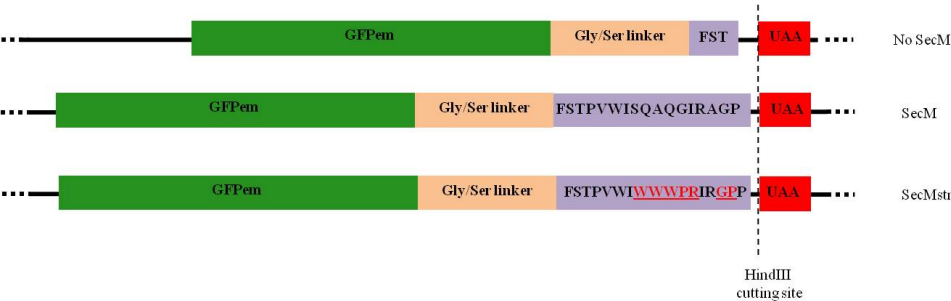

Figure 9.1.: Strategy for modification of the DNA in order to stall the GFPem on the ribosomes

A negative control with no stalling properties was also constructed, by deleting the last 14 residues of the arrest sequence.

The constructs were linearized, in order to remove the stop codon, and the stalling efficiency of the linear and circular plasmid was also compared. The linearization was performed by digestion with the HindIII Fast Digest enzyme, as described in Section 4.2.5. The successful linearization was confirmed by Agarose Gel Electrophoresis (Fig. 9.2).
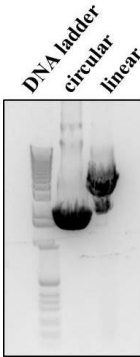

Figure 9.2.: Agarose Gel Electrophoresis the pRSET vectors, before (circular) and after (linear) digestion with the HimdIII endonuclease

9.3. Testing the Ribosome Stalling During Nascent Chain Synthesis

GFPem was expressed *in vitro* as described before (Section 4.6.2). After 2 h, the samples were tested for GFPem stalling on the ribosomes using two independent methods: co-precipitation and FCS measurements.

For the co-precipitation approach, adapted from [Rosenblum et al., 2012], the sample was overlaid on top of 200 μL sucrose cushion, and centrifuged: TLA 55/ 50 000 rpm/ 90 min. Only the heavy particles (i.e. ribosomes together with the stalled GFPem) are able to pass through the sucrose cushion, while the released GFPem remains in the supernatant. The fraction of bound GFPem was determined as the concentration of GFPem measured in the pellet, divided by the concentration of total GFPem (from pellet plus supernatant).

The stalling efficiency of the previously described DNA constructs (Section 9.2) was tested. (Fig. 9.3)
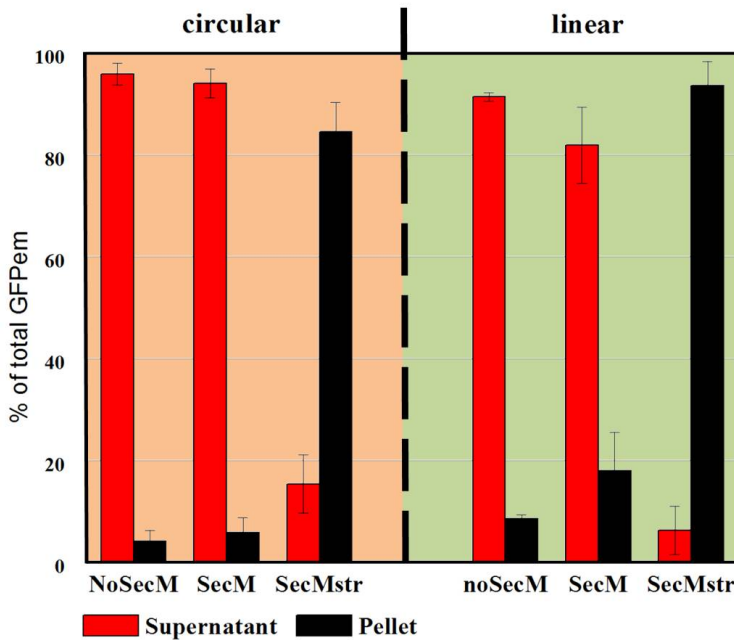

Figure 9.3.: Co-precipitation method used to test the stalling efficiency of the circular (pink background) and linear (green background) DNA constructs

As expected, in the case of the negative control, in which the arrest sequence was missing, the vast majority of the synthesized GFPem was released (95%). Surprisingly, the construct containing the SecM arrest sequence did not show a significantly better stalling than the negative control, as only a small fraction of GFPem was found in the pellet. In contrast to this, the SecMstr construct showed an impressive increase in stalling efficiency, since only 10% of the GFPem was found in the supernatant and the majority was measured in the pellet. (Fig. 9.3, pink background).

Moreover, the results show that the linearization of the constructs alone was rather insufficient to prevent the release of GFPem, but it did offer a small additional stalling effect to all the constructs. (Fig. 9.3, green background).

To confirm the improvement of the stalling efficiency of the SecM arrest sequence, FCS measurements, described in Section 4.10, were employed. The diffusion coefficient (D_0) of the GFPem synthesized in the samples described before was measured, and compared to the measured D_0 of free GFPem and Atto488 labeled ribosomes. Since the diffusion of ribosomes ($D_0 = 20 \mu m^2/s$) is significantly lower than the one of the free GFPem ($D_0 = 85 \mu m^2/s$), one can estimate whether the GFPem detected in the samples is bound or not on the ribosome by measuring its diffusion coefficient.

The measured diffusion coefficients are shown in Fig. 9.4. In the case of the GFPem synthesized using the linearized SecM plasmid, the D_0 was 55 $\mu m^2/s$, an intermediate value between the free GFPem and the Atto488 labeled ribosomes, meaning that most of the protein was released. In contrary, the measured D_0 of GFPem in the sample containing the linearized SecMstr was comparable to the D_0 of the ribosomes, which shows that the majority of the GFPem molecules were bound to the ribosomes.

Species		D_0
free GFPem		85 µm²/s
$^{SecM}_{lin}$GFPem	+	55 µm²/s
$^{SecM}_{lin}$GFPem		21 µm²/s
70S ribos-Atto488		20 µm²/s

Figure 9.4.: Fluorescence Correlation Spectroscopy used to test the stalling efficiency of the SecM and SecMstr arrest sequences

The co-precipitation and FCS data show that the SecMstr arrest sequence has an impressively improved stalling efficiency in comparison with the SecM sequence. For the single molecule experiments presented in this study, only the linearized plasmid containing SecMstr was used, to ensure the almost complete stalling of the GFPem on the ribosomes.

10

Tethering of biotinylated ribosomes on modified glass slides

10.1. General Considerations

Several aspects must be considered when immobilizing ribosomes on glass slides for performing single molecule experiments. First, the method must allow for specific, stable and reproducible attachment on the surface, with a low unspecific binding of ribosomes, translation factors and mRNA. Then, the ribosomes must contain an accessible functional group that enables surface tethering, while retaining the activity.

Several strategies for immobilization of active ribosomes have been described: unspecific attachment on nontreated quartz slides ([Perez and Gonzalez, 2011]), covalently linking to surface-exposed cysteine residues of ribosomal proteins ([Vanzi et al., 2005]) on amino-functionalized slides, or specific binding of biotinylated ribosomes on bioPEG modified slides coated with streptavidin. The last method was employed in this study, since it was reported to be highly robust and reproducible.

10.2. Immobilization Strategy

The slides were prepared as described in Section 4.5, using a mixture of PEG/bioPEG to passivate the glass surface and allow specific binding of biotinylated ribosomes. A flow chamber with a volume of 50 μL was assembled on a functionalized 20x40 mm glass slide, by adhering a coverslip on top of it using double sided sticky tape, that performed also as a spacer (Fig. 10.1).

After assembling the chamber, a solution containing 17 nM neutravidin was passed through the channel, and incubated for 2 min. Then, the slide was washed by flowing 5 mL Tico buffer into the channel, in order to remove the excess of unbound neutravidin. Theses steps ensure the binding of neutravidin
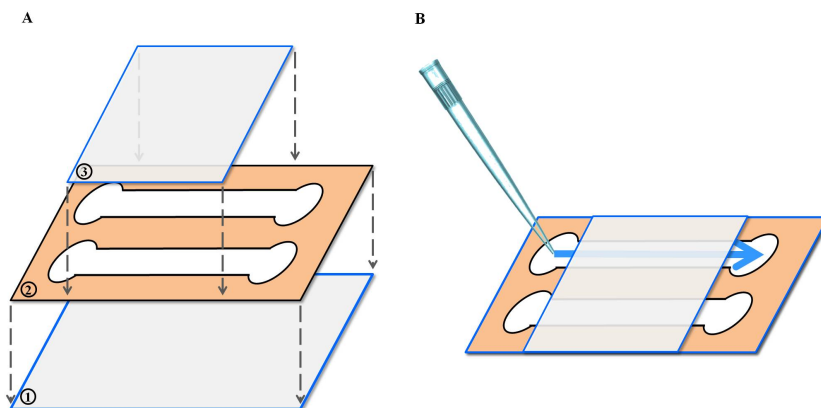
Figure 10.1.: Flow chamber for wide field measurements (B), assembled as described in (A) using a PEG/bioPEG glass slide (1), double sided sticky tape (2) and a second PEG glass slide (3).

molecules to the bio-PEG sites, so that another biotinylated molecule can be then bound to the existing neutravidin (Fig. 10.2).

The sample containing botinylated ribosomes was diluted to a final concentration of approximately 50 pM, and incubated in the flow chamber for 2 min. A wash step with 5 mL Tico buffer followed, to remove the unbound ribosomes.
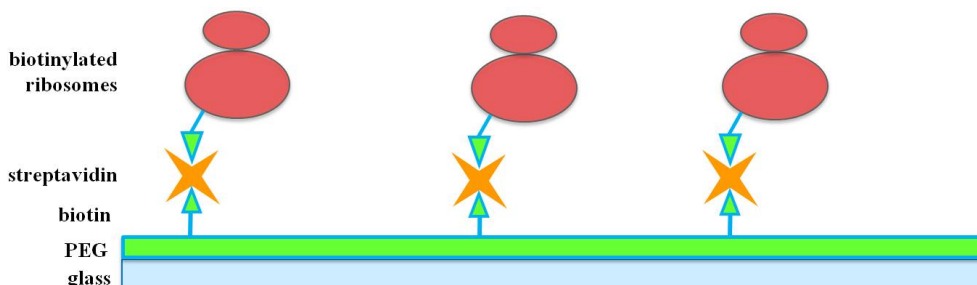

Figure 10.2.: Strategy for specific tethering of biotinylated ribosomes on modified PEG slides

The specific binding of Cy5 labeled bioCAN ribosomes was confirmed by performing negative controls, in which the flow chamber was prepared as described before, but without incubation with neutravidin. The number of red spots detected in the slides with and without neutravidin was compared at different concentrations, starting from 20 pM to 150 pM.

The negative control demonstrate that a low number of ribosomes bind unspecifically to the surface, since even at high sample concentration a low number of red spots are observed (Fig. 10.3, black curve). The binding curve in the case of neutravidin modified slides (Fig. 10.3, blue curve) shows that the number of Cy5 ribosomes bound to the surface increased exponentially with the increase in the ribosome concentration. The optimum concentration of biotinylated labeled ribosomes was determined

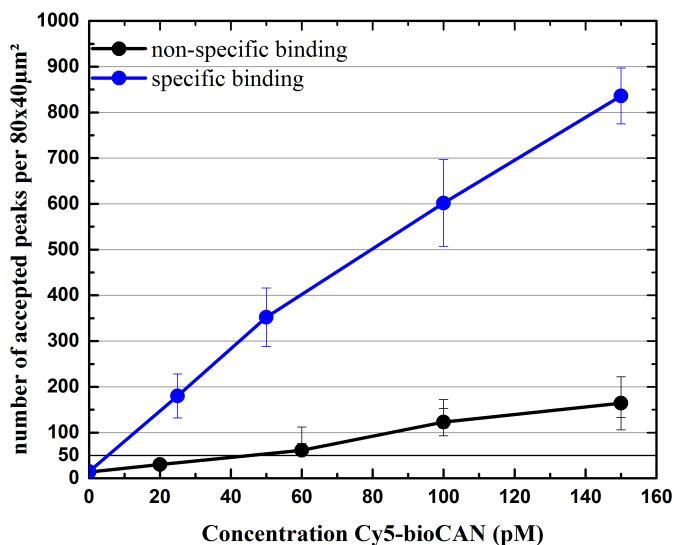**Figure 10.3.:** Specific (blue curve) and non specific (black curve) binding of biotinylated Cy5 labeled ribosomes on bioPEG modified glass slides

to be 50 pM, which was used for further wide field measurements. In this conditions, good statistics can be obtained from each experiment (approximately 300-400 particles per image) and the separation of spots is good enough to avoid artefacts in the analysis of the data.

11

Activity Test of the Ribosomes

11.1. Kinetics of GFPem Synthesis

Kinetics of GFPem synthesis was measured following its fluorescence signal, using a QM-7 spectrofluorometer, and a temperature controller was used to maintain a constant temperature of 37°C. The reaction components, with a total volume of 60 μL, prepared as described before (Section 4.6.2), were mixed in a 3 mm path length quartz cuvette. GFPem fluorescence emission spectra were recorded, exciting at λ_{exc}=465 nm and recording the emission between 480 nm and 650 nm, every 2.5 min up to 40 min, then every 5 min up to 60 min and finally every 10 min up to 240 min.

The recorded spectra were then corrected by substracting the background fluorescence spectra of the solvent measured in the same conditions. The resulting emission spectra were integrated, the area was converted in molar concentration using a calibration curve (described in Section 11.2), and plotted as a function of the measurement time.

11.2. GFPem Calibration Curve

The fluorescence emission spectra yield arbitrary fluorescence units as readouts. In order to convert these units into GFPem concentration, a calibration curve was made. GFPem standard was expressed in *E. coli* transformed with a plasmid containing exactly the same GFPem sequence as the one used for experiments. Also, a His-tag was attached to the end of the GFPem sequence in order to purify it using Nickel affinity chromatography. The GFPem stock was stored at -80°C in PBS, pH 7.4.

GFPem calibration solutions were prepared in Tico buffer, having concentrations between 5 nM and 300 nM, measured with a UV-VIS spectrometer. The fluorescence emission spectra of the solutions was measured in the same conditions as the sample: 37°C, slits: 0.5 nm (excitation monochromator) and 1 nm (emission monochromator). All the spectra were corrected for background intensities by

substracting the spectra of the solvent in the same conditions. The corrected spectra were integrated, and the areas were plotted against the GFPem concentration, to obtain the calibration curve.
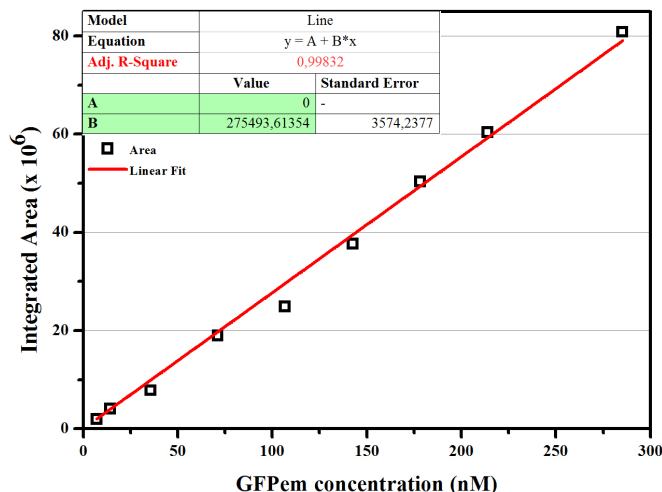

Model	Line	
Equation	y = A + B*x	
Adj. R-Square	0,99832	
	Value	**Standard Error**
A	0	-
B	275493,61354	3574,2377

Figure 11.1.: Calibration curve of GFPem for converting fluorescence arbitrary units into nM concentration

The calibration curve was remeasured periodically, to make sure that no errors are introduced by using an outdated one.

11.3. Activity of the Functionalized Ribosomes

The activity of the ribosome preparation was determined by the number of GFPem molecules produced, per ribosome, in an *in vitro* system. Accordingly, parallel reactions with a total volume of 25 μL were prepared as described before (Section 4.6.2), using the same concentration of modified ribosomes, and incubated at 37°C for 3 h, which is the time point after which the *in vitro* reaction reaches the saturation point. The reaction volume was then increased to 50 μL, and GFPem fluorescence emission spectra were measured as described before. The emission spectra were converted into molar concentration, and the average GFPem production, per ribosome, was compared.

11.4. The Influence of Functionalization on the Activity of the Ribosomes

11.4.1. Functionalization of the CAN 20/12-E Ribosomes

To validate our sample preparation procedure, the "home-made" CAN 20/12-E ribosomes were compared to the commercially available PURE system ribosomes. Then, the effect on the activity of the following modifications was investigated: *in vivo* biotinylation, described in Section 6, and fluorescence labeling using Cy5-NHS, described in Section 7).

The results (Fig. 11.2) show that the activity of the CAN 20/12-E ribosomes is comparable to the one of the PURE system ribosomes. In both cases, a fraction of 40% of the ribosomes produced GFP.
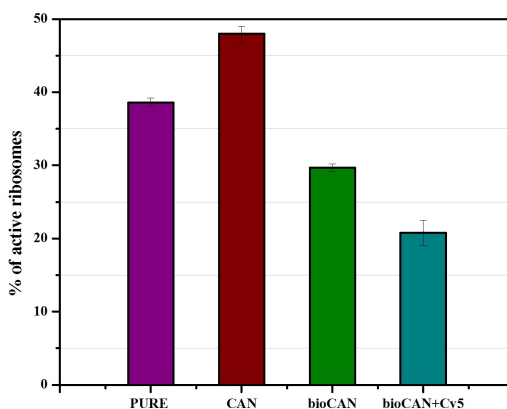

Figure 11.2.: Activity of the modified ribosomes

The procedure of *in vivo* biotinylation leads to an approximately 25% decrease in activity, which can be attributed not by the attachment of the biotin itself, but to the fact that bacteria were harvested at a later point of the cell growth. Overexpression of the mutant uL4 protein requires an extra induction step, so the cells were harvested at a later point than in the case of the wild-type ribosomes. Indeed, it has been shown that harvesting the cells in the early mid-log phase is optimal for the activity of the isolated ribosomes, in contrast to the late-log phase ([Bommer et al., 1997], [Dohme and Nierhaus, 1976]).

In addition to this, labeling with fluorescent dyes further reduces the activity of the ribosomes with 1/3 after. In order to check whether the attachment of the dyes or the labeling protocol is the reason for the loss of activity, a control experiment was performed. The ribosomes were treated using the same labeling protocol, but without adding the dye in the reaction mixture. The activity of this sample is comparable to the one of the labeled ribosomes, which leads to the conclusion that the effect of the labeling protocol itself, and not the presence of the dyes, is causing the loss of activity (Fig. 11.3).
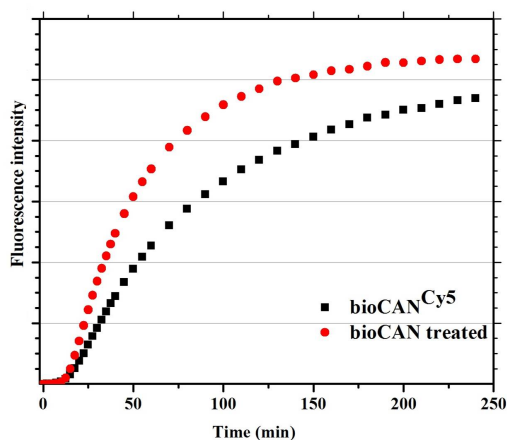
Figure 11.3.: Comparison of GFPem production for the bioCAN ribosomes labeled with Cy5 and bioCAN ribosomes undergoing the same treatment, without addition of the dye

11.4.2. Functionalization of the ZS-22 Ribosomes

In the case of ZS-22 ribosomes, the activity of the tightly-coupled 70S and the reassociated 70S was first compared. Then, the effect of functionalization by oligonucleotide hybridization was studied, by attaching both modified oligonucleotides simultaneously: the biotinylated one for binding to the 30S and the Cy5 labeled one for binding to the 50S. The results, presented in Fig. 11.4 show that the reassociated ribosomes have an activity comparable to the tightly coupled 70S, and that by functionalization with both Cy5 and biotinylated oligonucleotides, the activity does not decrease.
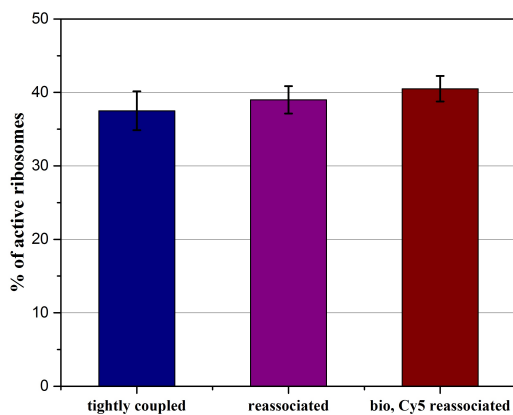

Figure 11.4.: The effect of functionalization on ZS-22 ribosomes

11.5. Number of Translation Cycles

In an *in vitro* transcription-translation kit, only a fraction of ribosomes is active, and one ribosome can undergo multiple cycles of translation. One question that arises from this is how many synthesizing cycles is a ribosome able to perform, and how can this number be improved.

Therefore, the circular construct containing the SecM arrest sequence was used, where the stalling was the most inefficient (Fig. 9.3), and considered the final amount of synthesized GFPem as the maximum that the system without stalling could achieve. In contrast to this, when the SecMstr was used, the ribosomes can undergo maximum one cycle of translation, since the stalling is extremely efficient. Considering these two quantities of GFPem, one can calculate the number of productive cycles. As shown in Fig.11.5, the CAN and bioCAN ribosomes underwent an average of merely two synthesizing cycles, while the Cy5 labeled bioCAN ribosomes slightly more than one cycle on average. This suggests that the biotinylation of the ribosomes affected only the activity, but not the number of active cycles. However, the additional labeling treatment affected the total productivity, by reducing both the fraction of active ribosomes and the number of productive cycles.
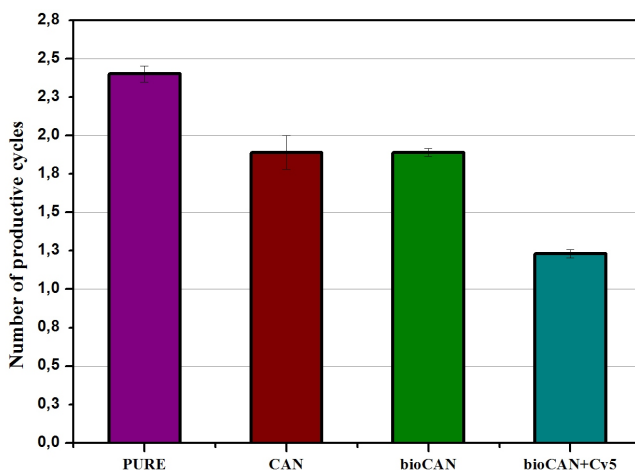

Figure 11.5.: The number of translation cycles performed by the modified ribosomes

Translation Initiation of Canonical mRNA with 70S Ribosomes

12.1. Experimental Design

In order to test the initiation of canonical mRNAs with 70S ribosomes, "empty" reassociated ribosomes were used, prepared from the ZS-22 strain, as described in Section 5. The ribosomes were labeled site-specifically on the engineered loop at the large subunit, as described in Section 8, with a Cy5 labeled oligonucleotide. Furthermore, a biotin molecule, for surface tethering was added site-specifically at the small subunit, using the same protocol. The DNA used for the *in vitro* synthesis of GFPem was described in Section 9, and it leads to a canonical mRNA after transcription, since it contains the SD sequence. In addition, a high excess of unlabeled 50S subunits was added to the reaction, in order to minimize the probability for a 30S subunit to reassociate with a labeled 50S subunit, after dissociation.

The 30S-binding initiation and the 70S-initiation events were identified using Two Colour Coincidence Detection (Fig. 12.1):

(A) In the case of 30S-binding initiation, the subunits dissociate during translation initiation, so that the labeled 50S subunit of a translating 70S ribosome would be replaced by a non labeled 50S subunit, and GFPem would be stalled on a non labeled ribosome.

(B) In the case of initiation with 70S, during translation initiation the subunits do not dissociate, and the GFPem would be stalled on a labeled 70S ribosome.
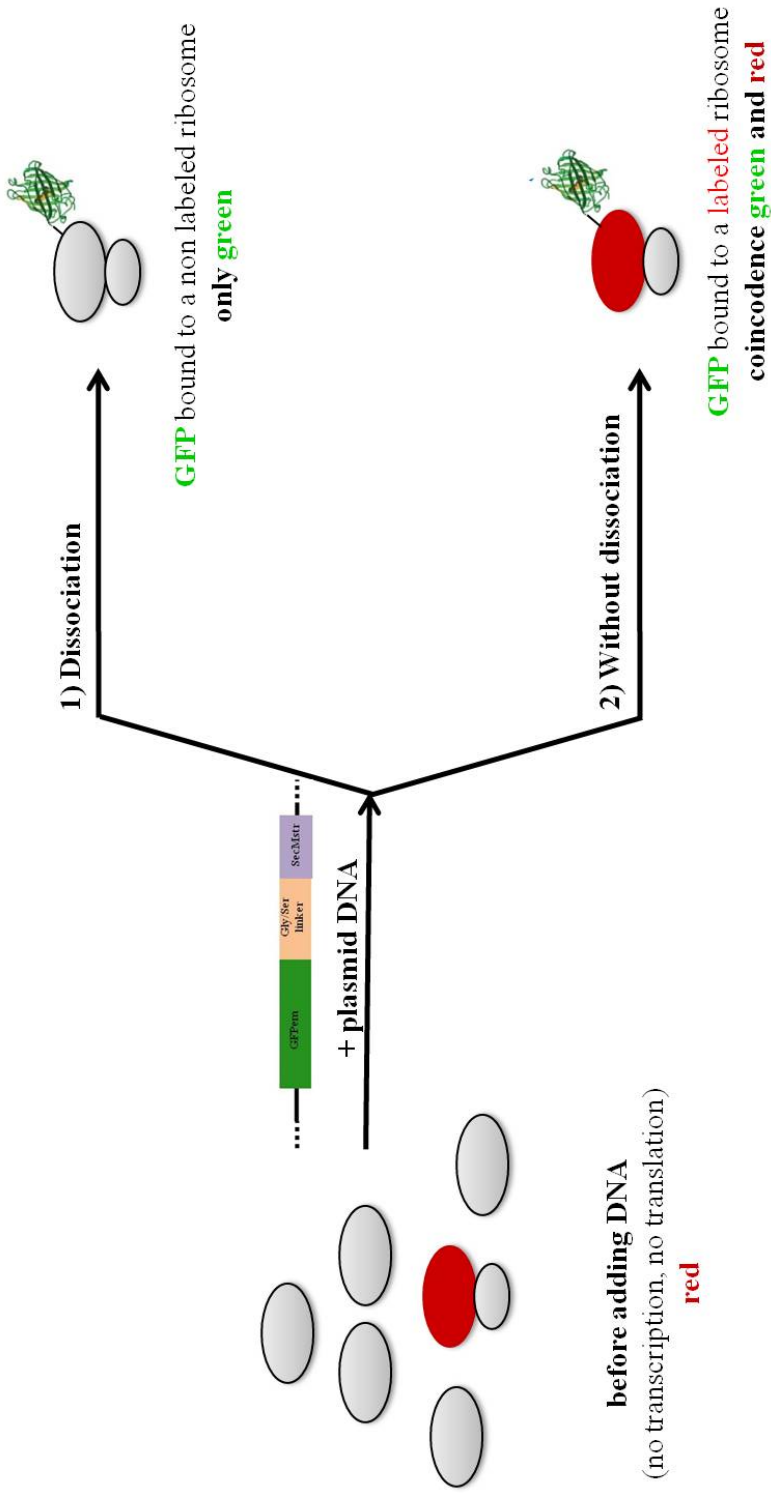
Figure 12.1.: Testing initiaton of a canonical mRNA by full 70S ribosomes. Reactions were prepared with the PURE system as an *in vitro* transcription-translation kit, using ribosomes labeled site-specifically at the large subunit, the optimized SecMstr DNA to ensure GFPem stalling, and a 5 times excess of unlabeled 50S subunits. If dissociation of ribosomes occurs during initiation, it would lead to a labeled 50S and a non labeled 30S which would associate to a non labeled 50S (in excess in the reaction mix) to produce a GFPem stalled to a non labeled ribosome. In contrast to this, if site-specifically labeled 70S initiate translation as full ribosomes, the GFPem would be bound to a Cy5 labeled ribosome. These two populations of GFPem, bound to a non labeled or to a labeled ribosome, can be identified and quantified with Two Colour Coincidence Measurements (TCCD).

Practically, the TCCD measurement was performed as described in Section 4.10.2. The samples presented in the next sections were diluted to a concentration of 10 pM ribosomes, and the oxygen scavenging system was added as explained in Section 4.9. In order to avoid solvation of molecular oxygen in the buffer during the measurement time, wells of approximately 700 μL were assembled, by cutting out one third of an eppendorf tube and attaching it to a PEG modified glass slide with UV curing adhesive (Fig. 12.2).
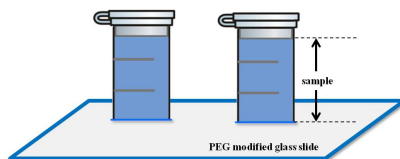

Figure 12.2.: Construction of the wells used for the TCCD experiments

Before performing the *in vitro* reaction, several control experiments were performed, in order to evaluate dissociation of ribosomes for other reasons than initiation of translation, such as:

- low concentration of ribosomes used for TCCD experiments

- components of the PURE system

- excess of 50S added in the reaction mix

These controls are detailed and discussed in the next two sections.

12.2. Controls. Stability of the Labeled Ribosomes

12.2.1. Stability of the Loop-oligonuceotide Interaction

As mentioned in Section 8.1, hybridization of labeled oligonucleotides on engineered loops leads to a complex with a K_D of 5 nM, higher than the usual picomolar concentration employed in single molecule studies. A potential dissociation of the labeled oligonucleotide in the experiment described in Section 12.1 would be falsely considered as an exchange of subunits, since the produced GFPem would be detected as diffusing bound to a non labeled ribosome (Fig 12.3).
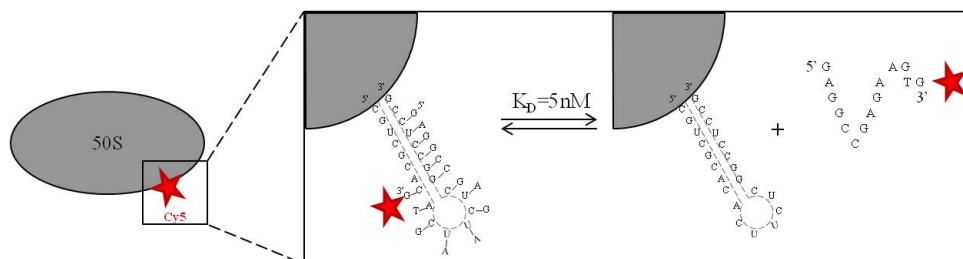

Figure 12.3.: Dissociation of the loop-labeled oligonucleotide complex

The stability of the complex was investigated at single molecule level, with wide-field measurements. 50S subunits of ZS-22 ribosomes were labeled with Cy5-labeled oligonucleotide, according to the protocol described before (Section 8.2). The sample was then diluted to a 50 pM concentration, in Tris-polymix buffer, and bound unspecifically on PEG-modified surfaces, immediately after dilution. Since the labeled oligonucleotide is not sticking to the glass surface at this concentration, the detected spots were identified as labeled 50S subunits. The oxygen-scavenging mix was added in order to minimize the bleaching and blinking of the dye, the slide was incubated at 37°C and the density of the spots was monitored for 2 h. The same procedure was repeated for the 30S subunit, hybridized with a Cy3-labeled oligonucleotide (Fig. 12.4)
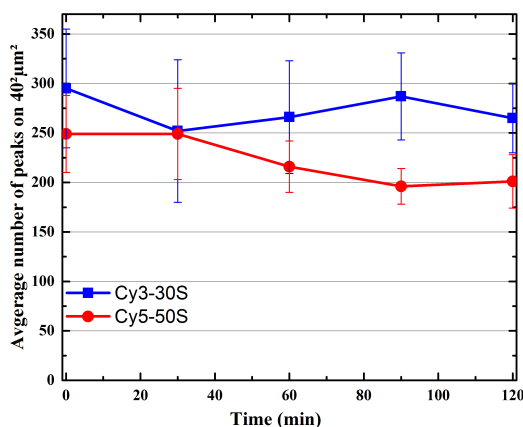

Figure 12.4.: Stability of the loop-oligonucleotide interaction, tested in wide field

The results presented in Fig 12.4 show that for Cy3, the density of detected spots does not decrease during two hours, proving that the Cy3 oligonucleotide bound to the small subunit is stable in this time range, at 37°C. However, in the case of the Cy5 labeled oligonucleotide bound to the large subunit, there is an obvious dissociation reaction in these conditions, since the number of spots decrease with approximately 10% after one hour and 20% after 2 hours. Therefore, single molecule experiments in which ribosomes labeled at the large subunit with the Cy5 oligonucleotide were employed, should not exceed one hour in order to avoid the dissociation step.

12.2.2. Stability of the Ribosomes in the Reaction System

When preparing samples containing ribosomes for single molecule experiments, there is a high chance that they dissociate into subunits due to the low concentrations. Therefore, the maximum TCCD measurement time was first determined, that allows acquisition of good statistics, but avoiding the dissociation step. In order to identify full ribosomes from single subunits, the 70S ribosomes were labeled with Cy5 at the large subunit and with Cy3 at the small subunit, as described in 8. In this way, the coincident blue and red signals correspond to a full ribosome, while the non coincident fluorescence

signals correspond to dissociated subunits. TCCD measurements were performed for one hour, immediately after labeling. The degree of red and blue coincidence was monitored in time, and compared to the value of the coincidence determined initially. The data shows that the number of coincident red and blue signals is constant (having a value of 20%) in the first 20 min of measurement (Fig. 12.5, red curve), which was chosen as the measurement time for the following TCCD experiments. After 20 min, the coincidence number decreased, presumably due to dissociation of subunits. A negative control was performed in which the dilution of double labeled ribosomes was made in PBS buffer, and TCCD measurements were made as before. The lack of Mg^{2+} in the buffer composition leads to dissociation of subunits, confirmed in the single molecule experiment, in which an extremely low degree of coincidence is observed (Fig. 12.5, black curve)
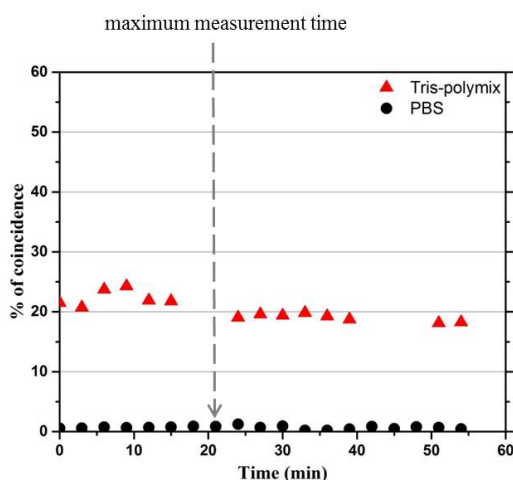

Figure 12.5.: Selection of the measurement time for TCCD measurements, to ensure the stability of the sample

Subsequently, controls were performed in order to analyse whether the ribosomal subunits dissociate during the 2 h incubation in the reaction system, at 37°C, without adding the DNA. These controls are extremely relevant, since we had to quantify the dissociation events that resulted exclusively by the initiation step. Double labeled ribosomes were used also in this case, and TCCD measurements performed before incubation show that 20% of the total particles were full ribosomes, while the rest of the molecules were supposedly single labeled subunits (Fig. 12.6).

Samples containing 500 nM double labeled ribosomes were then incubated in PURExpress mix, and in the reaction mix (PURExpress plus a 5 times excess of unlabeled 50S) respectively, without adding the DNA, for 2 h, at 37°C, and the fraction of double labeled particles was determined with TCCD. For both conditions, the percentage of double labeled ribosomes decreased to 17% after incubation (Fig. 12.6). This shows that the factors included in the PURE system mix and the presence of the excess of unlabeled 50S subunits determine dissociation of 70S ribosomes. This effect was taken into account when the *in vitro* reaction (Fig. 12.1) was performed and measured with TCCD, so that a positive control experiment was designed accordingly (Section 12.3, and Fig. 12.9).

Stability of the 70S ribosomes was analysed also on the surface, using PEG-modified glass slides. Double labeled ribosomes were bound unspecifically on the surface of PEGylated slides, and colocalization
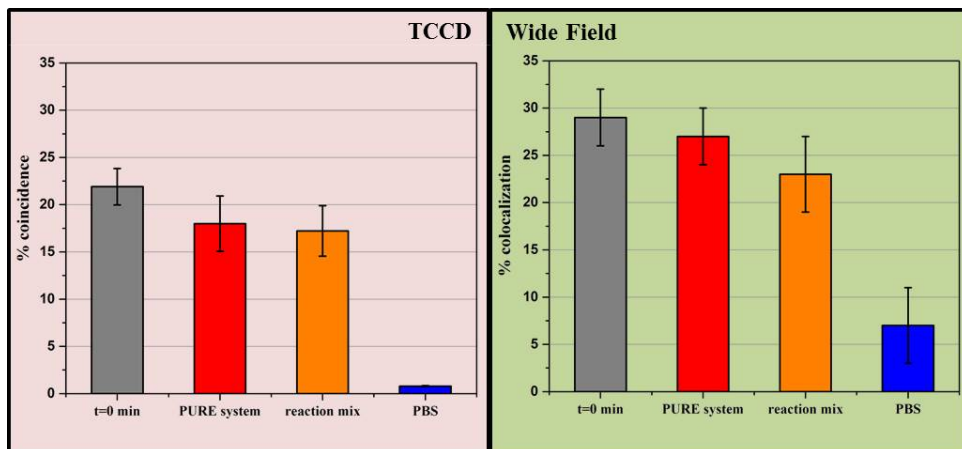
Figure 12.6.: Stability of the double labeled ribosomes, investigated with TCCD (pink background) and wide field (green background). The fraction of double labeled ribosomes was determined before incubation (grey column), and after incubation in PURE system mix (red column) and in the reaction mix (orange column). As a negative control, the double labeled ribosomes were incubated in PBS, in which dissociation occurs spontaneously (blue column)

of Cy5 and Cy3 was determined at time zero, with a wide field microscope (Section 4.11). The colocalization events correspond to full 70S, while single red and blue signals correspond to dissociated subunits. Immediately after labeling, a fraction of approximately 30% colocalized spots were detected. Afterwards, PURExpress mix and the oxygen scavenging system were added to the channel, the slide was incubated at 37°C, and colocalization was measured after 1.5 h. The measurement was repeated by incubating unspecifically bound ribosomes in the reaction mix, at 37°C for 1.5 h. The results, summarized in Fig 12.6 (green background) show that the fraction of full 70S ribosomes decreases to 27% after 1.5 hours incubation in PURE system and to 23% after 1.5 h incubation in the reaction mix. The negative control, in which the incubation was made in PBS indicates that dissociation of subunits occurs in these conditions, as the colocalization events decrease to 7%The results confirm the conclusion of the TCCD experiments illustrated in Fig. 12.6, that the incubation in the reaction mix leads to dissociation of the full 70S ribosomes.

12.3. Results of the Single Molecule Study

The *in vitro* reactions were prepared as detailed in Section 4.6.2, and contained 500 nM site-specifically Cy5 labeled ribosomes and 5.5 nM DNA. Moreover, 2.5 μM unlabeled 50S subunits were added, and the reaction mix was incubated at 37°C, for 2 h, and on ice for 15 min. The sample was then diluted to 5 nM ribosomes in Tris-polymix buffer, and FCS measurements were performed in order to calculate the diffusion coefficient of GFP. The obtained value, of 20 μm^2/s (Fig. 12.7), confirms that the GFPem is stalled on the ribosomes, and the release is minimal. The sample was then diluted to 10 pM ribosomes and TCCD measurements (Section 4.10.2) were performed. The red and blue bursts were recorded for 20 min, and the fraction of coincident bursts was determined using in-lab written Matlab routines.
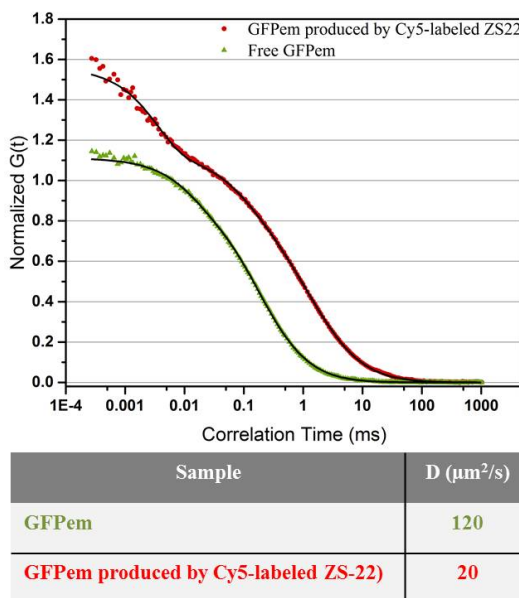
Sample	D (μm²/s)
GFPem	120
GFPem produced by Cy5-labeled ZS-22)	20

Figure 12.7.: Diffusion of GFPem produced by the Cy5-labeled ZS-22 ribosomes (red), compared to the diffusion of the free GFPem (green)

As described in Section 12.1, the coincident red and blue signals (approximately 16%, as shown in Fig. 12.9, orange column) correspond to initiation with 70S events, while the non-coincident blue bursts are identified as 30S-type initiation events.

However, because of the low concentrations to which the sample was diluted for the single molecule experiments, labeled ribosomal complexes containing a bound GFPem formed by initiation with 70S can dissociate. This event would produce a labeled 50S, an unlabeled 30S and a free GFPem, and it would be falsely interpreted as 30S-binding initiation, since the Cy5 and GFPem signal would not be coincident. Moreover, we showed (Fig. 12.6) that approximately 20% of ribosomes can dissociate because of the reaction conditions and not because of the initiation step, but these events would be detected as 30S-binding initiation events. Furthermore, blinking or bleaching of the Cy5 fluorophore can bias the interpretation of the TCCD experiments. For example, a labeled ribosome carrying GFPem (initiation with 70S), would be falsely detected as an unlabeled ribosome carrying GFPem (initiation with 30S) if the dye was in a non fluorescent state. In order to correct for these false 30S-binding initiation events, a positive control was prepared, consisting of an *in vitro* reaction containing the same components as previously described, but without adding the excess of unlabeled 50S subunits. The mix was incubated at 37°C, for 2 h and TCCD measurements were performed in the same manner as described before. Since in this case no exchange of subunits can take place, theoretically all the GFPem bursts should be coincident to a Cy5 signal, unless dissociation occurred during the incubation or the dilution step, or the fluorophore was in a non florescent state. Indeed, the result of the single molecule experiment shows that only approximately 45% of the GFPem was coincident to a Cy5 labeled ribosome.

Therefore, the percentage of 16% events with 70S-type initiation obtained before (Fig.12.9, orange col-
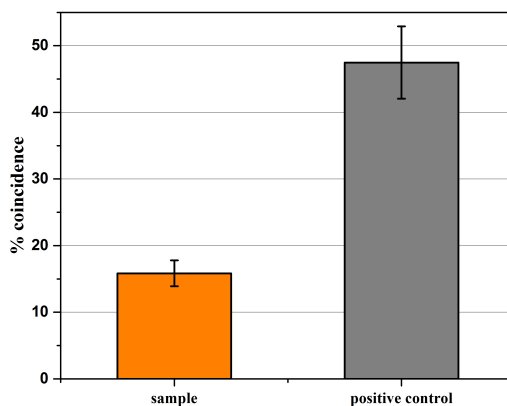
Figure 12.8.: Coincident events measured in the positive control (grey column) and the sample (orange column)

umn) was corrected to the maximum of 45% coincidence measured in the sample in which theoretically 100% coincidence should be observed (Fig.12.9, grey column). The final result, presented in Fig. 12.9, show that from the total number of successful translation events, 30% occurred with initiation by 70S ribosomes, and 70% developed in the classical 30S-binding type.
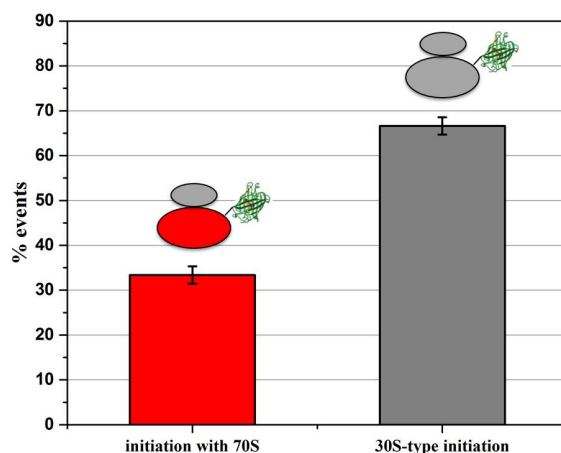
Figure 12.9.: Corrected values for initiation modes: initiation with 70S (red column) and 30S-type initiation (grey column)

This is the first study that tests initiation of canonical mRNAs by 70S ribosomes. The results presented here prove that besides the already described 30S-binding initiation mechanism, 30% of the canonical mRNAs were translated by full 70S ribosomes, without dissociation into subunits.

Part IV.

Discussions

13
Discussion

13.1. Reassociation of Ribosomes

In order to test the mechanism of initiation with 70S ribosomes, it is necessary that the ribosomes are purified as 70S particles, and do not contain bacterial mRNAs, since in our study, the constitutive mRNA would be translated first, followed by dissociation of subunits when the stop codon is reached. In this respect, reassociated ribosomes were employed (Section 5), prepared starting from crude 70S ribosomes, dissociated into subunits, which were then reassociated to form 70S particles. By employing sucrose gradient centrifugations we confirmed that the reassociated ribosomes stay associated also after storing the sample at -80°C.

One key step in this procedure is the reassociation step, in which the 30S and 50S subunits were incubated at 40°C in a 2:1 ratio. This ensures that most of the 50S subunits are consumed in the reaction, so that in the gradient purification, the corresponding peak will not overlap with the 70S peak. Moreover, in order to purify the pure 70S fraction, free of 50S, only two thirds of the peak were collected. An impurification with 50S would bring errors in the measurement of the ribosome concentration, and in the single molecule experiment, since the 50S subunit contains the fluorescent dye.

Regarding the activity, the reassociated ribosomes are comparable to the crude 70S (Section 11.4.2). In principle, it is expected that by reassociation, more active ribosomes are prepared, considering that factors, tRNAs, mRNAs, subunits, and polysomes are removed. Nevertheless, compared to the purification of crude 70S, the reassociation procedure takes longer, and it involves three rate-zonal purifications (for preparation of: tightly-coupled 70S, ribosomal subunits, and reassociated ribosomes) instead of one. The lengthy procedure and extra necessary steps can explain the decrease in activity of the purified reassociated 70S.

13.2. Functionalization of Ribosomes

In order to observe ribosomes at single molecule level, they have to be labeled with high quantum yield dyes, and for surface tethering, a biotin was added. For each functionalization, the labeling and purification protocols, and activity of the modified ribosomes are described.

In the case of labeling with fluorescent dyes, two approaches have been employed: on the one hand, unspecific labeling of the accessible lysines with NHS functionalized Cy5 (Section 7), and on the other hand, high-efficiency tagging of a mutant loop in the 23S rRNA via oligonucleotide hybridization (Section 8).

Labeling of ribosomes with NHS dyes leads to a non uniform population of fluorescently labeled 70S, since there are numerous accessible lysines at the surface of the ribosomes. In order to optimize the protocol in the sense of obtaining a high labeling ratio and activity, several parameters were investigated: the dye, the reaction buffer, the excess of dye, the incubation time and the temperature. Although the original protocol ([Milon et al., 2007]) employs a labeling buffer containing 15 mM Mg^{2+}, better results were obtained when the $Mg^{2}+$ concentration was reduced to 10 mM. Two different temperature conditions were tested: 4°C with overnight incubation, and 37°C using an incubation time of 20 min. The second one gave better results in respect to the activity of the labeled ribosomes. Two red fluorescent dyes were tested: Cy5-NHS and Alexa647-NHS. The first one provided a higher labeling ratio, presumably because of the smaller size and a low positive charge (+1, compared to -3), and it was chosen for further experiments. The conditions which lead to a high labeling ratio of 7 Cy5/ribosome and satisfactory activity are presented in Section 7, while increased incubation times lead to a considerably decreased activity. Longer reaction times and a higher excess of dye did not improve the labeling ratio, suggesting that this is the maximum number of lysines that are accessible for labeling on the surface of the ribosome. The labeled ribosomes were approximately 1/4 less active than the wild type ribosomes. This decrease in activity was determined by the effect of the labeling procedure and purification rather than the presence of the fluorophore on the ribosome.

The second labeling method involves specific hybridization of a Cy5-labeled oligonucleotide to engineered loops in the rRNA. Compared to the previously described method, this approach has numerous advantages: the ribosomes are purified as a homogenous population of single labeled particles, and approximately 98% of the ribosomes are labeled. Furthermore, the labeling site is engineered far from the spots of the ribosome involved in translation, so that the mutant labeled ribosomes retained more than 90% of activity as compared to the wild type ribosomes. However, several aspects have to be considered when performing single molecule experiments using the site-specifically single labeled ribosomes. First, the K_D of the loop-oligonucleotide complex is 5nM ([Dorywalska et al., 2005]), higher than the picomolar concentrations used for single molecule experiments. Nonetheless, it was reported ([Petrov and Puglisi, 2010]) that the relatively high apparent K_D is accompanied by slow rate of the oligonucleotide dissociation reaction (7 x 10^5 s^{-1}). This indicates that the oligonucleotide binding is sufficiently long lived for single-molecule experiments that are performed in picomolar concentration range. We performed control experiments in order to confirm that the labeled oligonucleotide is attached to the ribosome throughout the single molecule experiment, at 37°C, in Tris-polymix buffer, for 2 h. We showed (Section 12.2.1) that in the case of the Cy3 oligonucleotide bound to the small subunit, the complex is stable for 2 h, while the Cy5 labeleded oligonucleotide bound to the large subunit substantially dissociated after 1 h. Therefore, the sample was not measured at pM concentrations after longer than 1 h. In addition to this, having one label on the ribosome creates further complications for single molecule studies: the fast photobleaching and blinking of the fluorophore, phenomena

which complicate the interpretation of the results and limit the observation time. Therefore, an oxygen scavenging system has to be used in this case.

Ribosomes were also biotinylated for specific tethering on biotin functionalized glass slides coated with streptavidin. The first strategy involved the *in vivo* covalent binding of biotin to the N terminus of the ribosomal protein uL4 (Section 6), which lead to a population of ribosomes containing both the modified and the wild type particles. The activity test showed a 1/3 decrease in comparison to the non modified ribosomes, presumably due to the fact that the bacteria were harvested at the late exponential phase. When purifying wild type ribosomes, cells were harvested in the early exponential growth phase, at a maximum OD_{600} of 0.8. However, in the case of *in vivo* biotinylation, an additional induction step was necessary, which shifted the harvesting time to the late exponential growth phase. Several induction times were employed, and the activity and biotinylation of ribosomes was tested. A compromise between a reasonable biotinylation degree and activity is obtained with an induction time of 1h, while longer induction times increase the biotinylation rate, but decrease the activity. The second biotinylation approach involved hybridization of a biotinylated oligonucleotide to an engineered loop in the 16S rRNA (Section 8), which did not affect the activity of the ribosomes. The correct binding and specificity of the reaction was confirmed by labeling the ribosomes with an oligonucleotide with the same sequence, labeled with Cy3.

The method for functionalization of ribosomes is chosen according to the design of the single molecule experiment that will be performed. In single molecule studies on translation, the activity of the modified particles is obviously an issue that has to be considered. Moreover, the labeling method has to be chosen accordingly. On the one hand, a high number of fluorescent dyes unspecifically bound on the ribosome leads to a high background in red, but it ensures that all the particles are labeled with at least one fluorophore. On the other hand, site-specifically labeling of ribosomes provides a uniform sample of single labeled particles, but the single molecule study requires the presence of oxygen scavengers in the buffer, which are incompatible with *in situ* GFP production since the GFP chromophore maturation reaction requires molecular oxygen. For the current study in particular, the objective was to add a fluorophore exclusively on one subunit and a biotin on the other subunit of reassociated ribosomes. In this sense, two strategies were considered. The first one involved unspecifically labeling of tightly-coupled bioCAN 70S with Cy5-NHS, followed by dissociation into subunits, and reassociation of a red labeled 30S with a non labeled biotinylated 50S. This method allows the production of a low amount of sample, since only a small quantity of tightly coupled ribosomes can be labeled in the first step, and in addition, there is a loss of sample in the reassociation step. Also, compared to the wild type ribosomes, both the *in vivo* biotinylation and the labeling procedures lead to a decrease in activity.

The second possible strategy consisted of reassociation of unlabeled ZS22 ribosomes, followed by the labeling reaction with two oligonucleotides simultaneously: one specifically binding the large subunit, labeled with Cy5 and the second one specific for the small subunit, functionalized with biotin. This method has the advantage that labeling is made after the reassociation reaction, so that higher amounts of sample can be produced. Moreover, the activity of the ribosomes does not decrease after labeling, therefore we chose this procedure of functionalization for the single molecule study. GFPem production was performed in an eppendorf, at nanomolar concentration of ribosomes, and the reaction was analysed afterwards with single molecule methods, so that adding the oxygen scavenging cocktail for the final measurement did not interfere with the GFPem synthesis.

13.3. Stalling and the Number of Productive Cycles

When testing the dynamics of the ribosomal subunits during initiation using single molecule experiments, it is essential that the stalling of the produced protein (GFPem) is almost 100% efficient, so that the subunits will not dissociate after translation. In this respect, previous studies used the SecM arrest sequence, a short polypeptide induces translational stalling when synthesized on the ribosome, by interacting with the 100 Å ribosomal tunnel. However, when adding the SecM downstream the GFPem gene, our experiments showed that stalling efficiency was rather poor. By replacing the SecM arrest sequence with the SecMstr (detailed in Section 9), the release of GFPem was significantly reduced (Section 9.3). Another alternative for increasing the stalling effect of the DNA construct is the linearisation of the plasmid, thereby removing the stop codon and preventing the protein release. However, this method showed only a slight improvement in the stalling efficiency.

In order to understand the strong stalling effect of SecMstr, one has to consider that mechanical pulling forces acting on the nascent chain can weaken or even abolish stalling on the ribosome. The folding of the extremely stable β-barrel GFPem exerts considerably high forces (30 pN) (unpublished data), rendering the stalling on the SecM arrest peptide inefficient. The increased efficiency of the SecMstr can be attributed to the consecutive hydrophobic Trp residues, which stall translation even in the presence of a strong pulling force ([Cymer et al., 2015]). Moreover, the SecMstr sequence contains two consecutive Pro residues, proved to contribute to stalling. The aminoacid Pro, which contains an imino group instead of a primary amino group, is a poor substrate for peptide bond formation, both as a donor in the P site and as an acceptor in the A site of the ribosome. When a pair of two consecutive Pro are translated, stalling results from the slow rate of peptide-bond formation between the Pro located in the P-site and the Pro-tRNA in the A-site ([Doerfel et al., 2013], [Peil et al., 2013], [Chevance et al., 2014]). Also, the co-existence of two residues with a limited degree of freedom in the ribosomal peptidyl transferase centre inhibits a further amino acid incorporation.

Another interesting concept that was tested in this work was the number of productive cycles (Section 11.5). The results show that on average, ribosomes are able to undergo two synthesis cycles, a number that is considerably low for both modified and wild type ribosomes. The low number of cycles and consequently the weak productivity can be mostly attributed to the limitations of the *in vitro* system, namely accumulation of inhibitory by-products and depletion of energy resources, which constitute a major problem in the field. Employing a Continuous-Exchange Cell-Free (CECF) system ([Katzen et al., 2005], [Kim and Choi, 1996]), where an exchange of substrates and by-products takes place, raised the productivity of the sample (approximately 15 times) thanks to the higher number of productive cycles completed by the active ribosomes.

13.4. TCCD Measurements

There are several problems that have to be considered when performing TCCD measurements on samples containing ribosomes. First, the 70S ribosomes can dissociate into subunits when diluted to picomolar concentrations, leading to the release of GFPem, which would produce artefacts in the interpretation of the data analysis. For example, if a red labeled ribosome carrying GFPem (70S initiation type) dissociates during the dilution step, it would lead to a red labeled 50S, a free GFPem and a non labeled 30S. These components would not coincide in TCCD, therefore the event would be interpreted as a 30S binding event. In order to overcome this problem, a control experiment was performed, treated as the

sample, but in which the excess of 50S subunits was not added. The degree of coincidence corresponds to the maximum degree of coincidence that can be reached using this particular system, and the results of the final sample were compared to this number.

Another problem in TCCD studies is the imperfect overlap of the red and blue confocal detection volumes, which leads to an underestimation of the number of coinciding events. Optimal measurements require a careful choice of experimental conditions and acquisition parameters in order to maximize the overlap between the two detection volumes. For a precise calculation of the overlapping volume, it is necessary to measure a 100% double labeled standard, containing exactly the same fluorophores as the sample. The number of coinciding events of the sample should be then normalized to the number of coinciding events of the standard. In our case, the coincident events detected in the standard were more than 95%, therefore the result was not corrected.

Moreover, the photophysics of the dyes can lead to artefacts, especially in the case of single labeled biomolecules, since the fluorophores may cross into undetectable dark states during their trajectory across the confocal volume. Therefore, an oxygen scavenging system was used. Since the Glucoes oxydase/catalase (Gox) system has a high background in TCCD when used in usual working concentrations, we used the protocatechuic acid/protocatechuate-3,4-dioxygenase (PCA/PCD) system and Trolox. Moreover, we obtained better resuls with the PCA/PCD than with the Gox system also in wide field experiments in which we employed double labeled Cy3/Cy5 ribosomes unspecifically tethered on bare glass slides. For the same double labeled sample, the colocalization ratio was 30% when we used the Gox system, and 45% when we used the PCD system.

13.5. Surface Passivation for Single Molecule Studies

When biomolecules are probed at the single-molecule level, they can be immobilized on a glass surface, which allows a long-term observation. However, the immobilization procedure can lead to unwanted interactions of the biomolecules with the surface, so it is essential to passivate the glass slide in order to make it inert. Moreover, compared to proteins, ribosomes have a higher tendency to bind unspecifically to surfaces, therefore a rigorous protocol for preparation of microscopy slides had to be developed.

The first attempts to tether ribosomes on surfaces was by physical absorption on bare quartz slides, a method that retains a certain activity in translation ([Perez and Gonzalez, 2011]). Subsequently, further methods have been developed for glass surface passivation to allow only specific binding of ribosomes. We assayed three of these strategies: the BSA/bioBSA system ([Jeyachandran et al., 2010]), which displayed a high background in blue, the PEG/bioPEG blocking ([Lamichhane et al., 2010]), and the double passivation with PEG ([Chandradoss et al., 2014]), in which two rounds of incubation in PEG were performed to obtain a high density of polymeric layer. The most robust was the second one, presented in detail in Section 4.5. To achieve reproducibility, all steps in the passivation protocol were strictly followed. Since the PEG-NHS is extremely reactive, aliquots were made in the glovebox, in a nitrogen atmosphere, and stored at -20°C, and the PEGylation reaction was performed for the same reason as soon as the PEG-NHS ester was dissolved in buffer. Another crucial step is generating the hydrophilicity of the glass surface before the silanization reaction, by piranha etching and plasma cleaning, which generates free hydroxyl groups on a glass surface. After this procedure, it is recommended not to store the glass surface exposed to either water or air for a long period of time, since the hydrophilicity of the surface decreases in these conditions. PEGylated slides were also used for FCS

experiments, since sticking of the labeled ribosomes to the glass surface would lead to a decrease in the detected concentration and the results would be biased.

13.6. Initiation of Canonical mRNAs by 70S Ribosomes

The textbook knowledge on translation in bacteria puts forward a general initiation pathway: the 30S-binding initiation, described in detail in Section 1.6.1. In the current work, we want to underline the fact that this mechanism is not the only one through which initiation can occur, but rather the 70S particles can also initiate canonical mRNAs, without dissociation into subunits. Using single molecule experiments, we identified both mechanisms: the 30S-binding and initiation with 70S, in an *in vitro* transcription-translation system. Approximately 30% of initiation occurred with full ribosomes.

Several types of mRNA have been shown to be initiated by intact 70S: leaderless mRNAs, and the second cistron of a bicistronic mRNAs (Section 1.6.2), but the canonical mRNAs have not been studied in this respect. For both the leaderless and bicistronic mRNA, the initiation mechanism have been recently described. For the leaderless mRNA, in which the sequence starts immediately with the start codon, it is sterically straightforward to be accommodated in the mRNA tunnel of the 70S. In the case of the polycistronic mRNA, the ribosomes do not dissociate after translation of the first cistron, but rather scan until the next start codon, and initiate the second cistron. However, for the canonical mRNAs, which contain the SD sequence that binds the anti-SD of the 16S rRNA of the 30S subunit, these mechanisms can not be applied. In order to study the importance of initiation factors involved in this mechanism, one can employ *in vitro* systems devoid of these factors. The advantage of the PURE system, produced by mixing purified components of transcription and translation, is that it is available also in versions lacking certain factors, for example initiation factors. Moreover, introducing mutations in ribosomal complexes and comparing the occurence of 70S initiation events in this case, one can investigate the functionally important groups of the 70S that allow this type of initiation. In addition, further experiments in biologically relevant conditions, for example in the presence of a crowder or antibiotics, can be designed.

Recently, ribosomes with tethered subunits have been engineered ([Orelle et al., 2015]), which are functional in translation of canonical mRNAs, both *in vivo* and *in vitro*. In contrast to this, our study employs ribosomes which are not artificially linked, a case which is closer to the situation in the living bacteria. Therefore, it was surprising that approximately 30% of initiation occurred with 70S ribosomes. However, an interesting experiment would be to employ the ribosomes with tethered subunits in a single molecule study similar to the one described in this thesis.

13.7. Outlook

In this thesis, the results of the single molecule experiments in solution (TCCD) are presented. On the one hand, measurements in solution allow acquisition of a large number of events for a good statistical analysis, but on the other hand, the method does not provide information on the kinetics of the process. The current literature suggests that large-scale motions are the basis of important mechanistic events in translation, but the nature and timescale of these movements are still unknown. Therefore, experiments in solution should be complemented with imaging techniques using immobilized ribosomes.

So far, single molecule studies focused on translation were generally performed using ribosomal complexes immobilized via a biotinylated mRNA, so that a rather short sequence of the translated mRNA was studied. However, since we want to detect initiation, translation and folding of a fully active protein, our experiments were performed on ribosomes immobilized via the small subunit, and the full mRNA was translated. This raises further problems, since the ribosomes must be functionalized, and the modifications should not decrease activity, both in solution and after tethering on glass slides.

We showed that after functionalization, the ribosomes are active in solution (Section 11.4.2). On the glass slides, several problems occur, since unspecific binding could lead to random orientation and render ribosomes inactive. We chose the specific high-affinity biotin-streptavidin interaction and the blocking properties of polyethylene glycol (PEG) to achieve specific immobilization of ribosome complexes with low background binding (Section 10).

The experiment presented in this thesis can also be performed *in situ*, with ribosomes immobilized on a glass slide, and by measuring the GFPem and Cy5 fluorescence with a wide field. In this context, reassociated ZS22 ribosomes, functionalized with a biotin at the small subunit and Cy5 at the large subunit (using the method described in Section 8) are tethered on the surface, as described in Section 10 (Fig. 13.1). Using a wide field setup, the position of the Cy5 labels, corresponding to the large subunit, are identified. The PUExpress components, the DNA described in Section 9.2 and a 5 times excess of unlabeled 50S subunits are then added on the surface and the glass slide is incubated at 37°C to initiate transcription and translation. Successful translation and folding of GFPem is monitored in time, by detecting the apparition of green fluorescent peaks. The incubation time should not exceed one hour, since more than 10% of the Cy5 labeled oligonucleotide dissociates from the large subunit in these conditions (Fig. 12.4). The cases in which GFP is detected colocalized with a red fluorophore are considered as translation with full 70S ribosomes, while the cases in which GFP is detected bound on an non labeled ribosome is counted as a 30S-type initiation.
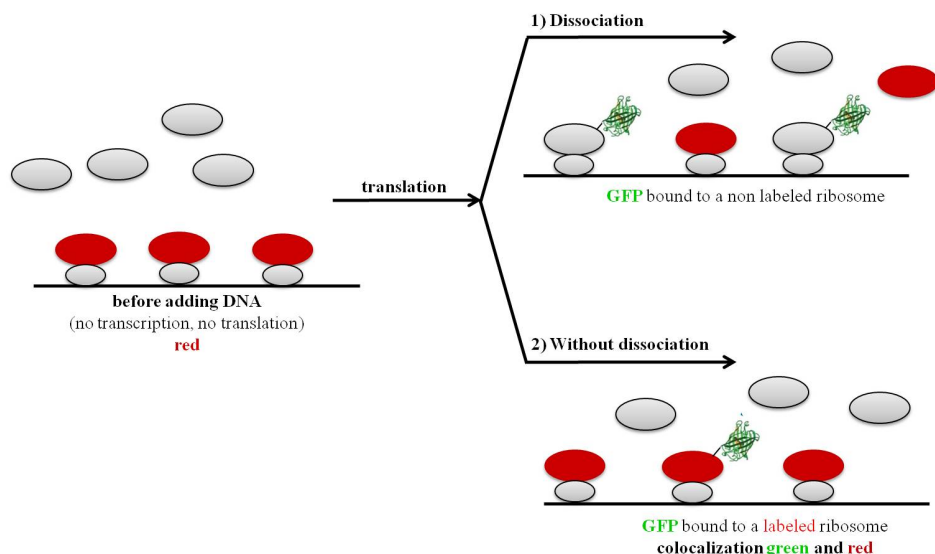

Figure 13.1.: Testing initiaton of a canonical mRNA by full 70S ribosomes, using tethered ribosomes

Acknowledgments

After having spent more than four years abroad, it's impossible not to become at least slightly emotional, maybe even melancholic. I still remember the first day in Germany. Heavy summer rain. My huge 30 kg luggage. The first German word that I learned: "Achtung!". The prophetic loud song in a shop in the airport. Queen. The show must go on. After four years, my Deutsch got better, I got used to the German "summertime" and most importantly, I finished the scientific project that I invested endless time and passion in.

It was not easy, one needs a strong mind not to give up. Maybe it's because of the sleepless nights, the days in which you go to work at 6 o'clock in the morning and return home late in the night, the uncertainty about the future. Or maybe all of them together. I couldn't have succeeded without the help and motivation of my supervisors and the whole Molecular Biophysics Group. First of all, I want to thank Prof. Dr. Jörg Fitter, for his scientific advice and professionalism, and Dr. Alexandros Katranidis, for sharing his knowledge about ribosomes, for insightful discussions and advice throughout these years. I must also mention the kind and generous scientific guidance of Prof. Dr. Knud Nierhaus, from Charité Universitätsmedizin Berlin, whose books, scientific articles and advice were a great source of inspiration for me. Moreover, I want to thank my group. Noémie, for helping me with the TCCD measurements, for her reliability and the fun times we had in the conference. Ralph, for the wide-field measurements and the lively discussions. Michele, for the time and patience in answering all my questions. Matteo, for all the support in the beginning of my PhD. Ramona, for helping me develop the rate-zonal fractionation of ribosomes. Ignatio, for the entertaining and relaxing lunch breaks.

Then, I want to acknowledge Dr. Thorsten Auth, for the perfect organization of the Biosoft Guest Student Programme that I participated in four years ago, and all the IHRS Biosoft professors and colleagues. I had the opportunity to meet brilliant students, together with whom I learned to think interdisciplinary.

In the end, I want to thank everyone that was beside me during this time. My parents for supporting me. My twin sister, Anca, for her lovely ways and fruitful midnight scientific conversations. Jenia, for being here in spite of my craziness and panic attacks, for inspiration and perfectly-timed holidays. Andreas, for encouraging me all the way. Daniel, for the enthusiasm and psychological support. My friends that I met in the train: Vahid, my serotonin boosting friend, Andreea, for her amazing optimism, Sergey, for all the waffles on the way back from work, and Silvia, for all the coffees that we shared.

Now, exhausted but content about my PhD time, I look forward to continue my scientific career, being convinced that the ribosome field will bring exciting discoveries in medicine and drug development. Show must go on...

Bibliography

Adhin, M. R. and van Duin, J. Scanning model for translational reinitiation in eubacteria. *Journal of Molecular Biology*, 213(4):811–818, 1990.

Aitken, C. E. and Puglisi, J. D. Following the intersubunit conformation of the ribosome during translation in real time. *Nature Structural and Molecular Biology*, 17(7):793–800, 2010.

Aitken, C. E., Marshall, R. A., and Puglisi, J. D. An oxygen scavenging system for improvement of dye stability in single-molecule fluorescence experiments. *Biophysical Journal*, 94(5):1826–1835, 2008.

Allen, G. S., Zavialov, A., Gursky, R., Ehrenberg, M., and Frank, J. The cryo-EM structure of a translation initiation complex from *Escherichia coli*. *Cell*, 121(5):703–712, 2005.

Angov, E., Hillier, C. J., Kincaid, R. L., and Lyon, J. A. Heterologous protein expression is enhanced by harmonizing the codon usage frequencies of the target gene with those of the expression host. *PLOS ONE*, 3(5):390–394, 2008.

Antoun, A., Pavlov, M. Y., Lovmar, M., and Ehrenberg, M. How initiation factors maximize the accuracy of tRNA selection in initiation of bacterial protein synthesis. *Molecular Cell*, 23(2):183–193, 2006.

Asai, T., Zaporojets, D., Squires, C., and Squires, C. L. An *Escherichia coli* strain with all chromosomal rRNA operons inactivated: complete exchange of rRNA genes between bacteria. *Proceedings of the National academy of Sciences of the United States of America*, 96(5):1971–1976, 1999.

Ban, N., Nissen, P., Hansen, J., Moore, P. B., and Steitz, T. A. The complete atomic structure of the large ribosomal subunit at 2.4 Å resolution. *Science*, 289(5481):905–920, 2000.

Beckett, D. T., Kovaleva, E., and Schatz, P. J. A minimal peptide substrate in biotin holoenzyme synthetase-catalyzed biotinylation. *Protein Science*, 8(4):921–929, 1999.

Biou, V., Shu, F., and Ramakrishnan, V. X-ray crystallography shows that translational initiation factor IF3 consists of two compact alpha/beta domains linked by an alpha-helix. *EMBO Journal*, 14(16):4056–4064, 1995.

Blaha, G., Burkhardt, N., and Nierhaus, K. H. Formation of 70s ribosomes: large activation energy is required for the adaptation of exclusively the small ribosomal subunit. *Biophysical Chemistry*, 96(2):153–161, 2002.

Bommer, U., Burkhardt, N., Juenemann, N., Spahn, C., Triana-Alonso, F., and Nierhaus, K. H. *Subcellular fractionation, A practical approach*, chapter Ribosomes and polysomes, pages 271–301. Oxford University Press, 1997.

Brakke, M. K. Zonal separations by density-gradient centrifugation. *Archives of Biochemistry and Biophysics*, 45(2):275–290, 1953.

Brenneis, M., Hering, O., Lange, C., and Soppa, J. Experimental characterization of Cis-acting elements important for translation and transcription in halophilic archaea. *PLoS Genetics*, 3(12):e229, 2007.

Brosius, J., Ullrich, A., Raker, M. A., Gray, A., Dull, T. J., Gutell, R. R., and Noller, H. F. Construction and fine and mapping of recombinant plasmids containing the rrnB ribosomal RNA operon of *E. coli*. *Plasmid*, 6:112–118, 1981.

Cabrita, L. D., Hsu, S.-T. D., Launay, H., Dobson, C. M., and Christodoulou, J. Probing ribosome-nascent chain complexes produced *in vivo* by NMR spectroscopy. *PNAS*, 2009.

Calogero, R. A., Pon, C. L., Canonaco, M. A., and Gualerzi, C. O. Selection of the mRNA translation initiation region by *Escherichia coli* ribosomes. *Proceedings of the National academy of Sciences of the United States of America*, 85(17):6427–6431, 1988.

Carter, A. P., Clemons, W. M., Brodersen, D. E., Morgan-Warren, R. J., Wimberly, B. T., and Ramakrishnan, V. Functional insights from the structure of the 30S ribosomal subunit and its interactions with antibiotics. *Nature*, 407(6802):340–348, 2000.

Carter, A. P., Clemons, W. M. J., Brodersen, D. E., Morgan-Warren, R. J., Hartsch, T., Wimberly, B. T., and Ramakrishnan, V. Crystal structure of an initiation factor bound to the 30S ribosomal subunit. *Science*, 291:498–501, 2001.

Celano, B., Pawlik, R. T., and Gualerzi, C. O. Interaction of *Escherichia coli* translation-initiation factor IF-1 with ribosomes. *European Journal of Biochemistry*, 178(2):351–355, 1988.

Chandradoss, S. D., Haagsma, A. C., Lee, Y. K., Hwang, J.-H., Nam, J.-M., and Joo, C. Surface passivation for single-molecule protein studies. *J Vis Exp*, 2014.

Cheng, Y. Single-particle cryo-EM at crystallographic resolution. *Cell*, 161(3):450–457, 2015.

Chevance, F. F. V., Le Guyon, S., and Hughes, K. T. The effects of codon context on in vivo translation speed. *PLoS Genetics*, 10(6):e1004392, 2014.

Christian, B. E. and Spremulli, L. L. Preferential selection of the 5'-terminal start codon on leaderless mRNAs by mammalian mitochondrial ribosomes. *Journal of Biological Chemistry*, 285(36):28379–28386, 2010.

Clemons, W. M. J., Brodersen, D. E., McCutcheon, J. P., May, J. L., Carter, A. P., Morgan-Warren, R. J., Wimberly, B. T., and Ramakrishnan, V. Crystal structure of the 30S ribosomal subunit from *Thermus thermophilus*: purification, crystallization and structure determination. *Journal of Molecular Biology*, 310(4):827–843, 2001.

Coombs, D. H. and Watts, N. R. Generating sucrose gradients in three minutes by tilted tube rotation. *Analytical Biochemistry*, 148(1):254–259, 1985.

Cymer, F., Hedman, R., Ismail, N., and von Heijne, G. Exploration of the arrest peptide sequence space reveals arrest-enhanced variants. *Journal of Biological Chemistry*, 290(16):10208–10215, 2015.

Dahlquist, K. D. and Puglisi, J. D. Interaction of translation initiation factor IF1 with the *E. coli* ribosomal A site. *Journal of Molecular Biology*, 299(1):1–15, 2000.

Dallas, A. and Noller, H. F. Interaction of translation initiation factor 3 with the 30S ribosomal subunit. *Molecular Cell*, 8(4):855–864, 2001.

Doerfel, L. K., Wohlgemuth, I., Kothe, C., Peske, F., Urlaub, H., and Rodnina, M. V. EF-P is essential for rapid synthesis of proteins containing consecutive proline residues. *Science*, 339(6115):85–88, 2013.

Dohme, F. and Nierhaus, K. H. Total reconstitution and assembly of 50S subunits from *Escherichia coli* ribosomes *in vitro*. *Journal of Molecular Biology*, 107(4):585–599, 1976.

Dorywalska, M., Blanchard, S. C., Gonzalez, R. L., Kim, H. D., Chu, S., and Puglisi, J. D. Site-specific labeling of the ribosome for single-molecule spectroscopy. *Nucleic Acids Research*, 33(1):182–189, 2005.

Dulebohn, D., Choy, J., Sundermeier, T., Okan, N., and Karzai, A. W. Trans-translation: the tmRNA-mediated surveillance mechanism for ribosome rescue, directed protein degradation, and nonstop mRNA decay. *Biochemistry*, 46(16):4681–4693, 2007.

Elvekrog, M. M. and Gonzalez, R. L., Jr. Conformational selection of translation initiation factor 3 signals proper substrate selection. *Nature Structural and Molecular Biology*, 20(5):628–633, 2013.

Enderlein, J. and Gregor, I. Using fluorescence lifetime for discriminating detector afterpulsing in fluorescence-correlation spectroscopy. *Review of Scientific Instruments*, 2005.

Evans, M. S., Ugrinov, K. G., Frese, M.-A., and Clark, P. L. Homogeneous stalled ribosome nascent chain complexes produced *in vivo* or *in vitro*. *Nature Methods*, 2(10):757–762, 2005.

Fabbretti, A., Pon, C. L., Hennelly, S. P., Hill, W. E., Lodmell, J. S., and Gualerzi, C. O. The real-time path of translation factor IF3 onto and off the ribosome. *Molecular Cell*, 25(2):285–296, 2007.

Fedyukina, D. V. and Cavagnero, S. Protein folding at the exit tunnel. *Annual Review of Biophysics*, 40(1):337–359, 2011.

Ferbitz, L., Maier, T., Patzelt, H., Bukau, B., Deuerling, E., and Ban, N. Trigger factor in complex with the ribosome forms a molecular cradle for nascent proteins. *Nature*, 431(7008):590–596, 2004.

Fortier, P. L., Schmitter, J. M., Garcia, C., and Dardel, F. The N-terminal half of initiation factor IF3 is folded as a stable independent domain. *Biochimie*, 76(5):376–383, 1994.

Garcia, C., Fortier, P. L., Blanquet, S., Lallemand, J. Y., and Dardel, F. 1H and 15N resonance assignments and structure of the N-terminal domain of *Escherichia coli* initiation factor 3. *European Journal of Biochemistry*, 228(2):395–402, 1995.

Grill, S., Gualerzi, C. O., Londei, P., and Bläsi, U. Selective stimulation of translation of leaderless mRNA by initiation factor 2: evolutionary implications for translation. *EMBO Journal*, 19(15): 4101–4110, 2000.

Grill, S., Moll, I., Hasenöhrl, D., Gualerzi, C. O., and Bläsi, U. Modulation of ribosomal recruitment to 5'-terminal start codons by translation initiation factors IF2 and IF3. *FEBS Letters*, 495(3):167–171, 2001.

Gualerzi, C. O., Brandi, L., Caserta, E., Garofalo, C., Lammi, M., La Teana, A., Petrelli, D., Spurio, R., Tomsic, J., and Pon, C. L. Initiation factors in the early events of mRNA translation in bacteria. *Cold Spring Harb Symp Quant Biol*, 66:363–376, 2001.

Gualerzi, C. O. and Pon, C. L. Initiation of mRNA translation in prokaryotes. *Biochemistry*, 29(25): 5881–5889, 1990.

Gualerzi, C. O., Severini, M., Spurio, R., La Teana, A., and Pon, C. L. Molecular dissection of translation initiation factor IF2. evidence for two structural and functional domains. *Journal of Biological Chemistry*, 266(25):16356–16362, 1991.

Gutmann, S., Haebel, P. W., Metzinger, L., Sutter, M., Felden, B., and Ban, N. Crystal structure of the transfer-RNA domain of transfer-messenger RNA in complex with SmpB. *Nature*, 424(6949): 699–703, 2003.

Ha, T. and Tinnefeld, P. Photophysics of fluorescent probes for single-molecule biophysics and super-resolution imaging. *Annual Review of Physical Chemistry*, 63:595–617, 2012.

Hartz, D., McPheeters, D. S., and Gold, L. Selection of the initiator tRNA by *Escherichia coli* initiation factors. *Genes & Development*, 3:1899–1912, 1989.

Hashem, Y., des Georges, A., Fu, J., Buss, S. N., Jossinet, F., Jobe, A., Zhang, Q., Liao, H. Y., Grassucci, R. A., Bajaj, C., Westhof, E., Madison-Antenucci, S., and Frank, J. High-resolution cryo-electron microscopy structure of the *Trypanosoma brucei* ribosome. *Nature*, 494(7437):385–389, 2013.

Jansen, R., Bussemaker, H. J., and Gerstein, M. Revisiting the codon adaptation index from a whole-genome perspective: analyzing the relationship between gene expression and codon occurrence in yeast using a variety of models. *Nucleic Acids Research*, 31(8):2242–2251, 2003.

Jeyachandran, Y. L., Mielczarski, J. A., Mielczarski, E., and Rai, B. Efficiency of blocking of non-specific interaction of different proteins by BSA adsorbed on hydrophobic and hydrophilic surfaces. *Journal of Colloid and Interface Science*, 341(1):136–142, 2010.

Julián, P., Milon, P., Agirrezabala, X., Lasso, G., Gil, D., Rodnina, M. V., and Valle, M. The Cryo-EM structure of a complete 30S translation initiation complex from *Escherichia coli*. *PLoS Biology*, 9 (7):e1001095, 2011.

Kaberdina, A. C., Szaflarski, W., Nierhaus, K. H., and Moll, I. An unexpected type of ribosomes induced by kasugamycin: a look into ancestral times of protein synthesis? *Molecular Cell*, 33(2): 227–236, 2009.

Kaempfer, R. Initiation factor IF-3: a specific inhibitor of ribosomal subunit association. *Journal of Molecular Biology*, 71(3):583–598, 1972.

Karzai, W. A., Roche, E. D., and Sauer, R. T. The SsrA-SmpB system for protein tagging, directed degradation and ribosome rescue. *Nature Structural Biology*, 7(6):449–455, 2000.

Katranidis, A., Atta, D., Schlesinger, R., Nierhaus, K. H., Choli-Papadopoulou, T., Gregor, I., Gerrits, M., Büldt, G., and Fitter, J. Fast biosynthesis of GFP molecules: a single-molecule fluorescence study. *Angewandte Chemie. International Edition in English*, 48(10):1758–1761, 2009.

Bibliography

Katzen, F., Chang, G., and Kudlicki, W. The past, present and future of cell-free protein synthesis. *Trends in Biotechnology*, 23(3):150–156, 2005.

Keiler, K. C. and Feaga, H. A. Resolving nonstop translation complexes is a matter of life or death. *Journal of Bacteriology*, 196(12):2123–2130, 2014.

Keiler, K. C. Mechanisms of ribosome rescue in bacteria. *Nature Reviews. Microbiology*, 13(5):285–297, 2015.

Keiler, K. C., Waller, P. R., and Sauer, R. T. Role of a peptide tagging system in degradation of proteins synthesized from damaged messenger RNA. *Science*, 271(5251):990–993, 1996.

Kim, D. M. and Choi, C. Y. A semicontinuous prokaryotic coupled transcription/translation system using a dialysis membrane. *Biotechnol Prog*, 12(5):645–649, 1996.

Kisselev, L. and Buckingham, R. Translational termination comes of age. *EMBO Journal*, 25(11), 2000.

Kisselev, L., Ehrenberg, M., and Frolova, L. Termination of translation: interplay of mRNA, rRNA and release factors? *The EMBO Journal*, 22, 2003.

Klein, D. J., Moore, P. B., and Steitz, T. A. The contribution of metal ions to the structural stability of the large ribosomal subunit. *RNA*, 10(9):1366–1379, 2004.

Komine, Y., Kitabatake, M., Yokogawa, T., Nishikawa, K., and Inokuchi, H. A tRNA-like structure is present in 10Sa RNA, a small stable RNA from *Escherichia coli*. *Proceedings of the National academy of Sciences of the United States of America*, 91(20):9223–9227, 1994.

La Teana, A., Gualerzi, C. O., and Brimacombe, R. From stand-by to decoding site. adjustment of the mRNA on the 30S ribosomal subunit under the influence of the initiation factors. *RNA*, 1(8): 772–782, 1995.

Lamichhane, R., Solem, A., Black, W., and Rueda, D. Single-molecule FRET of protein-nucleic acid and protein-protein complexes: surface passivation and immobilization. *Methods*, 52(2):192–200, 2010.

Laursen, B. S., SÃ¸rensen, H. P., and Mortensen, K. K. Initiation of protein synthesis in bacteria. *Microbiology and Molecular Biology Reviews*, 69(1):101–123, 2005.

Lawrence, M. G., Shamsuzzaman, M., Kondopaka, M., Pascual, C., Zengel, J. M., and Lindahl, L. The extended loops of ribosomal proteins uL4 and uL22 of *Escherichia coli* contribute to ribosome assembly and protein translation. *Nucleic Acids Research*, 44(12):5798–5810, 2016.

Li, G.-W., Oh, E., and Weissman, J. S. The anti-Shine-Dalgarno sequence drives translational pausing and codon choice in bacteria. *Nature*, 484(7395):538–541, 2012.

Li, H., Ying, L., Green, J., Balasubramanian, S., and Klenerman, D. Ultrasensitive coincidence fluorescence detection of single DNA molecules. *Analytical Chemistry*, 75(7):1664–1670, 2003.

Marshall, R. A., Aitken, C. E., Dorywalska, M., and Puglisi, J. D. Translation at the single-molecule level. *Annual Review of Biochemistry*, 77:177–203, 2008.

Marshall, R. A., Aitken, C. E., and Puglisi, J. D. GTP hydrolysis by IF2 guides progression of the ribosome into elongation. *Molecular Cell*, 35(1):37–47, 2009.

McCutcheon, J., Agrawal, R. K., Philips, S. M., Grassucci, R. A., Gerchman, S. E., Clemons, W. M. J., and Ramakrishnan, J., V. and. Frank. Localization of translation initiation factor IF3 on the small ribosomal subunit. *Proc. Natl. Acad. Sci. USA*, 96:4301–4306, 1999.

Mears, J. A., Cannone, J. J., Stagg, S. M., Gutell, R. R., Agrawal, R. K., and Harvey, S. C. Modeling a minimal ribosome based on comparative sequence analysis. *Journal of Molecular Biology*, 321(2): 215–234, 2002.

Meinnel, T., Sacerdot, C., Graffe, M., Blanquet, S., and Springer, M. Discrimination by *Escherichia coli* initiation factor IF3 against initiation on non-canonical codons relies on complementarity rules. *Journal of Molecular Biology*, 290:825–837, 1999.

Milon, P., Konevega, A. L., Peske, F., Fabbretti, A., Gualerzi, C. O., and Rodnina, M. V. Transient kinetics, fluorescence, and FRET in studies of initiation of translation in bacteria. *Methods in Enzymology*, 430:1–30, 2007.

Moll, I., Grill, S., Gualerzi, C. O., and Bläsi, U. Leaderless mRNAs in bacteria: surprises in ribosomal recruitment and translational control. *Molecular Microbiology*, 43(1):239–246, 2002.

Müller, B. K., Zaychikov, E., Bräuchle, C., and Lamb, D. C. Pulsed interleaved excitation. *Biophysical Journal*, 89(5):3508–3522, 2005.

Myasnikov, A. G., Marzi, S., Simonetti, A., Giuliodori, A. M., Gualerzi, C. O., Yusupova, G., Yusupov, M., and Klaholz, B. P. Conformational transition of initiation factor 2 from the GTP- to GDP-bound state visualized on the ribosome. *Nature Structural and Molecular Biology*, 12(12):1145–1149, 2005.

Nierhaus, K. H. Mg^{2+}, K^+, and the ribosome. *Journal of Bacteriology*, 196(22):3817–3819, 2014.

Nilsson, O. B., Hedman, R., Marino, J., Wickles, S., Bischoff, L., Johansson, M., Müller-Lucks, A., Trovato, F., Puglisi, J. D., O'Brien, E. P., Beckmann, R., and von Heijne, G. Cotranslational protein folding inside the ribosome exit tunnel. *Cell Rep*, 12(10):1533–1540, 2015.

Nissen, P., Hansen, J., Ban, N., Moore, P. B., and Steitz, T. A. The structural basis of ribosome activity in peptide bond synthesis. *Science*, 289:920–930, 2000.

Orelle, C., Carlson, E. D., Szal, T., Florin, T., Jewett, M. C., and Mankin, A. S. Protein synthesis by ribosomes with tethered subunits. *Nature*, 524(7563):119–124, 2015.

Orte, A., Clarke, R., and Klenerman, D. Single-molecule two-colour coincidence detection to probe biomolecular associations. *Biochemical Society Transactions*, 38(4):914–918, 2010.

Pavlov, M. Y., Antoun, A., Lovmar, M., and Ehrenberg, M. Complementary roles of initiation factor 1 and ribosome recycling factor in 70S ribosome splitting. *EMBO Journal*, 27(12):1706–1717, 2008.

Peil, L., Starosta, A. L., Lassak, J., Atkinson, G. C., Virumäe, K., Spitzer, M., Tenson, T., Jung, K., Remme, J., and Wilson, D. N. Distinct XPPX sequence motifs induce ribosome stalling, which is rescued by the translation elongation factor EF-P. *Proceedings of the National academy of Sciences of the United States of America*, 110(38):15265–15270, 2013.

Bibliography

Pelham, H. R. B. and Jackson, R. J. An efficient mRNA-dependent translation system from reticulocyte lysates. *European Journal of Biochemistry*, 67(1):247–256, 1976.

Perez, C. E. and Gonzalez, R. L., Jr. *In vitro* and *in vivo* single-molecule fluorescence imaging of ribosome-catalyzed protein synthesis. *Current Opinion in Chemical Biology*, 15(6):853–863, 2011.

Petersen, H. U., Danchin, A., and Grunberg-Manago, M. Toward an understanding of the formylation of initiator tRNA methionine in prokaryotic protein synthesis. a two-state model for the 70S ribosome. *Biochemistry*, 15(7):1362–1369, 1976.

Petrov, A. and Puglisi, J. D. Site-specific labeling of *Saccharomyces cerevisiae* ribosomes for single-molecule manipulations. *Nucleic Acids Research*, 38(13):e143, 2010.

Pioletti, M., Schlünzen, F., Harms, J., Zarivach, R., Glühmann, M., Avila, H., Bashan, A., Bartels, H., Auerbach, T., Jacobi, C., Hartsch, T., Thomas, A., and Franceschi, F. Crystal structures of complexes of the small and ribosomal subunit with tetracycline, edeine and IF3. *The EMBO Journal*, 20(8): 1829–1839, 2001.

Pon, C. L. and Gualerzi, C. O. Mechanism of protein biosynthesis in prokaryotic cells. effect of initiation factor IF1 on the initial rate of 30S initiation complex formation. *FEBS Letters*, 175(2): 203–207, 1984.

Proshkin, S., Rahmouni, A. R., Mironov, A., and Nudler, E. Cooperation between translating ribosomes and RNA polymerase in transcription elongation. *Science*, 328(5977):504–508, 2010.

Ramakrishnan, V. and Moore, P. B. Atomic structures at last: the ribosome in 2000. *Current Opinion in Structural Biology*, 11(2):144–154, 2001.

Rasnik, I., McKinney, S. A., and Ha, T. Nonblinking and long-lasting single-molecule fluorescence imaging. *Nature Methods*, 3(11):891–893, 2006.

Roberts, B. E. and Paterson, B. M. Efficient translation of tobacco mosaic virus RNA and rabbit globin 9S RNA in a cell-free system from commercial wheat germ. *Proc. Nat. Acad. Sci.*, 70(8):2330–2334, 1973.

Romero, D. A., Hasan, A. H., Lin, Y.-f., Kime, L., Ruiz-Larrabeiti, O., Urem, M., Bucca, G., Mamanova, L., Laing, E. E., van Wezel, G. P., Smith, C. P., Kaberdin, V. R., and McDowall, K. J. A comparison of key aspects of gene regulation in *Streptomyces coelicolor* and *Escherichia coli* using nucleotide-resolution transcription maps produced in parallel by global and differential RNA sequencing. *Molecular Microbiology*, 94(5):963–987, 2014.

Rosenblum, G., Chen, C., Kaur, J., Cui, X., Goldman, Y. E., and Cooperman, B. S. Real-time assay for testing components of protein synthesis. *Nucleic Acids Research*, 40(12):e88, 2012.

Saeki, H. and Svejstrup, J. Q. Stability, flexibility, and dynamic interactions of colliding RNA polymerase II elongation complexes. *Molecular Cell*, 35(2):191–205, 2009.

Schaffitzel, C., Hanes, J., Jermutus, L., and Pluckthun, A. Ribosome display: an *in vitro* method for selection and evolution and of antibodies from libraries. *Journal of Immunological Methods*, 1999.

Schilling-Bartetzko, S., Bartetzko, A., and Nierhaus, K. H. Kinetic and thermodynamic parameters for tRNA binding to the ribosome and for the translocation reaction. *Journal of Biological Chemistry*, 267(7):4703–4712, 1992.

Schlünzen, F., Wilson, D. N., Tian, P., Harms, J. M., McInnes, S. J., Hansen, H. A. S., Albrecht, R., Buerger, J., Wilbanks, S. M., and Fucini, P. The binding mode of the trigger factor on the ribosome: implications for protein folding and SRP interaction. *Structure*, 13(11):1685–1694, 2005.

Schmeing, M. T. and Ramakrishnan, V. What recent ribosome structures have revealed about the mechanism of translation. *Nature*, 461(7268):1234–1242, 2009.

Sette, M., Spurio, R., van Tilborg, P., Gualerzi, C. O., and Boelens, R. Identification of the ribosome binding sites of translation initiation factor IF3 by multidimensional heteronuclear NMR spectroscopy. *RNA*, 5(1):82–92, 1999.

Sette, M., van Tilborg, P., Spurio, R., Kaptein, R., Paci, M., Gualerzi, C. O., and Boelens, R. The structure of the translational initiation factor IF1 from *E.coli* contains an oligomer-binding motif. *The EMBO Journal*, 16(6):1436–1443, 1997.

Shalev-Benami, M., Zhang, Y., Matzov, D., Halfon, Y., Zackay, A., Rozenberg, H., Zimmerman, E., Bashan, A., Jaffe, C. L., Yonath, A., and Skiniotis, G. 2.8-Å cryo-em structure of the large ribosomal subunit from the eukaryotic parasite leishmania. *Cell Rep*, 16(2):288–294, 2016.

Shaner, N., Steinbach, P. A., and Tsien, R. Y. A guide to choosing fluorescent proteins. *Nature Methods*, 2(12):905–909, 2005.

Shimizu, Y., Inoue, A., Tomari, Y., Suzuki, T., Yokogawa, T., Nishikawa, K., and Ueda, T. Cell-free translation reconstituted with purified components. *Nature Biotechnology*, 19(8):751–755, 2001.

Shine, J. and Dalgarno, L. The 3' terminal sequence of *Escherichia coli* 16S ribosomal RNA: complementarity to nonsense triplets and ribosome binding site. *Proc Natl Acad Sci USA*, 71(4):1342–1346, 1974.

Simonetti, A., Marzi, S., Myasnikov, A. G., Fabbretti, A., Yusupov, M., Gualerzi, C. O., and Klaholz, B. P. Structure of the 30S translation initiation complex. *Nature*, 455(7211):416–420, 2008.

Slupska, M. M., King, A. G., Fitz-Gibbon, S., Besemer, J., Borodovsky, M., and Miller, J. H. Leaderless transcripts of the crenarchaeal hyperthermophile *Pyrobaculum aerophilum*. *Journal of Molecular Biology*, 309(2):347–360, 2001.

Sprink, T., Ramrath, D. J. F., Yamamoto, H., Yamamoto, K., Loerke, J., Ismer, J., Hildebrand, P. W., Scheerer, P., Buürger, J., Mielke, T., and Spahn, C. M. T. Structures of ribosome-bound initiation factor 2 reveal the mechanism of subunit association. *Science Advances*, 2(3), 2016.

Steitz, J. A. and Jakes, K. How ribosomes select initiator regions in mRNA: base pair formation between the 3' terminus of 16S rRNA and the mRNA during initiation of protein synthesis in *Escherichia coli*. *Proceedings of the National academy of Sciences of the United States of America*, 72 (12):4734–4738, 1975.

Steitz, T. A. A structural understanding of the dynamic ribosome machine. *Nature Reviews. Molecular Cell Biology*, 9(3):242–253, 2008.

Tsai, A., Petrov, A., Marshall, R. A., Korlach, J., Uemura, S., and Puglisi, J. D. Heterogeneous pathways and timing of factor departure during translation initiation. *Nature*, 487(7407):390–393, 2012.

Bibliography

Udagawa, T., Shimizu, Y., and Ueda, T. Evidence for the translation initiation of leaderless mRNAs by the intact 70S ribosome without its dissociation into subunits in eubacteria. *Journal of Biological Chemistry*, 279(10):8539–8546, 2004.

Uemura, S., Iizuka, R., Ueno, T., Shimizu, Y., Taguchi, H., Ueda, T., Puglisi, J. D., and Funatsu, T. Single-molecule imaging of full protein synthesis by immobilized ribosomes. *Nucleic Acids Research*, 36(12):e70, 2008.

Uemura, S., Aitken, C. E., Korlach, J., Flusberg, B. A., Turner, S. W., and Puglisi, J. D. Real-time tRNA transit on single translating ribosomes at codon resolution. *Nature*, 464(7291):1012–1017, 2010.

Vanzi, F., Takagi, Y., Shuman, H., Cooperman, B. S., and Goldman, Y. E. Mechanical studies of single ribosome/mRNA complexes. *Biophysical Journal*, 89(3):1909–1919, 2005.

Widengren, J. and Schwille, P. Characterization of photoinduced isomerization and back-isomerization of the cyanine dye Cy5 by fluorescence correlation spectroscopy. *The Journal of Physical Chemistry A*, 104(27):6416–6428, 2000.

Wimberly, B. T., Brodersen, D. E., Clemons, W. M. J., Morgan-Warren, R. J., Carter, A. P., Vonrhein, C., Hartsch, T., and Ramakrishnan, V. Structure of the 30S ribosomal subunit. *Nature*, 407(6802): 327–339, 2000.

Woolhead, C. A., McCormick, P. J., and Johnson, A. E. Nascent membrane and secretory proteins differ in FRET-detected folding far inside the ribosome and in their exposure to ribosomal proteins. *Cell*, 116(5):725–736, 2004.

Worbs, M., Huber, R., and Wahl, M. C. Crystal structure of ribosomal protein L4 shows RNA-binding sites for ribosome incorporation and feedback control of the S10 operon. *EMBO Journal*, 19(5): 807–818, 2000.

Yamamoto, H., Wittek, D., Gupta, R., Qin, B., Ueda, T., Krause, R., Yamamoto, K., Albrecht, R., Pech, M., and Nierhaus, K. H. 70S-scanning initiation is a novel and frequent initiation mode of ribosomal translation in bacteria. *Proceedings of the National Academy of Sciences*, 113(9):E1180–E1189, 2016.

Yanofsky, C. and Ito, J. Nonsense codons and polarity in the tryptophan operon. *Journal of Molecular Biology*, 21(2):313–334, 1966.

Yusupova, G. Z., Yusupov, M. M., Cate, J. H., and Noller, H. F. The path of messenger RNA through the ribosome. *Cell*, 106(2):233–241, 2001.

Zaniewski, R., Petkaitis, E., and Deutscher, M. P. A multiple mutant of *Escherichia coli* lacking the exoribonucleases RNase II, RNase D, and RNase BN. *Journal of Biological Chemistry*, 259(19): 11651–11653, 1984.

Zhao, M., Jin, L., Chen, B., Ding, Y., Ma, H., and Chen, D. Afterpulsing and its correction in fluorescence correlation spectroscopy experiments. *Applied Optics*, 42(19):4031–4036, 2003.

Zheng, X., Hu, G.-Q., She, Z.-S., and Zhu, H. Leaderless genes in bacteria: clue to the evolution of translation initiation mechanisms in prokaryotes. *BMC Genomics*, 12:361, 2011.

Zondervan, R., Kulzer, F., Orlinskii, S. B., and Orrit, M. Photoblinking of Rhodamine 6G in Poly(vinyl alcohol): Radical dark state formed through the triplet. *The Journal of Physical Chemistry A*, 107 (35):6770–6776, 2003.

List of Figures

List of Tables

Abbreviation

Translation specific

30S	small subunit of the bacterial ribosome
50S	large subunit of the bacterial ribosome
70S	bacterial ribosome
aSD	anti Shine-Dalgarno
ATP	adenosine triphosphate
DNA	dezoxyribonucleic acid
E. coli	Escherichia coli
EF-G	elongation factor G
EF-Tu	elongation factor Tu
fMet	N-formylmethionine
GDP	guanosine-5'-diphosphate
GFP	green fluorescent protein
GFPem	emerald green fluorescent protein
GTP	guanosine-5'-triphosphate
IF	initiation factor
lmRNA	leaderless mRNA
mRNA	messenger RNA
ORF	open reading frame
PTC	peptidyl-transferase center
RF	release factor
RNA	ribonucleic acid
RNAP	RNA polymerase
RNase	ribonuclease
RNC	ribosome-nascent chain complex
RRF	ribosome recycling factor
rRNA	ribosomal RNA
SD	Shine-Dalgarno
SecM	secretion monitor
SmpB	small protein B
TF	trigger factor
tmRNA	transfer-messenger RNA
tRNA	transfer RNA
UTR	untranslated regions

. Abbreviation

Chemicals

AcOH	acetic acid
Amp	ampicilin
APS	ammonium persulfate
bioPEG	biotinylated polyethylene glycol
Ca(OAc)$_2$	calcium acetate
CaCl$_2$	calcium chloride
Cm	chloramphenicol
DMSO	dimethyl sulfoxide
EDTA	ethylenediamine tetraacetic acid
Gox	glucoxe oxydase
H$_2$O$_2$	hydrogen peroxide
Hepes	(4-(2-hydroxyethyl)-1-piperazineethanesulfonic acid
IPTG	isopropyl-thio-β-D-galaktosidose
KCl	potasium chloride
KOAc	potasium acetate
Mg(OAc)$_2$	magnesium acetate
MgCl$_2$	magnesium chloride
MgSO$_4$	magnesium sulphate
miliQ	salt free, sterile, RNase free water
MnCl$_2$	manganese chloride
MOPS	3-(N-morpholino)propanesulfonic acid sodium salt
NaCl	sodium chloride
NaHCO$_3$	sodium bicarbonate
NaOH	sodium hydroxyde
NH$_4$Cl	ammonium chloride
NH$_4$OAc	ammonium acetate
NHS	N-hydroxysuccinimide
PAA	polyacrilamide
PBS	phosphate-buffered saline
PCA	protocatechuic acid
PCD	protocatechuate-3,4-dioxygenase
PEG	polyethylene glycol
PURE	protein synthesis using recombinant elements
RbCl	rubidium chloride
TEMED	tetramethylethylenediamine
Tet	tetracycline
Tris-HCl	Tris hydrochloride
Tris-OAc	Tris(hydroxymethyl)aminomethane acetate salt

Units

A_{260}	absorbance at 260nm
h	hour
min	minute
OD_{600}	optical density at 600 nm
rpm	rotations per minute

Methods

cryo-EM	cryo-electron microscopy
FCS	fluorescence correlation spectroscopy
FRET	fluorescence resonance energy transfer
NMR	nuclear magnetic resonance spectroscopy
TCCD	two-color coincidence detection

Schriften des Forschungszentrums Jülich
Reihe Schlüsseltechnologien / Key Technologies

Schriften des Forschungszentrums Jülich
Reihe Schlüsseltechnologien / Key Technologies

Weitere ***Schriften des Verlags im Forschungszentrum Jülich*** unter
http://wwwzb1.fz-juelich.de/verlagextern1/index.asp

JÜLICH
Forschungszentrum